



MASTERARBEIT

Titel der Masterarbeit

„FGFR4 blocking strategies in colorectal cancer and
Ba/F3 cells“

verfasst von

Daniel Drev BSc

angestrebter akademischer Grad

Master of Science (MSc)

Wien, 2014

Studienkennzahl lt. Studienblatt:

A 066 834

Studienrichtung lt. Studienblatt:

Masterstudium Molekulare Biologie

Betreut von:

A.o. Univ. Prof. Dr. Brigitte Marian

Acknowledgements

The end of my master thesis marks an important chapter in my life. Here, I want to thank all the people that helped me on this journey.

First of all, I want to thank my supervisor Dr. Brigitte Marian for her inspiration, her advice and of course for the opportunity to work in her lab. Brigitte had always an open ear for my thoughts and questions. Thank you for supporting me in the last year.

I am very grateful to Christine Heinzle, who introduced me into this project and always supported me and my work. Moreover, I want to say a big thanks to my entire lab, namely Andrea, Mohamed, Xenia, Zeynep, and our newest member Steffi. Thank you for all the fun we had, your scientific and technical support as well as for all the stimulating discussions.

I want to thank the FGF group, namely Dr. Walter Berger, Dr. Michael Grusch, Dr. Bettina Grasl-Kraupp, Dr. Klaus Holzmann and their teams for fruitful discussions as well as advices.

Special thanks to Irene Herbacek for performing myriads of FACS analysis for me, to Anita Brandstetter and the Histological Facility as well as to Dr. Petra Heffeter for helping me with the mice experiments.

Last but not least, I want to thank my beloved ones. My father Hubert, my mother Marion and her partner Martin always supported me financially and encouraged me to study, thank you for your trust in me! Also, I want to thank my brother Benni for all the fun we had, especially after long learning sessions. This helped me to stay focused. Special thanks to my girlfriend Vanita, for our time together and all the laugh we had in the last years. I can always count on your support and advice. Also, I am deeply thankful for my grandfather and –mother, Dieter and Gerti. You two are amazing, thank you for your backup. I would also like to thank all my friends and companions for all the fun we had outside of university, you guys are great!

Table of Contents

i.	List of figures	V
ii.	List of tables	VI
iii.	Abbreviations	VII
1	Introduction.....	1
1.1	Definition of cancer	1
1.2	Epidemiology	1
1.2.1	Cancer epidemiology.....	1
1.2.2	Epidemiology of Colorectal Cancer	3
1.3	Tumorigenesis of Colon Cancer	3
1.4	Hallmarks of Cancer.....	5
1.4.1	Permanent Proliferation.....	5
1.4.2	Evading Growth Suppressors	6
1.4.3	Resisting Apoptosis	6
1.4.4	Immortalization	7
1.4.5	Neo-Angiogenesis.....	7
1.4.6	Invasion and Metastasis	7
1.4.7	Enabling Characteristic: Genome Instability and Mutation	8
1.4.8	Enabling Characteristic: Inflammation	9
1.4.9	Emerging Hallmark: Altered Energy Metabolism.....	9
1.4.10	Emerging Hallmark: Evading the Immune System	9
1.5	Receptor Tyrosine Kinases.....	10
1.6	Fibroblast Growth Factor Receptors	11
1.6.1	Structure.....	11
1.6.2	Interaction between FGFR and FGF	12

1.6.3	FGFR downstream signaling	13
1.6.4	Termination of FGFR signaling	14
1.6.5	Deregulation of FGFR-signaling in cancer	15
1.7	Fibroblast Growth Factor Receptor 4	16
1.7.1	Structure of FGFR4	16
1.7.2	Physiological role of FGFR4	17
1.7.3	FGFR4 and cancer	17
1.7.4	SNP of FGFR4 at position G388R	18
1.7.5	Blocking strategies for FGFR4	20
1.8	Ba/F3 model system	21
2	Aim of the study	22
3	Material and methods	23
3.1	Cell biology	23
3.1.1	Cell lines and passaging	23
3.1.2	Viability assays	24
3.1.3	Transfection of Ba/F3 cells	24
3.1.4	Selection of transfected Ba/F3 cells	25
3.1.5	Fluorescence activated cell sorting (FACS)	25
3.1.6	Viral transduction of cells	26
3.2	Working with RNA	27
3.2.1	RNA Isolation	27
3.2.2	cDNA Synthesis	28
3.3	Working with DNA	29
3.3.1	Polymerase chain reaction (PCR)	29
3.3.2	Restriction Fragment Length Polymorphism (RFLP) for G388R	30
3.3.3	Polyacrylamid gel electrophoresis	31

3.3.4	Transformation of bacterial cells	31
3.3.5	Glycerol stocks.....	32
3.3.6	Preparation of plasmids	32
3.3.7	Quality control of plasmids	33
3.4	Working with proteins	33
3.4.1	Protein isolation	33
3.4.2	Evaluation of protein concentration	34
3.4.3	SDS Polyacrylamide gel electrophoresis (SDS-PAGE).....	34
3.4.4	Western blot.....	36
3.4.5	Ponceau S staining.....	36
3.4.6	Detection of proteins	37
3.5	In vivo experiments	37
3.5.1	Xenograft tumors in SCID mice	37
3.5.2	Embedding and sectioning	38
3.5.3	Tissue staining	38
4	Results	43
4.1	Establishing FGFR overexpressing Ba/F3 cell lines	43
4.1.1	Evaluation of purified plasmids.....	43
4.1.2	Transfection of Ba/F3 cells and sorting.....	46
4.1.3	Verification of FGFR overexpressing cells	49
4.2	Inhibition of FGFR4 and its effect on viability	52
4.2.1	IL-3 (in) dependency of Ba/F3 cells	52
4.2.2	Inhibition of FGFR4.....	52
4.3	Viability of FGFR4 overexpressing Ba/F3 cells stimulated with FGF	56
4.4	Impact of Genetic FGFR4 Blockade on the Signaling of Ba/F3 Cells Overexpressing FGFR458	
4.5	Establishing new FGFR overexpressing Ba/F3 cell lines	62

4.6	Signaling of FGFR overexpressing cells induced with FGF	63
4.7	In vivo – SW480, HCT116 and HT29 xenografts	65
5	Discussion	71
5.1	IL-3 (in)dependency of Ba/F3 cells	71
5.2	FGF mediated signaling of transfected Ba/F3 cells	72
5.3	FGFR4 inhibition - PD173074.....	74
5.4	Blockade of FGFR4 by adenoviral constructs	74
5.5	Impact of FGFR4 Blockade on Tumor Growth.....	76
5.6	Summary.....	76
6	Abstract	78
7	Kurzfassung	79
8	Bibliography.....	80
9	Curriculum Vitae.....	88

i. List of figures

Figure 1: <i>Global cancer incidence and mortality rates.</i>	2
Figure 2: <i>Regional distribution of mortality and incidence rates of colorectal cancer cases.</i> ...	3
Figure 3: <i>Colon carcinoma progression and involved tumor suppressors/oncogenes.</i>	4
Figure 4: <i>The 6 Hallmarks of cancer.</i>	5
Figure 5: <i>Emerging Hallmarks and Enabling Characteristics of Cancer.</i>	8
Figure 6: <i>RTK subfamilies.</i>	10
Figure 7: <i>Structure of FGFRs.</i>	11
Figure 8: <i>FGFR downstream signaling.</i>	14
Figure 9: <i>SNP of FGFR4 at position 388 of the transmembrane domain.</i>	19
Figure 10: <i>Design of inhibitory FGFR4 constructs.</i>	27
Figure 11: <i>Design of a western blot.</i>	36
Figure 12: <i>Possible plasmid conformations and their visualization on an agarose-gel</i>	44
Figure 13: <i>Quality control of prepared plasmids.</i>	45
Figure 14: <i>FACS Ba/F3 cells after transfection using an anti-FGFR4 PE-labeled or an anti-FGFR3 APCy surface antibody.</i>	47
Figure 15: <i>FACS plots of newly transfected Ba/F3 cells after 2-3 sorting cycles.</i>	48
Figure 16: <i>Verification of FGFR3IIIb and IIIc expression in BaF3 transfectants using Standard PCR.</i>	50
Figure 17: <i>G388R RFLP of FGFR4-Ba/F3 transfectants.</i>	51
Figure 18: <i>Viability of Ba/F3 cells using different amounts of IL-3.</i>	52
Figure 19: <i>Cell viability of Ba/F3 Gly transfectants treated with TKI PD173074.</i>	54
Figure 20: <i>Adenoviral inhibition of FGFR4.</i>	55
Figure 21: <i>Viability assays of Ba/F3 transfectant cells stimulated with FGF1 and FGF2.</i>	57
Figure 22: <i>Effects of sol4 and dn4 constructs on PLCy1 and S6 signaling.</i>	59
Figure 23: <i>STAT3 and ERK1/2 signaling of virally inhibited Ba/F3 transfectants with or without FGF1.</i>	61
Figure 24: <i>Comparing viability of Ba/F3 cell lines with different IL-3 concentrations.</i>	62
Figure 25: <i>MTT assay of new transfected Ba/F3 cell lines.</i>	63
Figure 26: <i>PLCy1 signaling of Ba/F3 transfectants stimulated with FGF1.</i>	64
Figure 27: <i>S6 and ERK signaling of FGF1 stimulated Ba/F3 transfectants.</i>	65

Figure 28: <i>relative FGFR4 expression of different colon cancer cell lines.</i>	66
Figure 29: <i>In vivo tumor growth of A: HCT116, B: HT29 and C: SW480 infected with co-v, dn4, and sol4.</i>	67
Figure 30: <i>HE and Ki-67 staining of SW480 tumor tissue.</i>	68
Figure 31: <i>HE and Ki-67 staining of HCT116 tumor tissue.</i>	69
Figure 32: <i>Ki-67 stained lungs of the experiment using HCT116 cell line.</i>	70

ii. List of tables

Table 1: <i>FGFs and their receptors.</i>	12
Table 2: <i>Cell lines and their characteristics.</i>	23
Table 3: <i>List of all plasmids and their characteristics.</i>	25
Table 4: <i>Standard primer pairs and their sequences.</i>	29
Table 5: <i>List of TaqMan probes used in this project.</i>	30
Table 6: <i>Pipetting protocol for BSA standard curve.</i>	34
Table 7: <i>Antibodies used in this project.</i>	37
Table 8: <i>Immuno-histological staining antibodies.</i>	39
Table 9: <i>Materials used in this project and their distributors.</i>	42

iii. Abbreviations

μF	micro Farad
μg	microgram
μL	microliter
ALCL	Anaplastic Large Cell Lymphomas
ALK	Anaplastic Lymphoma Kinase
ALT	Alternative Lengthening of Telomeres
APC	Adenomatous Poliposis Coli
APCy	Allophycocyanin
APS	Ammoniumperoxodisulfate
Arg	Cells expressing FGFR4 R388
ATCC	American Type Culture Collection
ATP	Adenosine triphosphate
BAD	Bcl-2-Associated Death promoter
Bcl-2	Basal cell lymphoma-2
Bcl-x _L	Basal cell lymphoma-extra-large
BIM	B-cell lymphoma 2 Interacting Mediator of cell death
BSA	Bovine Serum Albumin
cDNA	complementary DNA
CFP	Cyan-Fluorescence-Protein
cm	centimeter
co-v	control virus
CRC	Colorectal Cancer
ddH ₂ O	double distilled water
DEPC	Diethylpyrocarbonate
DMSO	Dimethyl sulfoxide
dn	dominant negative
dn4	dominant negative FGFR4
DNA	Deoxyribonucleic Acid
ECM	Extracellular Matrix
EDTA	Ethylenediaminetetraacetic Acid
EGFR	Epidermal Growth Factor Receptor
EMT	Epithelial-Mesenchymal Transition
EtOH	Ethanol
FACS	Fluorescence Activated Cell Sorting
FCS	Fetal Calf Serum
FGF	Fibroblast Growth Factor
FGFR	Fibroblast Growth Factor Receptor
FGFR4-Arg	FGFR4 R388
FGFR4-Gly	FGFR4 G388
FRS2	FGFR Substrate 2
g	gramm

GAPDH	Glyceraldehyde 3-Phosphate Dehydrogenase
Gly	Cells expressing FGFR4 G388
GRB2	Growth Factor Receptor Bound 2
h	hour
HCC	Hepatocellular Cancer
HE	Hematoxylin and Eosin
HRP	Horse Radish Peroxidase
HSPG	Heparansulfateproteoglycanes
Ig	Immunoglobulin
IL-3	Interleukin 3
KD (FGFR4-K504M)	Kinase Dead FGFR4
kDa	kilo Dalton
LOH	Loss Of Heterozygosity
MAPK	Mitogen-Activated Protein Kinase
MCL-1	Myeloid Cell Leukaemia-1
MEM	Minimal Essential Media
mg	milligram
min	minutes
mL	milliliter
mM	milimolar
MOI	Multiplicity Of Infection
MT1-MMP	Membrane Type 1 Matrix Metalloproteinase
ng	nanogram
nm	nanometer
nM	nanomolar
NPM	Nucleophosmin
PAGE	Polyacrylamid Gel Electrophoresis
PBS	Phosphate Buffered Saline
PCR	Polymerase Chain Reaction
PDGFRs	Platelet Derived Growth Factor Receptors
PE	Phycoerythrin
Penstrep	Penicillin/Streptomycin
PI3-kinase	Phosphoinositide 3-Kinase
PKB	Protein kinase B
PKC	Protein kinase C
PLCy1	Phospholipase Cy1
PVDF	Polyvinylidene Fluoride
q-PCR	real time quantitative PCR
RB	Retinoblastoma-associated protein
RFLP	Restriction Fragment Length Polymorphism
RMS	Rhabdomyosarcomas
RNA	Ribonucleic Acid
rpm	revolutions per minute
RT	Reverse Transcriptase
RTK	Receptor Tyrosine Kinase

SCID	Severe Combined Immuno-Deficient
SDS	Sodium Dodecyl Sulfate
sec	seconds
SH2	Src Homology 2
SH3	Src Homology 3
SNPs	Single Nucleotide Polymorphisms
sol4	Soluble FGFR4
SOS	Son Of Sevenless
Spry	Sprouty
STAT	Signal Transducers Activators of Transcription
TAE buffer	Tris base, Acetic acid and EDTA buffer
TBS	Tris-Buffered Saline
TBST	TBS containing Tween
TEMED	Tetramethylethylenediamine
TKI	Tyrosine Kinase Inhibitors
TM	Transmembrane
V	Volts
VEGFR	Vascular Endothelial Growth Factor Receptor
WHO	World Health Organization

1 Introduction

1.1 Definition of cancer

Cancer can be defined as a disease “in which abnormal cells divide without control and are able to invade other tissues” (National Cancer Institute, 07.03.2014). Although this seems to be a simple definition, there are more than 100 different types of this disease. Cancer is usually grouped into categories, based on the organ or cell type they originate from. Carcinomas (from the greek word karkinos – growth) develop from cells lining inner or outer surfaces of the body. Sarcoma (from the greek word sarx for flesh) begins in cells originating from the mesenchyme, like muscle, bones or fat tissue. Another type is called leukemia, a group of cancers that develop in the bone marrow which can cause high numbers of abnormal blood cells. Both lymphoma and myeloma describe cancers that arise from cells of the immune system. The last group harbors central nervous system cancers, which originate from the tissues of brain or spinal cord (National-Cancer-Institute 2014).

1.2 Epidemiology

1.2.1 Cancer epidemiology

The World Health Organization (WHO) reports, that in 2012 32.6 million people were living with cancer and that 8.2 million died because of cancer which makes it one of the leading causes of death worldwide. Figure 1 shows incidence and mortality rates of men/women clustered into regions. In developed countries, incidence rates are much higher compared to less developed countries, but there is less regional variation of the mortality rates. The cancer incidence rate is about 25% higher in males than females, although these rates can vary more than five-fold in different regions. The most prominent driver of higher incidence rates in males is prostate cancer (WHO, 2014).

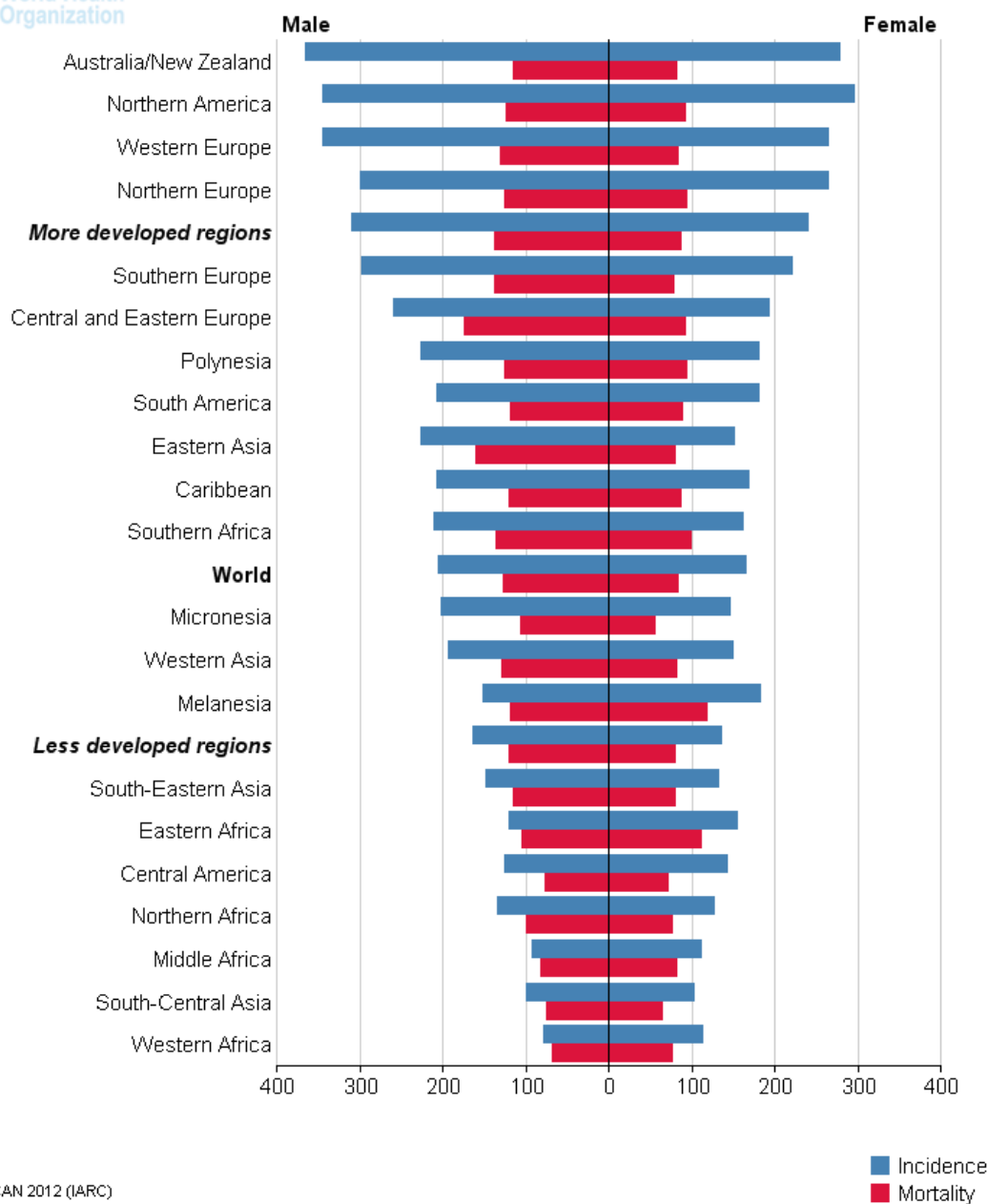


Figure 1: Global cancer incidence and mortality rates. Estimated age-standardized rates per 100000 (Globocan 2012).

Lung cancer is the leading cause of death for men, followed by liver, stomach and colorectal cancer (CRC) whereas for women it is breast, lung, colorectal and cervix cancer (WHO, Globocan 2012).

1.2.2 Epidemiology of Colorectal Cancer

CRC is the second most common cancer in women and the third in men. In 2012, there were more than 1.3 million cases of CRC. The highest incidence rates were observed in Australia/New Zealand, Europe and Northern America. Rates were lowest in Africa and South-Central Asia (figure 2). More than 690.000 people died because of CRC in 2012, accounting for 8.5% of all cancer deaths (WHO, Globocan 2012).

International Agency for Research on Cancer Colorectum: both sexes, all ages

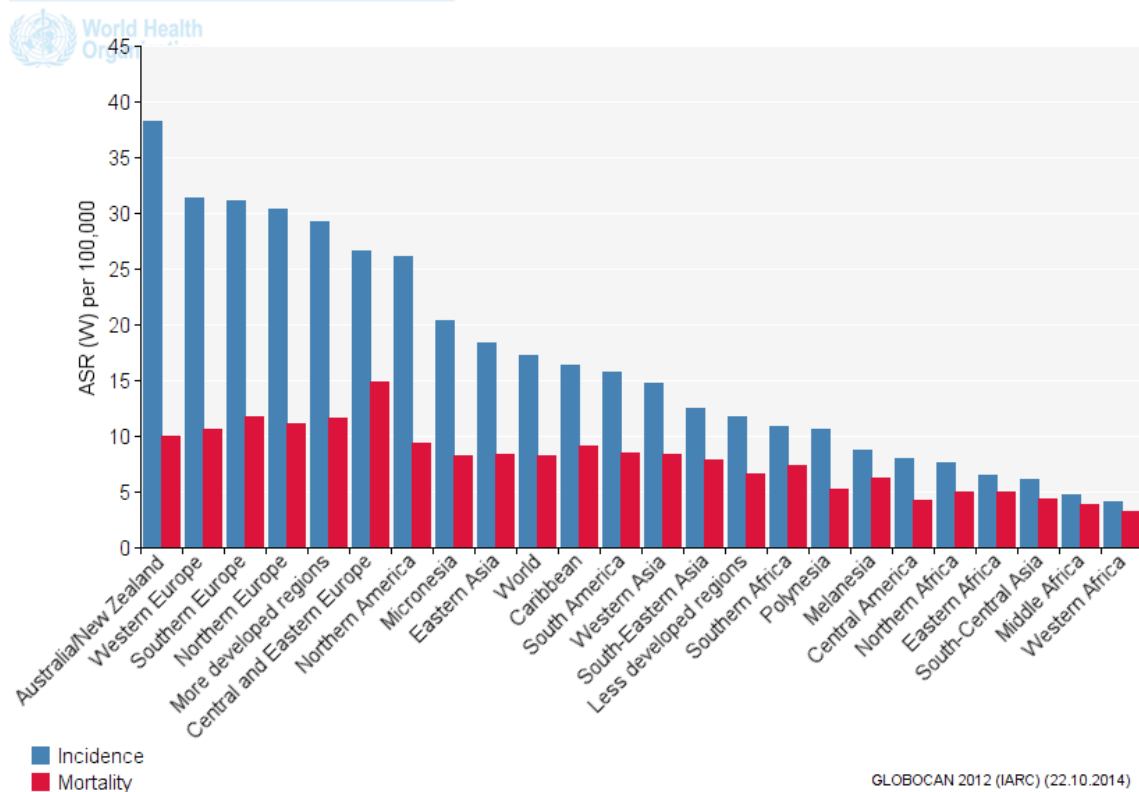


Figure 2: Regional distribution of mortality and incidence rates of colorectal cancer cases (Globocan 2012).

1.3 Tumorigenesis of Colon Cancer

A normal cell can acquire cancerous attributes through a process called tumor progression. This process usually takes place at many sites in the body but rarely develops into a clinically detectable tumor. The drivers of tumor progression are random mutations and epigenetic

changes that affect genes regulating cell proliferation, survival or genetic stability to mention just a few (Weinberg 2007).

Epidemiology studies have shown that age plays an important role in tumor progression. For example, the risk of colon cancer in the USA is more than 1000 times larger for a 70 year old man than for a 10 year old boy (Weinberg 2007). This fact was found for many other tumors as well, which indicates that tumor progression is a multistep process that takes decades to develop (Armitage and Doll 1954, Boland and Ricciardiello 1999, Hanahan and Weinberg 2011).

The link between multiple genetic alterations and the resulting phenotype is best documented for colon cancer. Because this disease is relatively common in Western industrialized countries and the colon epithelium is easily accessible via colonoscopy, tissue samples have been collected from many different stages (Weinberg 2007).

In 1989, Vogelstein et al investigated the genomes of differently sized tumors originating from the colon. They hypothesized, that tumor progression should lead to increased tumor size and accumulation of mutations. Vogelstein et al. discovered that many early stage adenomas showed a loss of heterozygosity (LOH) in the long arm of chromosome 5. About half of the slightly larger tumors carried in addition a mutated K-Ras oncogene and even larger adenomas also suffered from LOH on chromosomes 17 and 18 (Vogelstein, Fearon et al. 1989).

Soon after this remarkable discoveries, the genes lost due to LOH on chromosom 5 and 18 were identified as adenomatous poliposis coli (APC) and p53 tumor suppressor genes.

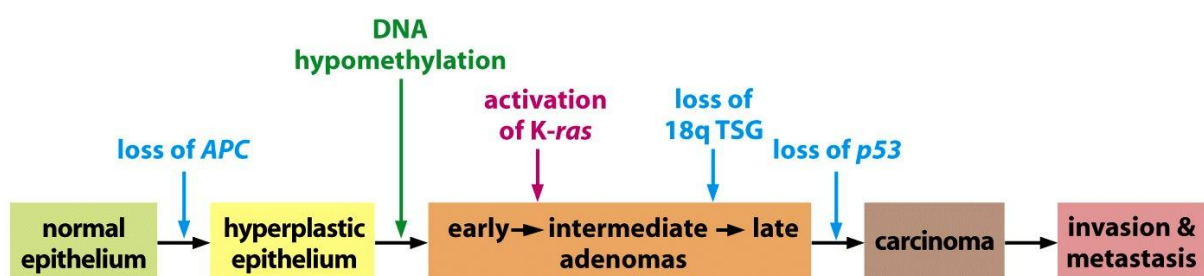


Figure 3: *Colon carcinoma progression and involved tumor suppressors/oncogenes (Weinberg 2007).*

Figure 3 depicts a possible route of tumor progression from normal to cancer cells capable of sustained growth and metastasis. About 90% of all colon carcinomas suffer from loss of APC,

which seems to be an early step in this process. However, only 40 to 50% develop an activating mutation of K-Ras and 50 to 70% acquire a LOH of p53 which indicates that after loss of APC, cancer cells are not restricted on a specific genetic path to evolve towards fully malignant tumors (Weinberg 2007).

1.4 Hallmarks of Cancer

In order to create an organizing principle to explain the complexities of neoplastic disease, Hanahan and Weinberg defined 6 hallmarks, 2 emerging hallmarks and 2 enabling characteristics of cancer which contribute to tumorigenesis (figure 4).

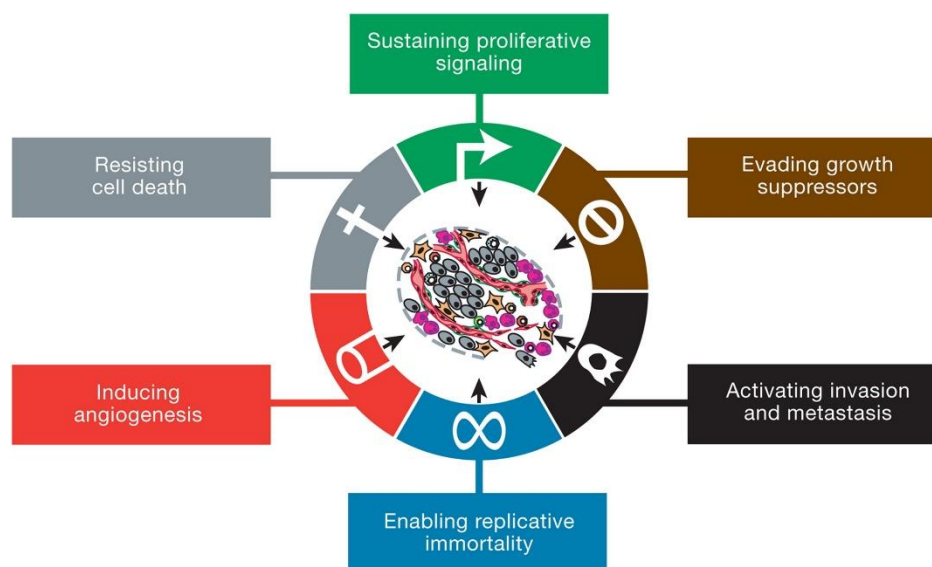


Figure 4: *The 6 Hallmarks of cancer (Hanahan and Weinberg 2011).*

1.4.1 Permanent Proliferation

Cell number homeostasis is crucial to retain normal tissue architecture and function. One of the most prominent characteristics of cancer cells is their ability of chronic proliferation. There are many alternative ways to ensure permanent cell division (Hanahan and Weinberg 2011). Cancer cells can produce ligands for their growth factor receptors either themselves or stimulate tumor-associated stroma to supply them with growth factors (Bhowmick, Neilson et al. 2004, Cheng, Chytil et al. 2008). Moreover, elevation of receptor protein levels can increase the sensitivity of a cell towards growth factors, which has been shown for fibroblast growth factor receptors (FGFRs). Alternatively, mutations in growth factor receptors can lead to permanent activation (Kunii, Davis et al. 2008, Haugsten, Wiedlocha et al. 2010). Growth

factor receptor dependent signaling can also be activated by mutations of downstream signaling proteins like Ras, Raf and phosphoinositide 3-kinase (PI3-kinase) (Shaw and Cantley 2006, Jiang and Liu 2009, Davies and Samuels 2010).

1.4.2 Evading Growth Suppressors

For a cancer cell, being able to evade growth suppressors is also important. Many mediators that negatively regulate cell growth and proliferation are encoded by tumor suppressor genes. Two prominent examples are the retinoblastoma-associated (RB) and p53 proteins which are mutated or missing in many cancers. In response to extracellular signals, RB protein can arrest or drive cell cycle. In contrast, p53 integrates intracellular signals and can trigger cell cycle arrest or under extreme situations apoptosis. Contact inhibition is another important way to trigger growth suppression (Hanahan and Weinberg 2011).

1.4.3 Resisting Apoptosis

Another crucial point in tumorigenesis is the feature to resist programmed cell death or apoptosis. Apoptosis can be triggered by 2 main pathways, extrinsically when so-called death receptors are activated by their ligands or intrinsically induced by intracellular stress. The latter is regulated by proteins of the anti-apoptotic basal cell lymphoma-2 (Bcl-2) family and pro-apoptotic Bcl-2 binding proteins (for examples Bax, Bak). Activation of either one of the 2 main pathways results in activation of caspases and ultimately to cell death (Adams and Cory 2007). One way to circumvent programmed cell death is the loss of the damage sensor and tumor suppressor p53. The same outcome could be achieved by overexpression of anti-apoptotic factors (e.g. members of the Bcl-2 family) or survival signals, for example due to FGFR signaling. Alternatively, apoptosis can be avoided by down regulation of proapoptotic factors (Bax, Bak) or by interruption of the ligand dependent death receptor pathway (Weinberg 2007, Heinzle, Sutterluty et al. 2011). In contrast, autophagy enables cells to survive starvation and stress by removal of damaged proteins and organelles. This means, that although this mechanism has tumor suppressor properties, it can potentially enable cancer cells to survive extreme situations like starvation or drug treatment in a dormancy like state (White and DiPaola 2009).

1.4.4 Immortalization

The end of chromosomes consists of tandem repeats that protect them from end-to-end joining. Upon cell division, these repeats or telomeres are shortened. This shortening is viewed as a “molecular clock”, loss of the protective telomeres drives cells into either senescence – viable but non-proliferating - or crisis/apoptosis and ensures tissue homeostasis and function. Because cancer cells usually show high proliferation rates, they have to achieve replicative immortality in order to propagate. About 90% of all tumor cells show telomerase activity, the rest of them are enabled to divide infinite number of times by a mechanism called alternative lengthening of telomeres (ALT). It has been proposed, that the majority of cancer cells suffer from genomic instability due to shortened telomeres which also increase their mutational potential before rescued by induced telomerase activity (Blasco 2005).

1.4.5 Neo-Angiogenesis

The nourishment of tumors as well as the cleansing away of carbon dioxide and other metabolic products is ensured by blood vessels. In normal tissue, sprouting of new vessels from existing ones is a rare process and is only transiently activated for processes like wound healing or female reproductive cycling (Klagsbrun and D'Amore 1991). In tumorigenesis, cancer cells influence surrounding tissues in various ways, resulting in neo-angiogenesis and thereby ensuring tumor growth and progression (Hanahan and Folkman 1996). Recent studies have demonstrated, that angiogenesis can be regulated through cell surface receptors and their ligands, for example vascular endothelial growth factor receptor (VEGFR) signaling of vascular endothelial cells (Weinberg 2007). Besides VEGFR, FGF signaling via FGFRs seems to play an additional important role in angiogenesis. FGFs can activate essential angiogenesis pathways in endothelial cells and FGFR inhibitors are tested as anti-angiogenic drugs (Heinzle, Sutterluty et al. 2011).

1.4.6 Invasion and Metastasis

Cell-to-cell and cell-to-extracellular matrix (ECM) contacts play an important role in tissue architecture and function. E-cadherin is a prominent example for a cell-to-cell adhesion molecule. Overexpression of E-cadherin is known to suppress invasion and metastasis, reduced expression favors these phenotypes (Berx and van Roy 2009). In addition to E-

cadherin, other adhesion and contact molecules showed altered expression in many invasive tumors. N-cadherin, for example, is usually expressed early stages of development in migrating cells like neurons or mesenchymal cells, but also up regulated in many aggressive cancer cells (Cavallaro and Christofori 2004). Epithelial-mesenchymal transition (EMT) refers to a regulatory program of cells which makes them capable of increased motility, invading surrounding tissue and resisting programmed cell death. By acquiring EMT, cancer cells are enabled to invade and metastasize (Polyak and Weinberg 2009). Various studies observed EMT related migration of cancer cells stimulated with FGF. FGFR1 signaling can lead to an invasive phenotype in mouse epithelial cells and the single nucleotide polymorphism (SNP) variant FGFR4-Arg can stimulate cell migration (Heinzle, Sutterluty et al. 2011). Beside alterations of cancer cells themselves, crosstalk and composition of the surrounding tumor stroma seems to be an important factor for invasiveness and tumor progression (Weinberg 2007).

1.4.7 Enabling Characteristic - Mutations and Genome Instability

Besides the 6 Hallmarks, Hanahan and Weinberg also describe 2 emerging Hallmarks and 2 enabling characteristics, which all contribute to tumorigenesis (figure 5)

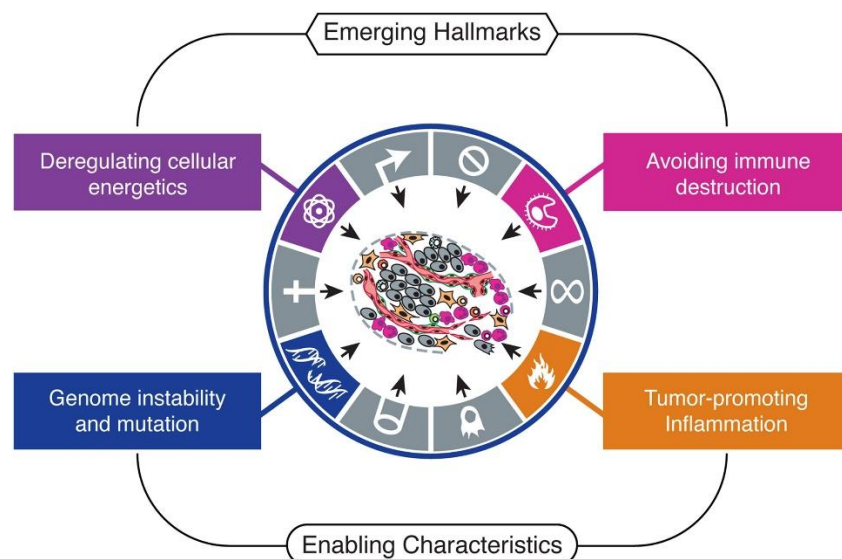


Figure 5: *Emerging Hallmarks and Enabling Characteristics of Cancer (Hanahan and Weinberg 2011).*

Acquiring hallmarks described above depends almost always on alterations of cancer cell genomes, allowing selection of neoplastic cells that can outgrow their environment.

Epigenetic changes are one possibility to change the genome and its stability. Back in 1983, Feinberg and Vogelstein compared normal and tumor tissue and found low level of CpG methylation for the latter (Feinberg and Vogelstein 1983). Recent studies strongly indicate, that a combination of both hypomethylation of oncogenes like Wnt and hypermethylation of tumor suppressors, for example APC plays an important role in multi-step tumorigenesis (Hammoud, Cairns et al. 2013). Besides epigenetic changes, defects in the DNA maintenance machinery can lead to undetected or unrepaired DNA damage as well as to increased sensitivity towards mutagenic agents. Moreover, karyotype and chromosomal deletions are often observed in different tumors and as a consequence of shortened telomeres in early tumor stages (see 1.4.4 *Immortalization*) (Weinberg 2007).

1.4.8 Enabling Characteristic - Inflammation

The vast majority of solid tumors are surrounded by a large variety of immune cells. There are contradictory reports whether this reflects an anti-tumor reaction of the immune system or is a result of subversive stimulation of the tumor. However, recent studies strongly indicate that the resulting inflammation supplies the tumor microenvironment with growth, survival, pro-angiogenic factors as well as matrix modifying enzymes and signals that can initiate EMT (Grivennikov and Karin 2010).

1.4.9 Emerging Hallmark - Altered Energy Metabolism

High proliferation rates together with hypoxia and other factors affect the energy metabolism of cancer cells. In the presence of oxygen, cancer cells can reprogram their metabolic functions to so-called aerobic glycolysis. This metabolic program is characterized by a ~18-fold lower efficiency of adenosine triphosphate (ATP) production compared to mitochondrial ATP synthesis. Tumors benefit from various glycolysis intermediates, allowing them to synthesize large amounts of nucleosides and amino acids and thereby enable high proliferation rates (Weinberg 2007).

1.4.10 Emerging Hallmark - Evading the Immune System

The immune system plays an important role in antagonizing tumor formation. Higher cancer incident rates for viral-associated forms of cancer in immune compromised persons reflect

the obvious anti-viral role of the immune system (Weinberg 2007). Besides, experiments with engineered mice showed, that animals with deficiencies in CD8⁺ cytotoxic t-lymphocytes, CD4⁺ T cells or natural killer cells showed elevated tumor incidence when treated with carcinogens (Kim, Emi et al. 2007, Teng, Swann et al. 2008). An increasing body of evidence suggests various interactions between cancer cells and the immune system. Function of immune-cells can be impaired by immunosuppressive factors, either secreted by the tumor or cells of the inflammatory stroma (Weinberg 2007).

1.5 Receptor Tyrosine Kinases

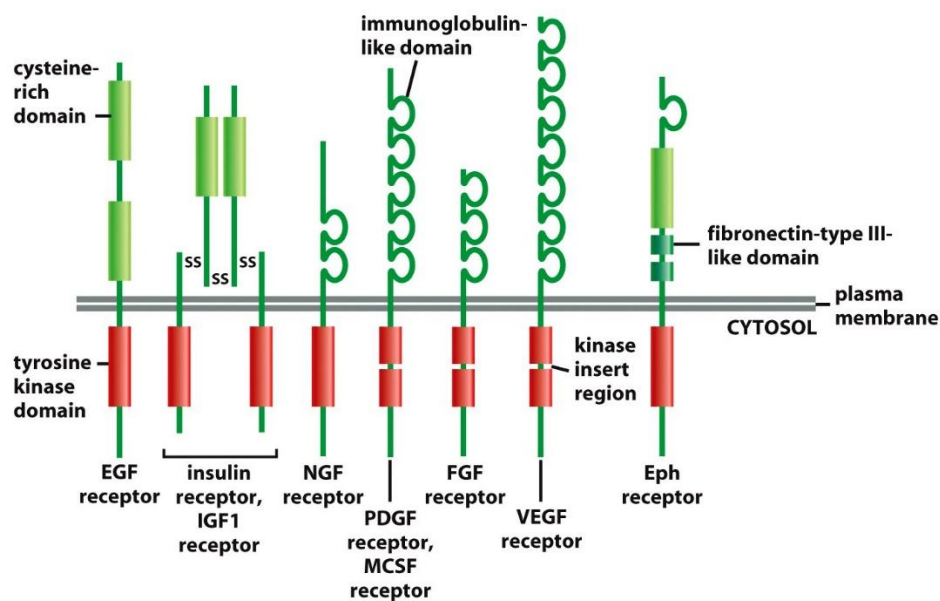


Figure 6: RTK subfamilies. Only 1 or 2 members of each subfamily are shown. The kinase domains of some of the RTKs are split (Alberts 2008).

There are 58 genes encoding receptor tyrosine kinases (RTKs) which can be assigned to 20 structural families (figure 6). They consist of an extracellular, a transmembrane and an intracellular domain. Upon ligand binding to the extracellular domain, two RTKs dimerize, bringing the kinase domains in close proximity. Next, adjacent kinase domains phosphorylate each other on various tyrosines, a mechanism referred to as transautophosphorylation. Phosphorylated tyrosines can act as binding sites for many different signaling proteins. After binding, those signal molecules are activated either by phosphorylation or via induced conformational changes. In many cases, binding to the phosphorylation scaffold and close proximity to the protein next in the signaling cascade is sufficient for downstream signaling.

RTKs and its signaling through ligands can activate numerous downstream signaling pathways, regulating important functions including cell survival, proliferation and migration (Alberts 2008).

1.6 Fibroblast Growth Factor Receptors

1.6.1 Structure

Important members of the RTK family are the FGFRs, regulating cellular functions like embryogenesis, cell survival, proliferation and neoangiogenesis. There are four FGFR genes consisting of up to 20 exons and encoding FGFR1-4. The resulting proteins are composed of an extracellular FGF binding, a single-pass transmembrane and an intracellular kinase domain (figure 7).

The extracellular domain of a typical FGFR consists of three immunoglobulin (Ig)-like loops (IgI, IgII and IgIII). The linker between IgI and IgII comprises a 4-8 amino acids long stretch and is referred to as acidic box (AB). IgI and linker containing the AB have auto-inhibitory functions but do not contribute to FGF binding (Olsen, Ibrahimi et al. 2004). Instead, FGFs can bind to a pocket formed by IgII and IgIII whereby this complex is stabilized by heparin. Diversity of FGFR is achieved by varying ligand specificity but also by alternative splicing. One example is splicing of IgIII to IgIIIb or IgIIIc isoforms of FGFR1-3, which happens in a tissue specific manner. IIIb is predominantly expressed in epithelial tissues, whereas IIIc is usually found in mesenchymal tissues (Beenken and Mohammadi 2009, Turner and Grose 2010).

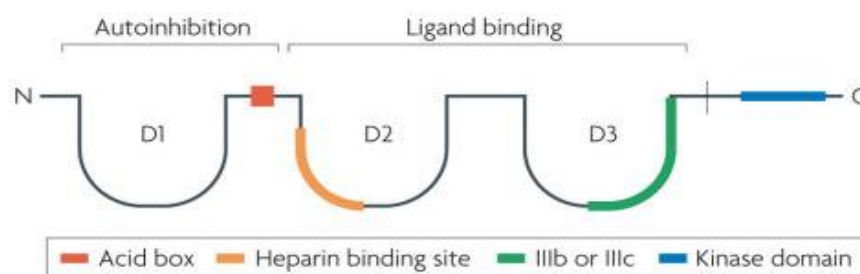


Figure 7: Structure of FGFRs. D2 (IgII) and D3 (IgIII) bind specific FGFs which leads to dimerization and autophosphorylation. For FGFR1-3, the lower part of D3 (green) is spliced to either FGFRIIIb or IIIc, which affects ligand specificity (Beenken and Mohammadi 2009).

1.6.2 Interaction between FGFR and FGF

There are 18 FGFs that contribute to FGFR signaling. They can be distributed to two different subgroups: hormone like FGFs (FGF 19, FGF21 and FGF23) and canonical FGFs. The latter can further be divided into five different groups: FGF1- (FGF1, FGF2), FGF4- (FGF4, FGF5, FGF6), FGF7- (FGF3, FGF7, FGF10, FGF22), FGF8- (FGF8, FGF17, FGF18) and FGF9-group (FGF9, FGF16, FGF20). All FGFs with the exception of FGF group 1 are secreted, the latter is only released upon cell death. For a detailed list of FGFs and their receptor affinities see table 1.

Receptor	Ligands
FGFR1-IIIb	FGF1, FGF2, FGF3, FGF10, FGF22
FGFR1-IIIc	FGF1, FGF2, FGF4, FGF5, FGF6, FGF8, FGF9, FGF16, FGF17, FGF18, FGF20, FGF21, FGF23
FGFR2-IIIb	FGF1, FGF3, FGF7, FGF10, FGF22
FGFR2-IIIc	FGF1, FGF2, FGF4, FGF5, FGF6, FGF8, FGF9, FGF16, FGF17, FGF18, FGF20, FGF21, FGF23
FGFR3-IIIb	FGF1, FGF9, FGF16
FGFR3-IIIc	FGF1, FGF2, FGF4, FGF5, FGF6, FGF8, FGF9, FGF16, FGF17, FGF18, FGF20, FGF21
FGFR4	FGF1, FGF2, FGF4, FGF5, FGF6, FGF8, FGF9, FGF16, FGF17, FGF18, FGF19, FGF20, FGF21, FGF23

Table 1: *FGFs and their receptors (Heinzle, Sutterluty et al. 2011).*

After canonical FGFs are secreted or released from decaying cells, they are stored in the ECM based on their affinity for heparansulfateproteoglycans (HSPG), an abundant molecule in this microenvironment. Upon proteolytic cleavage or action of FGF binding proteins, FGFs are released and able to activate FGFR signaling by binding to a specific receptor (Heinzle, Sutterluty et al. 2011). Although FGFs show high affinity for FGFRs, HSPG and its analogue heparin can increase this affinity by more than 10-fold (Ibrahimi, Zhang et al. 2004). Thereby, heparin is obligatory for FGF mediated signaling by binding to both FGF and FGFR, forming a ternary complex. Two of those complexes are able to dimerize, bringing the intracellular kinase domains in close proximity leading to conformational changes, transphosphorylation and downstream signaling (Schlessinger, Plotnikov et al. 2000).

1.6.3 FGFR downstream signaling

After dimerization and phosphorylation, tyrosine residues of the kinase domains function as binding sites for adaptor proteins. Those adaptor or scaffold proteins can be phosphorylated by the activated FGFR, resulting in the activation of various downstream signaling pathways (figure 8). FGFR substrate 2 (FRS2) is one of the main adaptors, binding almost exclusively to FGFR. It binds to FGFR close to the membrane via its phosphotyrosine binding (PTB) domain and upon activation recruits Src homology 2 (SH2) domain of growth factor receptor bound 2 (GRB2) which in turn binds son of sevenless (SOS). The latter activates Ras and its downstream pathways, including mitogen-activated protein kinase (MAPK) and PI3K/Akt pathway. Recruitment of GAB1 by GRB2 via Src homology 3 (SH3) domain leads to Ras-independent PI3K activation (Knights and Cook 2010, Turner and Grose 2010).

Another main substrate for FGFR is phospholipase C γ (PLC γ) which binds close to the carboxyl terminus via its SH2 domain. When phosphorylated, PLC γ activates protein kinase C (PKC) which in turn elevates MAPK pathway signaling by phosphorylating Raf (Turner and Grose 2010).

Moreover, experiments using cells overexpressing FGFRs 1, 3 and 4 showed activation of the signal transducers activators of transcription (STAT) downstream of the receptor (Heinzle, Sutterluty et al. 2011).

Activation of MAPK and PI3K pathways promote cell survival and cell cycle progression. In the MAPK pathway, ERK1/2 can cause degradation of pro-death protein B-cell lymphoma 2 interacting mediator of cell death (BIM) (Ley, Balmano et al. 2003) whilst protein kinase B (PKB) of the PI3K pathway can decrease intracellular levels of pro-apoptotic protein Bcl-2-associated death promoter (BAD) (Datta, Dudek et al. 1997). In addition, both pathways can also activate pro-survival pathways by elevating protein levels of basal cell lymphoma-extra-large (Bcl-x_L) and myeloid cell leukaemia-1 (MCL-1) (Balmano and Cook 2009).

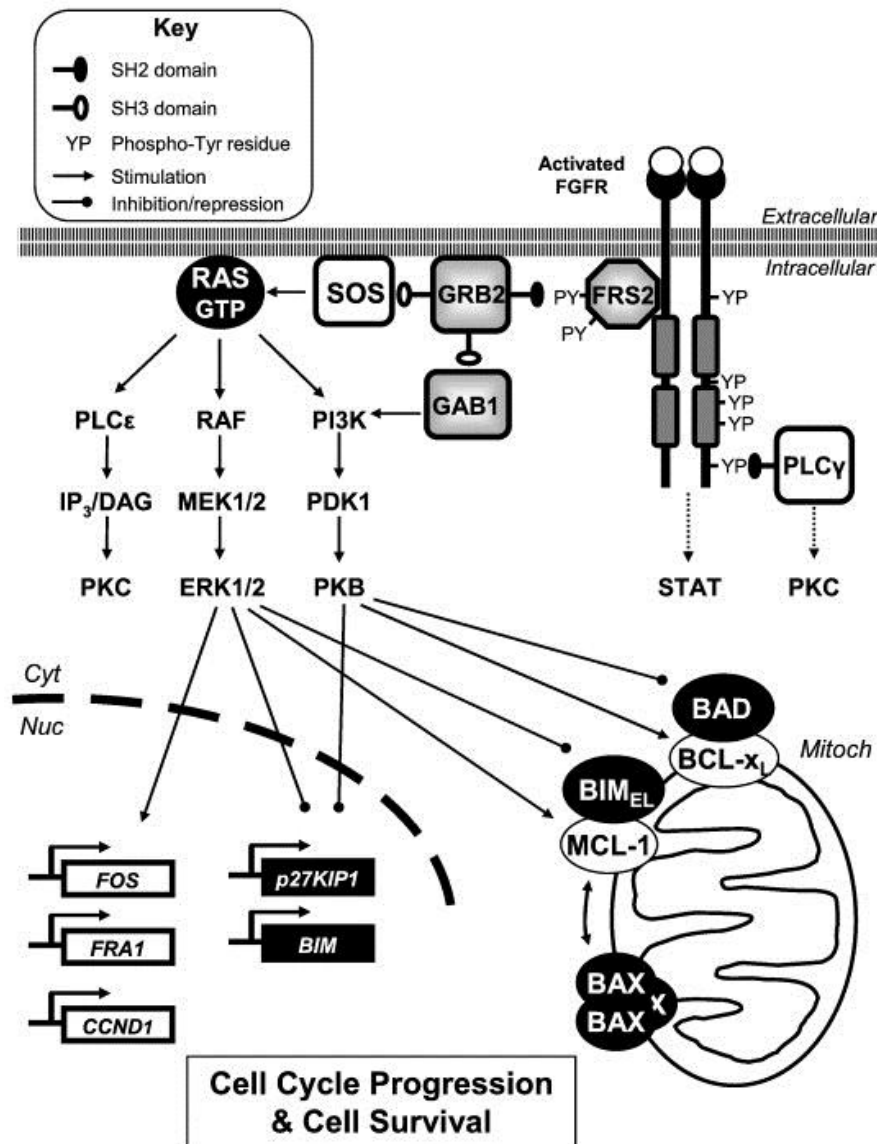


Figure 8: FGFR downstream signaling (Knights and Cook 2010).

1.6.4 Termination of FGFR signaling

In healthy cells, activation of FGFRs and their downstream targets goes hand in hand with initiation of negative feedback loops and mechanisms to regulate duration and intensity of the signal. One of the most important negative regulators of FGF signaling are Sprouty (Spry) proteins. They are expressed in response to FGF signaling, although the exact inhibitory mechanism remains unclear (Heinzle, Sutterluty et al. 2011). Other regulators are MAPK phosphatases or proteins of the Sef family, both inhibiting ERK phosphorylation (Turner and Grose 2010). Autoinhibition is another way to prevent uncontrolled FGF signaling. A compelling body of evidence suggests, that the alternatively spliced Ig1 together with the AB

domain electrostatically engages the heparin binding site on IgII and thereby inhibiting FGF binding (Kalinina, Dutta et al. 2012). Overexpression of co-receptor of FGFR – klotho- β – seems to be another strategy to inhibit FGFR signaling, as previously shown for FGFR4 (Poh, Wong et al. 2012). Similar to other RTKs, FGFRs and their signaling can be attenuated by receptor internalization and subsequent degradation (Heinzle, Sutterluty et al. 2011).

1.6.5 Deregulation of FGFR-signaling in cancer

Deregulated FGFR signaling can communicate a powerful combination of increased proliferation, survival, migration and neoangiogenesis, which all contribute to the Hallmarks of cancer. Therefore, it is not surprising that FGF signaling plays an important role in tumorigenesis once its regulatory mechanisms fail (Heinzle, Sutterluty et al. 2011).

Amplification of FGFR genes, as most commonly observed for FGFR 1-2, leads to increased sensitivity towards their ligands and finally to stimulation of cell growth (Heinzle, Sutterluty et al. 2011). Alternatively, FGFR gene translocation under the control of strong promoters result in FGFR overexpression and thereby deregulation of FGF signaling (Avet-Loiseau, Facon et al. 1999).

SNPs are able to alter FGFR activity and/or function impacting on cancer risk and aggressiveness. So far, the best studied SNP for FGFRs results in a glycine to arginine substitution at position 388 of the transmembrane domain of FGFR4 (Haugsten, Wiedlocha et al. 2010). The FGFR4-Arg isoform is related to increased migratory behavior and more aggressive tumors as observed, for example, for tumors of breast, prostate and colon (Bange, Prechtel et al. 2002, Wang, Stockton et al. 2004, Spinola, Leoni et al. 2005, Heinzle, Gsur et al. 2012).

Splicing of FGFR1-3 happens in a tissue specific manner, as described above. In cancer cells, switching of IIIb to IIIc enables a cell to be stimulated by factors intended to activate the mesenchyme, contributing to tumorigenesis (Yan, Fukabori et al. 1993, Carstens, Eaton et al. 1997). FGFR2IIIb variants are characterized by anti-tumorigenic attributes, which is converted to pro-tumorigenic by switching to IIIc (Ricol, Cappellen et al. 1999). Experiments with CRC cells showed, that Inhibition of FGFRIIIc decreased growth as well as survival and blocked migration (Sonvilla, Allerstorfer et al. 2010).

Enhanced autocrine stimulation by FGFs is a common characteristic of malignancies. Overexpression of FGF2, for example, has been observed in breast or lung cancer (Berger, Setinek et al. 1999, Smith, Fox et al. 1999). Besides, there are reports about autocrine loops fueled by FGF5 in lung, esophagus, prostate and colon cancers (Hanada, Perry-Lalley et al. 2001). The latter is also commonly influenced by overexpression of FGF18 stimulating FGFR3IIIc (Sonvilla, Allerstorfer et al. 2010) and FGF19 mediated FGFR4 activity (Desnoyers, Pai et al. 2008).

Deregulation of signal termination is another effective way to alter FGF signaling. Decreased Spry expression is linked to tumorigenesis and has been observed for many tumors, for example lung (Sutterluty, Mayer et al. 2007), prostate (Kwabi-Addo, Wang et al. 2004), breast (Lo, Yusoff et al. 2004) and liver cancer (Fong, Chua et al. 2006). In addition, disruption of ubiquitinating proteins like c-Cbl or mutated ubiquitination sites on FGFRs can cause prolonged FGF signaling or recycling of the receptor instead of degradation (Cho, Guo et al. 2004).

1.7 Fibroblast Growth Factor Receptor 4

So far, FGFR4 is the least studied FGFR. In contrast to FGFR1-3, there are no splicing variants of IgIII that can effect ligand specificities as described above. Moreover, knockout of FGFR4 does not result in an embryonic lethal phenotype in mice. In addition, IC_{50} values of small inhibitors targeting FGFRs for FGFR4 are multiples of FGFR1-3, suggesting differences in its kinase domains (Heinzle, Erdem et al. 2014).

1.7.1 Structure of FGFR4

The FGFR4 gene spans more than 11kb on chromosome 5q. GeneBank lists two different full-length entries of FGFR4 consisting of 762 and 802 amino acids. In the absence of alternative splicing of the Ig-loop III FGF binding characteristics are very similar to those of IIIc receptors (table 1) (Heinzle, Erdem et al. 2014). In addition to FGF1 and FGF2, FGFR4 ligands include members of FGF4, FGF8 and hormonal FGF19 subfamilies (Zhang, Ibrahimi et al. 2006). Alternative splicing of FGFR4 may result in soluble FGFR4 (sol4) variants that contribute to negative regulation of FGFR4 signaling (Ezzat, Zheng et al. 2001), either by functioning as

ligand traps, cause non-functional dimerization (Vorlova, Rocco et al. 2011) or auto-inhibition (Kalinina, Dutta et al. 2012).

1.7.2 Physiological role of FGFR4

FGFR3 and FGFR4 are both the highest expressed FGFRs in mouse pre-implantation stage (Rappolee, Patel et al. 1998). In addition, studies showed an increase in FGFR4 expression until day E14-E15 before they begin to attenuate (Korhonen, Partanen et al. 1992). FGFR4 expression was observed during organogenesis in muscles, liver, the gut, pancreatic ducts, lungs and kidney but not in the brain or the spinal cord (Stark, McMahon et al. 1991, Korhonen, Partanen et al. 1992, Rappolee, Patel et al. 1998). Nonetheless, knockout of the FGFR4 gene did not cause any developmental abnormalities, but induced changes in the cholesterol metabolism of adult mice (Yu, Wang et al. 2000).

Recent studies suggest, that muscle cell differentiation and regeneration is mainly regulated by FGFR1IIIc as well as FGFR4 and stimulated via FGF6 (Armand, Laziz et al. 2006). In regenerating muscles, FGF6 induces FGFR 1 down regulation while at the same time enhances FGFR4 expression, leading to de-differentiation (Armand, Launay et al. 2003).

Another interesting feature of FGFR4 is its stimulation – all members of the hormone-like subfamily (FGF19, FGF21 and FGF23) show high mitogenic activity for this receptor (Zhang, Ibrahimi et al. 2006). The rather low activation potential of this subfamily is compensated by co-receptors consisting of klotho proteins, which boost hormone-like FGF mediated signaling (Heinzle, Erdem et al. 2014). Experiments with mice showed, that the interplay between FGF19 and FGFR4 seems also essential for regulating the cholesterol metabolism (Yu, Wang et al. 2000), filling of the gallbladder (Choi, Moschetta et al. 2006) and tissue homeostasis in the liver (Yu, Wang et al. 2002).

1.7.3 FGFR4 and cancer

Mutated FGFR4 is a potential candidate oncogene. Alterations in this gene have been observed in embryonic rhabdomyosarcomas (RMS) which correlated with more aggressive tumors (Taylor, Cheuk et al. 2009, Shukla, Ameer et al. 2012). The underlying mechanism was traced back to activating mutations in the kinase domains of FGFR4, strongly inducing downstream STAT3, while attenuating ERK and Akt signaling (Taylor, Cheuk et al. 2009). In

addition, mutations in the extracellular or transmembrane domain can result in altered FGFR4 signaling, for example ligand-independent dimerization through disulfide bonds (Roidl, Foo et al. 2010, Heinzle, Erdem et al. 2014).

Similar to FGFR1-3, upregulation of FGFR4 or its ligands seems to play an important role in multiple tumor types, for example liver, RMS, breast, prostate, thyroid, and colon cancer. The interplay between FGFR4 and FGF19 is best characterized in tumors of the liver as well as the colon (Heinzle, Erdem et al. 2014). In vitro studies with colon cancer cells showed, that inhibition of FGFR4 resulted in reduced proliferation and migration (Heinzle, Gsur et al. 2012).

1.7.4 SNP of FGFR4 at position G388R

The discovery of the SNP at position G388R in the transmembrane domain of FGFR4 (figure 9) by Axel Ulrich and his group moved FGFR4 into the focus of interest. Glycine at position 388 was found in the majority (about 60%) of the population, the wild-type FGFR4 is referred to as FGFR4-Gly. About 30% of the population are heterozygous for the Gly/Arg allele, while approximately 10% are FGFR4-Arg homozygous (Bange, Prechtel et al. 2002).

Similar mutations on other RTKs are correlated with increased kinase activities or prolonged signaling due to slowed receptor internalization. The role of FGFR4-Arg seems to be more subtle. This is reflected by many contradictory reports about the role of FGFR4-Arg in various tumors. Some studies found evidence for increased aggressiveness and tumor progression for patients hetero- or homozygous for FGFR4-Arg, others failed to detect any impact. In vitro studies with cell lines derived from breast, prostate and colon cancer showed increased migration and invasion when overexpressing FGFR4-Arg (Heinzle, Erdem et al. 2014). Expression of FGFR4-Gly in FGFR-Arg expressing colon cancer cells attenuated migration (Heinzle, Gsur et al. 2012).

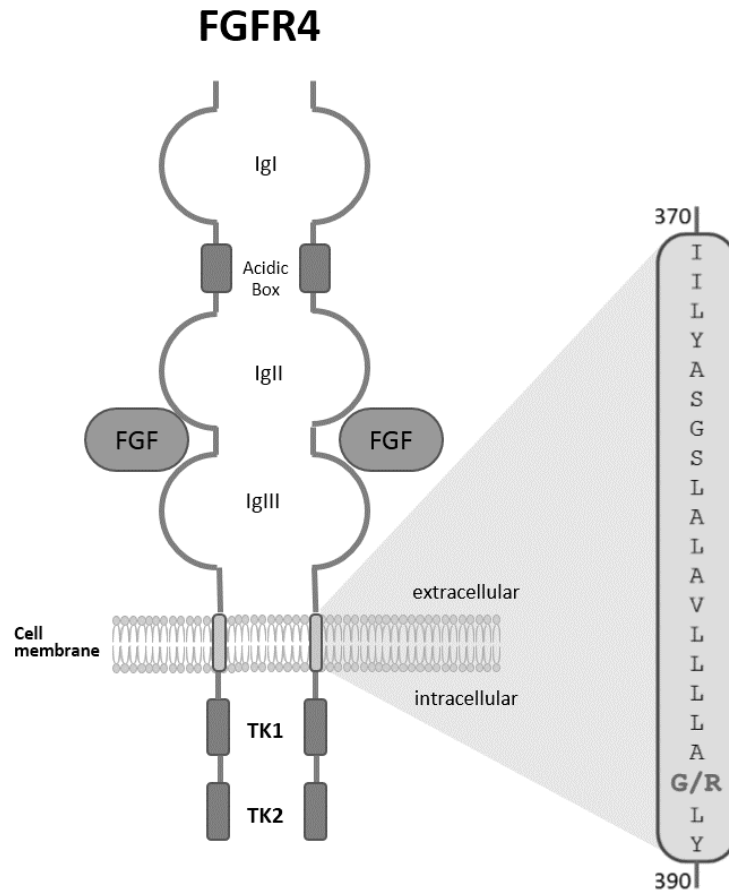


Figure 9: *SNP of FGFR4 at position 388 of the transmembrane domain (Heinzle, Erdem et al. 2014).*

The mechanism behind FGFR4-Arg and its correlation with increased motility is unclear. It seems possible, that the altered amino acid in the transmembrane domain results in a more stable receptor with prolonged signaling or an increased kinase domain activity (Wang, Stockton et al. 2004, Wang, Yu et al. 2008). Sugiyama et al showed, that FGFR4-Arg reduced lysosomal degradation of membrane type 1 matrix metalloproteinase (MT1-MMP) thereby stabilizing this metastasis enhancing protein. In addition, prolonged MT1-MMP activity increased FGFR4-Arg auto-phosphorylation. In contrast, FGFR4-Gly and MT1-MMP had inhibitory effects on each other (Sugiyama, Varjosalo et al. 2010). Besides these pro-metastatic effects, there are also various reports about a tumor suppressive function of FGFR4-Arg in certain tumor types. This could indicate diverging roles of FGFR4 in different tissues and should be considered when targeting this receptor for cancer therapy (Heinzle, Erdem et al. 2014).

1.7.5 Blocking strategies for FGFR4

So far, there are only few studies targeting the FGFR4 for cancer therapy. This might be explained by the rather small subgroup of patients affected by mutations or amplifications of FGFR4 compared to other receptors. In addition, underlying mechanisms of FGFR4 and all the consequences of its signaling are not fully understood yet. The low sequence homology to the other three FGFRs seems to affect the efficiency of developed small molecule tyrosine kinase inhibitors (TKI). Although no FGFR TKI are approved for cancer therapy so far, several drugs targeting VEGFRs or platelet-derived growth factor receptors (PDGFRs) show inhibitory effects on FGFRs (Heinzle, Erdem et al. 2014).

The TKI PD173074 has recently been used to successfully inhibit FGFR1 (Nguyen, Tsunematsu et al. 2013), FGFR2 as well as FGFR3 (Beenken and Mohammadi 2009). PD173074 is also used to inhibit FGFR4, although the inhibitory potential for FGFR4 is weaker compared to FGFR1-3. Therefore, effects caused by PD173074 in cells (over)-expressing (mutant) FGFR4 may not be solely caused by FGFR4-blockade (Heinzle, Erdem et al. 2014).

Specific targeting of FGFR4 can be achieved by using anti-FGFR4 antibodies. French et al investigated LD1, a FGFR4 monoclonal antibody, using in vitro studies as well as a hepatocellular cancer (HCC) mouse model. They showed, that LD1 blocked FGF1 and FGF19 binding to FGFR4 which resulted in attenuated FGFR4 signaling, colony formation and proliferation. Additionally, tumor growth in LD1 treated HCC mice was reduced compared to control groups (French, Lin et al. 2012).

Expression of autoinhibitory fragments of FGFR4 or dominant negative FGFR4 (dn4) constructs are alternative approaches to inhibit FGFR4 signaling and downstream functions. As described above (*Termination of FGFR signaling*), a construct expressing IgI and AB is able to engage the heparin binding site of FGFR and therefore inhibit FGF binding and signaling (Kalinina, Dutta et al. 2012). Dominant negative (dn) FGFR constructs lack a functional kinase domain and dimerization with a functional receptor will not result in autophosphorylation (Alberts 2008). Mouse studies have shown, that dnFGFR constructs are able to attenuate tumor growth (Turner and Grose 2010). Grasl-Kraupp and her group showed, that inhibition of FGFR4 by expression of dn4 and sol4 constructs in HCC cells resulted in decreased clonogenicity and anchorage-independent growth in vitro, as well as reduced tumor growth rates when injected into Severe Combined Immuno-Deficient (SCID) mice in vivo (Gauglhofer, Paur et al. 2014).

1.8 Ba/F3 model system

Targeting and inhibiting one specific FGFR is crucial for some experiments, but difficult to achieve. TKI are not specific enough, especially when working with cells expressing endogenous levels of FGFR4 as well as several other RTKs (Heinzle, Erdem et al. 2014). Even highly specific dnFGFR constructs could form heterodimers and thereby falsify the results (Turner and Grose 2010). Ba/F3 cells are perfectly suitable for inhibiting one receptor out of a large subfamily of receptors due to their lack of endogenous RTKs. The response after transfection with one specific receptor and treatment with an inhibitor can be directly measured, without the interference of unrelated down-stream signaling (Warmuth, Kim et al. 2007).

Ba/F3 is an interleukin 3 (IL-3) dependent, murine bone marrow-derived cell line. Identification of surface antigens and configuration of their Ig loci classifies them as early B-cells of the lymphoblastoid lineage (Palacios and Steinmetz 1985). Although large numbers of experiments failed to induce spontaneous IL-3 independency (Daley and Baltimore 1988), there are numerous studies which observed transformed Ba/F3 cells after transfection with RTKs (Daley and Baltimore 1988, Smedley, Demiroglu et al. 1999, Jiang, Paez et al. 2004, Jiang, Greulich et al. 2005, Ceccon, Mologni et al. 2013). By identifying IL-3 independent cells, the transforming potential of a transfected receptor can be easily tracked. This strategy was used to demonstrate the oncogenic potential of the bcr/abl fusion protein (Daley and Baltimore 1988), the FGFR1/ZNF198 fusion protein (Smedley, Demiroglu et al. 1999), the FLT3 receptor (Jiang, Paez et al. 2004) and mutated epidermal growth factor receptors (EGFRs) (Jiang, Greulich et al. 2005).

Jiang et al observed, that IL-3 independent Ba/F3 cells expressing either mutated EGFR-G719R or EGFR-L858R differed in their sensitivity to the TKI Gefitinib (Jiang, Greulich et al. 2005). A similar strategy was used to find potential inhibitory drugs for fusion protein NPM-ALK, which is responsible for up to 80% of all anaplastic large cell lymphomas (ALCL). Recently, Ba/F3 cells expressing different mutated NPM-ALK proteins were used to identify potential drugs for ALCL treatment (Ceccon, Mologni et al. 2013).

2 Aim of the study

Previous results obtained in the group indicates that blocking of FGFR4 could help to improve cancer therapy of patients with deregulated FGFR4 background. For blocking, genetic strategies as well as small molecule compounds are available. However none of these are highly specific. For dn genetic constructs co-inhibition with related receptors has been discussed and chemicals are generally not specific (Heinzle, Erdem et al. 2014). Usually the impact of a blocking strategy on a specific target is assessed by analyzing down-stream events. For FGFR4 this is difficult, because most cells express several FGFRs and FGFR4 is the weakest in terms of signaling. Using a model system that does not express any other FGFRs should help to avoid interference of other receptors and permit the identification of FGFR4-specific events.

Part one of this master thesis therefore aims to produce and characterize Ba/F3 cells stably overexpressing FGFR4. To ensure, that these cell lines express the correct receptors, PCRs will be performed. Sorting using FACS will allow us to work with cell lines which express their respective receptors at same levels.

Then the cell lines will be used to test the inhibitory potential and toxicity of each blocking strategy by

- a. monitoring the viability via MTT and CellTiter-Glo assays
- b. signaling activity by phospho-specific western blot

Part two of the thesis will determine the impact of dominant-negative genetic constructs on tumor growth rates in vivo.

3 Material and methods

All used materials and their distributors are listed at the end of this chapter in table 2.

3.1 Cell biology

3.1.1 Cell lines and passaging

In Table 2, all used cell lines and their specifications are listed.

Alias/ATCC	Tissue	Type	Culture properties	Media	Split ratio	Mutations
HCT116/CCL-247	Colon (human)	Colorectal carcinoma	adherent	MEM with 10% FCS and 4% Penstrep	1:10-1:20	Codon 13 of ras proto-oncogene
HT29/HTB-38	Colon (human)	Colorectal adenocarcinoma	adherent	MEM with 10% FCS and 4% Penstrep	1:10-1:20	-
SW480	Colon (human)	Colorectal adenocarcinoma	adherent	MEM with 10% FCS and 4% Penstrep	1:10-1:20	Codon 12 of ras proto-oncogen
Ba/F3	Bone marrow (mouse)	immortalized murine bone marrow-derived pro-B-cell	suspension	RPMI-1640 with 10% FCS, 10% WEHI-3 and 4% penstrep (BaF-media)	1:10-1:20	

Table 2: *Cell lines and their characteristics.*

All adherent cell lines were split at 80-90% confluence using PBS/EDTA and trypsin/EDTA. In addition, stable transfectants were incubated with either 30µg/mL (SW480) or 50µg/mL (Ba/F3) G418.

Trypsin/EDTA

Trypsin/EDTA	5mL
1x PBS	45mL

3.1.2 Viability assays

3.1.2.1 MTT assay – EZ4U

This assay is based on the reduction of yellow/orange tetrazolium salt to red/purple formazan derivatives. Since this reduction requires functional mitochondria, it is possible to indirectly measure the viability of cells.

2500 to 15000 cells were seeded into 96-well plates in a volume of 100µL BaF-media and incubated for 3 to 5 days at 37°C. For viability evaluation, EZ4U substrate was added according to the protocol. After 2h to 4h, absorption was measured at 450nm wavelength with a 620nm reference wavelength using a Tecan Infinity 200 PRO device.

3.1.2.2 CellTiter-Glo assay – Luminescent cell viability assay

With a CellTiter-Glo assay, one can measure the ATP production of cells which is highly correlated with cell viability. Luciferin is oxygenated by luciferase in the presence of Mg^{2+} , oxygen and ATP and the resulting luminescence signal is analyzed.

Similar to the MTT assay, we seeded 2500 to 15000 cells in 96-well plates and incubated them for 3 to 5 days at 37°C. After that, cells were pipetted onto opaque 96-well plates and mixed with the CellTiterGlo assay. Luminescent signal was measured with a Tecan Infinity 200 PRO and an integration time of 1000ms.

3.1.3 Transfection of Ba/F3 cells

One of the most straight forward methods for transformation of eukaryotic cells is electroporation. An externally applied electrical field causes a temporal increase of the permeability of the cells plasma membrane and plasmids can enter the cell.

For electroporation, 1×10^7 cells were washed and resuspended in 700µL 1xPBS together with 20µg plasmid DNA. After 10min incubation at room temperature, cells were electroporated at 350V / 975µF in a Bio Rad Gene Pulser. In the next step, electroporated cells were incubated at room temperature for 10min and then transferred into 10mL flask containing RPMI-1640, 10% FCS, 10% WEHI-3, and 4% penstrep. For a list of all used plasmids, see table 3.

	Vector backbone	Gene of interest	Mutation	Selection bacteria	Selection mammalian
1	pMSCV-puro	FGFR4 Gly		Ampicilin	Puromycin
2	pMSCV-puro	FGFR4 E550	kinase active	Ampicilin	Puromycin
3	pMSCV-puro	FGFR4 K535	kinase active	Ampicilin	Puromycin
4	pMSCV-puro	empty		Ampicilin	Puromycin
5	pcDNA3	FGFR4 K645E	kinase active	Ampicilin	Neomycin (G418)
6	pcDNA3	FGFR4 K504M	kinase dead	Ampicilin	Neomycin (G418)
7	pcDNA3	FGFR4 Gly		Ampicilin	Neomycin (G418)
8	pcDNA3	FGFR4 Arg	G388R	Ampicilin	Neomycin (G418)
9	pcDNA3	FGFR3IIIb		Ampicillin	Neomycin (G418)
10	pcDNA3	FGFR3IIIc		Ampicillin	Neomycin (G418)

Table 3: List of all plasmids and their characteristics. Vectors 1 to 4 were kindly provided by Javed Khan, 5/6 by Daniel Donoghue and 7/8 by Axel Ullrich.

3.1.4 Selection of transfected Ba/F3 cells

For stable transfections, the gene of interest together with the selection marker has to be inserted into the cells genome. This can be achieved by treating those cells with a chemical which kills untransfected cells.

24h after electroporation, cells were split 1:2 but no selective reagents were added. 48h after transfection, cells were split again and selected by incubation with 50µg/mL G418 at 37°C for another 48h. These splitting and selection steps were repeated for 7 to 10 days, until the cells showed a normal proliferation rate and no signs of apoptosis.

3.1.5 Fluorescence activated cell sorting (FACS)

1×10^6 cells were washed twice with 1xPBS, resuspended in 100µL 1xPBS and incubated with 30µL FCS for 20min at room temperature. Afterwards, the Phycoerythrin (PE) or Allophycocyanin (APCy) labeled antibody was added in a concentration of 1:10 and incubated for 2h at room temperature and in darkness. After an additional washing step, cells were resuspended in 300 to 400 µL 1xPBS and fluorescence was recorded.

3.1.5.1 Cell sorting

Cells were washed and incubated with a PE or APCy labeled antibody similar to the FACS approach described above. Instead in 1x PBS, cells were resuspended in 1mL serum free RPMI-

1640 media and sorted in our FACS sorting facility. Positive cells were centrifuged at 1600rpm for 5min, transferred into 10mL flasks containing RPMI-1640, 50µg/mL G418, 10% FCS, 10% WEHI-3, 4% Penstrep, 10µg/mL Ciprofloxacin as well as 0.5µg/mL Amphotericin B and incubated at 37°C for 3 to 5 days.

3.1.6 Viral transduction of cells

When working with adenoviruses, additional safety protocols were used. The generation of aerosols was prevented and in addition, all used materials and the work benches were cleaned with proline after their use. Adenoviruses were kindly provided by Bettina Grasl-Kraupp. 24h after seeding, the cells were infected with an adequate dilution of the virus and experiments were performed.

We used 2 different adenoviral constructs in this project. The dn4 construct consists of a transmembrane domain, 3 Ig-like loops and an AB (figure 10 A), while its cytosolic tyrosine kinase domain has been replaced by a cyan-fluorescence-protein (CFP) tag thereby preventing dimerization and autophosphorylation (Alberts 2008).

The second construct expresses a sol4 mutant consisting of an AB linked to Ig-like loop I, as depicted in figure 10 B. Binding to FGFR4 and causes inhibition of its heparin binding properties, thereby blocking FGF mediated signaling (Kalinina, Dutta et al. 2012).

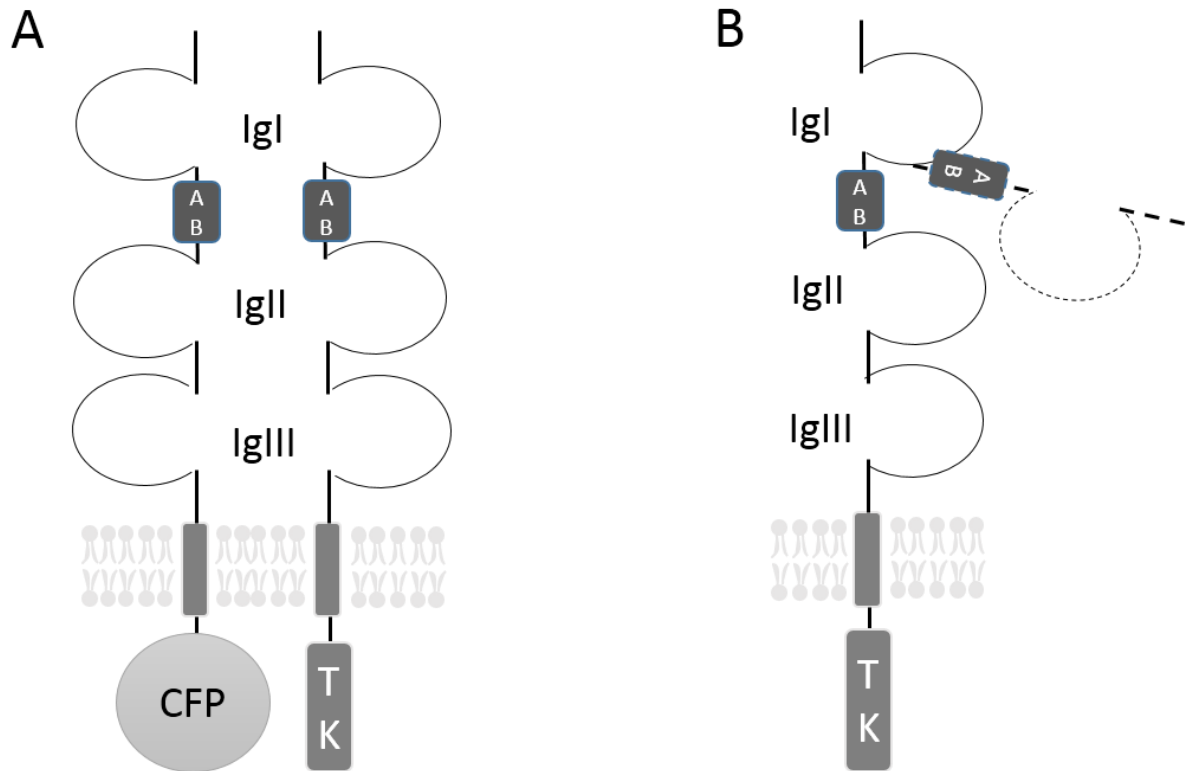


Figure 10: Design of inhibitory FGFR4 constructs. A: Schematic inhibition of FGFR4 by dn4 construct. The TK domain was substituted by a CFP-tag. B: Auto inhibitory construct sol4. The construct consists of an AB linked to IgI (Adapted from Christine Heinzle).

3.2 Working with RNA

3.2.1 RNA Isolation

Before RNA isolation, benches were cleaned with 70% ethanol (EtOH) to minimize the risk of RNase contamination of samples. In addition, scrapers were incubated 10min in 0.1M NaOH followed by 10min in 70% EtOH.

After the culture supernatant was aspirated, we added 1mL Trifast per 6cm petri dish and incubated them on ice for 5min. Next, cells and Trifast were scrapped off the plates using RNAase free scrapers and transferred into Eppendorf tubes. After adding 200µL chloroform, the tubes were vortexed for 30sec and incubated on ice for 10min. Afterwards, the tubes were centrifuged at 15000 rpm for 15min at 4°C. The RNA containing transparent phase was collected in a new tube. After adding 500µL isopropanol and vortexing for 30 sec, the tubes were incubated on ice for 10 min. In the next step, precipitated RNA was centrifuged at

12200rpm for 10 min at 4°C. Next, we discarded the supernatant and the RNA pellet was washed with 1mL 70% EtOH. After a last centrifugation step at 15000 rpm for 15min at 4°C, the supernatant was discarded and the RNA pellets were dried in a lamina for 15 – 20 min. Depending on the pellet size, we dissolved it in 30 – 50µL Diethylpyrocarbonate (DEPC) H₂O and stored the RNA at -80°C.

3.2.2 cDNA Synthesis

Complementary DNA (cDNA) synthesis was performed using isolated RNA, reverse transcriptase (RT) and a thermo cycler.

Quality and concentration of isolated RNA was measured with a Nano drop spectrophotometer device. 5µg RNA were diluted in 10µl nuclease free water and transferred into PCR tubes. After adding 2.5µl of random hexamer primer master mix, the samples were incubated at 70°C for 5min. In the next step we added 6.5µl RT master mix and incubated at 25°C for 5min. Finally, reverse transcription was initiated by adding 1µl Revert Aid M-MuLV reverse transcriptase to each sample and incubating at 25°C for 10min, followed by an 1h synthesis step at 42°C and a 10min deactivation at 70°C. The cDNA samples were diluted with 80 µl nuclease free water and stored at -20°C.

Random hexamer primer master mix

Random hexamer primer mix (100µM)	1µl
Nuclease free water	1.5µl

RT master mix

5x first strand buffer	4µl
dNTP mix (10mM)	2µl
RNAse inhibitor	0.5µl

3.3 Working with DNA

3.3.1 Polymerase chain reaction (PCR)

PCR is used to amplify specific sequences of DNA, e.g. to detect a specific gene of interest. As control, we always detected the housekeeping gene GAPDH in parallel. Used standard primers and their characteristics are listed in table 4.

3.3.1.1 Standard PCR

Standard PCR components

DNA	x μ L (2 μ g)
Primer 1 (10 μ M)	1 μ L
Primer 2 (10 μ M)	1 μ L
2x PCR Mastermix	12.5 μ L
DEPC-H ₂ O	x μ L to a total volume of 25 μ L

Conditions

95°C	2min	} 40x
95°C	40sec	
60°C	40sec	
72°C	40sec	
72°C	10min	

Primer Name	Sequence 5'→ 3' forward reverse	Annealing temperature In °C	Product size In bp
FGFR3IIIb	AACGGCAGGGAGTTCCGCGGC CCCGTCCCCGCTCCGACACATTG	62	429
FGFR3IIIc	AACGGCAGGGAGTTCCGCGGC CCCGGCGTCCTCAAAGGTG	58	435
FGFR4	AGCACTGGAGTCTCGTGATG CATAGTGGGTCGAGAGGTAG	56	525
GAPDH	CGGGAAGCTTGTGATCAATGG GGCAGTGATGGCATGGACTG	60	358

Table 4: Standard primer pairs and their sequences.

After PCR, samples were loaded onto a 6% polyacrylamide (PAA) gel for analysis (see also chapter 3.3.3 *Polyacrylamid gel electrophoresis*).

3.3.1.2 Real Time quantitative PCR (q-PCR)

q-PCR approaches are similar to standard PCRs, with the important difference that for each cycle of amplification, the quantity of the DNA sequence of interest can be measured in real time. In this project we used the TaqMan technique; all assays were measured using ABI 7500 Fast Real Time PCR System from Lifetechnologies.

3.3.1.2.1 TaqMan assays

A TaqMan probe consists of a fluorescent reporter, a quencher as well as a DNA sequence which connects both and is complementary to the DNA sequence of interest. Because of the close proximity of quencher and reporter, there is no detectable signal. After binding of the probe to DNA and subsequent degradation by polymerase exonuclease activity, the quantity of probe specific DNA sequences can be measured. Used TaqMan probes are listed in table 5.

TaqMan assay		Conditions	
cDNA (2µg)	1µL	95°C	10min
TaqMan probe	1µL	95°C	15sec
5x TaqMan Mastermix	4µL	60°C	1min
DEPC H ₂ O	14µL		
		} 40x	

TaqMan probe	number	exon	Amplicon lenght
FGFR4 total	Hs01106913_g1	7-8	84bp
FGFR4 TK	Hs00608744_g1	17-18	134bp
MT-MMP1	Hs01037009_g1	9-10	92bp
GAPDH	Hs99999905_m1	3	122bp

Table 5: List of TaqMan probes used in this project.

3.3.2 Restriction Fragment Length Polymorphism (RFLP) for G388R

The SNP at position 388 of the transmembrane domain of FGFR4 can be examined by a standard PCR and subsequent restriction digestion.

3.3.2.1 RFLP Standard PCR

We performed a standard PCR as described in 3.3.1.1 *Standard PCR*.

Conditions

94°C	12 min	} 40x
94°C	30 sec	
66°C (first 5 cylce)/62°C	30 sec	
72°C	40 sec	
72°C	7 min	

RFLP Primer

5' → 3'

Forward	GGCCAGTCTCACCCTGACC
Reverse	TGCTGGAGTCAGGCTGTCAC

3.3.2.2 Restriction enzyme digestion

PCR product, buffer and restriction enzyme MspI were incubated at 37°C for 1h and analyzed by gel electrophoresis using a 6% PAA gel (see 3.3.3 *Polyacrylamid gel electrophoresis*).

Digestion reaction

PCR product	10µL
MspI	1µL
10x Tango buffer	1.5µL
H ₂ O	2.5µL

3.3.3 Polyacrylamid gel electrophoresis

To separate DNA according to its size, we performed a PAA gel electrophoresis.

	6% PAA gel	12% PAA gel	50x TAE	
TAE (50%)	150µl	150µl	Tris	2M
PAA (40%)	1125µl	2250µl	Acetic acid	1M
ddH ₂ O	6175µl	5050µl	EDTA pH=8	50mM
TEMED	5µl	5µl	in ddH ₂ O	
APS (0,1g/mL)	50µl	50µl		

After polymerization of the gel, 10µL of the DNA and 2µL 6x loading buffer were loaded onto the gel. As marker, we used 1µL 50bp, 100bp or 1000bp ladder, according to the expected DNA fragment length. We applied 125V for approximately 1h in 1x TAE buffer. After that, the gel was stained for 15min using DNA Serva Clear and 5min washed in ddH₂O. Fluorescence was measured with a Typhoon TR O using a laser with an excitation maximum at 488nm and a 530nm filter.

3.3.4 Transformation of bacterial cells

The uptake of DNA into bacteria is dependent on their competence, a state which is either natural or induced by laboratory conditions. Competent E. coli JM-109 cells were kindly provided by the lab of Prof. Michael Grusch.

2µL plasmid DNA (200ng) were incubated with 100µL competent JM-109 cells on ice for 20min. After a 60sec heat shock at 42°C, 1mL SOC media was added and the cells were incubated for 1h at 37°C under shaking. Then, bacterial cells were centrifuged at 2000g for

3min and after discarding of the supernatant, cells were plated onto agar plates containing ampicillin. After incubation at 37°C overnight, 6 colonies were chosen at random and incubated in 1mL SOB containing 100ng ampicillin.

SOB medium

Tryptone	2%
Yeast extract	0.5%
NaCl	0.05%
KCl	0.0186%
MgSO ₄	0.24%
in ddH ₂ O	

SOC medium

Glucose	20mM
MgCl ₂	10mM
Fill up with SOB	

3.3.4.1 PCR analysis of colonies

To check if the correct plasmid was taken up by the bacterial cells, we performed a PCR analysis with appropriate primers.

5µL bacterial suspension of the overnight culture were mixed with 30µL DEPC H₂O and 6.5µL of this dilution were used as template for subsequent PCR (see also 3.3.1.1 *Standard PCR*)

3.3.5 Glycerol stocks

We used glycerol stocks to store successfully transformed bacterial clones.

Transformed bacterial clones were inoculated in 2mL LB medium containing 0.2mg ampicillin and incubated under constant shaking overnight. Next day, 700µL of the bacterial suspension was diluted with 300 µL 80% Glycerol and stored at -80°C.

3.3.6 Preparation of plasmids

Plasmids are small, double stranded, circular and uncoated DNA molecules that can replicate independently of a cells chromosomal DNA. They are usually found in bacteria and can be transferred from one bacterium to another via horizontal gene transfer. Plasmids or vectors have become an easy and powerful tool in molecular cloning which allows the easy and fast amplification of a gene of interest. Besides the gene of interest, plasmids often contain at least 2 different selective markers to allow selection in both bacterial and eukaryotic cells.

For preparation of plasmids, we used Qiagen Plasmid Mega Kits. 500mL LB-media containing 50mg ampicillin were inoculated with a bacterial strain expressing the correct plasmid. After constant shaking at 37°C for 16 to 18h, plasmid preparation was carried out following the Qiagen Plasmid Mega Kit protocol. The purified plasmids were dissolved in an appropriate amount of DEPC-H₂O.

3.3.7 Quality control of plasmids

To evaluate the quality of prepared plasmids, we performed a restriction enzyme digestion and subsequent agarose gel electrophoresis.

0.5µg of plasmid DNA were diluted in 8.5µl nuclease free water and transferred into Eppendorf tubes. After adding 1µl 10x fast digest buffer and 0.5µl EcoRI restriction enzyme, samples were incubated at 37°C for 30min under constant shaking. The agarose for the gel was weight, dissolved in ddH₂O and heated up in the microwave. After that, 50x TAE was added, so the final concentration was 1x TAE. As soon as the gel solidified, samples were loaded together with 2µl 6x loading buffer and gel electrophoresis was performed in 1x TAE by applying 100V for 1h.

3.4 Working with proteins

3.4.1 Protein isolation

3.4.1.1 Protein isolation of adherent cells

To inhibit phosphatases, cells were washed with Tris-buffered saline (TBS) containing 1mM Na₃VO₄ and 10mM NaF. Lysis of the cells was carried out by adding 150µl lysis-buffer and incubation on ice for 30min. While incubated on ice, lysates were vortexed every 10min. Afterwards, samples were sonificated 3 times for 1sec using a Bandelin Sonoplus device at 70% of maximum power, centrifuged with 15000 rpm at 4°C for 5min and stored at -20°C.

3.4.1.2 Protein isolation of suspension cells

First, we added 1mM Na₃VO₄ and 10mM NaF to each petri dish. Next, suspension cells were transferred into 15ml falcons and centrifuged with 2500 rpm for 5min. After discarding the

supernatant, the cell pellets were washed with TBS containing Na_3VO_4 and NaF. The next steps of protein isolation were carried out according to the protocol in chapter 3.4.1.1 *Protein isolation from adherent cells*.

10x TBS buffer

Tris	500mM
NaCl	1500mM
HCl	Adjust pH to .7,6
ddH ₂ O	Fill up to 1L

1x TBS + Na_3VO_4 /NaF

Na_3VO_4	1mM
NaF	10mM
1x TBS	Fill up to 1L

Lysis-buffer

Tris/HCl pH=7.4	50mM
NaCl	500mM
SDS	0.1%
Sodium Deoxycholat	0.5%
NP40	1%
NaN_3	0.05%
Complete	2.5%
in ddH ₂ O	

3.4.2 Evaluation of protein concentration

We performed a bovine serum albumin (BSA) standard curve by using a $1\mu\text{g}/\mu\text{l}$ BSA dilution and the pipetting protocol of table 6.

$\mu\text{g}/\mu\text{l}$ BSA	0	1	2	3	4	5	6	7	8	9
μl ddH ₂ O	9	8	7	6	5	4	3	2	1	0
μl Lysis buffer	1	1	1	1	1	1	1	1	1	1

Table 6: Pipetting protocol for BSA standard curve.

Then we diluted each sample 1:10 ($1\mu\text{l}$ protein lysate + $9\mu\text{l}$ ddH₂O.) and added $150\mu\text{l}$ of 1:5 thinned down Coomassie reagent. After 10min of incubation at room temperature, we measured absorption of both protein probes and BSA standard curve at 590nm and calculated the protein concentrations using EXCEL.

3.4.3 SDS Polyacrylamide gel electrophoresis (SDS-PAGE)

3.4.3.1 Standard SDS-PAGE

First, a separating gel was cast and overlaid with EtOH. After its polymerization (30-45min), it was overlaid with a stacking gel. Before loading the gel, protein samples were mixed with the adequate amount of 4x sample buffer and heated up to 80°C for 5min. Samples and $5\mu\text{l}$ page

ruler protein ladder was loaded onto the gel. Electrophoresis was carried out in 1x electrophoresis buffer at 60V for the first 15min (until proteins reached the separating gel) and then at 100V for about 1.5-2h.

	7% Resolving gel	4% Stacking gel
ddH ₂ O	2.8ml	1.9ml
1M Tris, pH 6,8	-	313µl
1,5M Tris pH 8,8	1.25ml	-
10% SDS	50µl	25µl
40% PAA	875µl	250µl
TEMED	2.5µl	2.5µl
10% APS	25µl	12.5µl

1x Electrophoresis buffer

Glycine	200mM
Tris	25mM
SDS	1%
in ddH ₂ O	

4x Sample loading buffer

Glycerin	40%
2-Mercaptoethanol	20%
SDS	8%
Tris, pH=6,8	250mM
Bromphenolblue	Traces of
in ddH ₂ O	

3.4.3.2 Tricine SDS-PAGE

The main difference between a standard and a tricine SDS-PAGE is the preparation of the gel and the running buffer. All sample preparation steps were carried out as described in chapter 3.4.3.1 *Standard SDS-PAGE*.

Separating and stacking gel were casted and overlaid according to the protocol of the standard SDS-PAGE, after 10 – 15min polymerization was finished. After adding anode (outer tank) and cathode (inner part –gel) buffer we applied 60V for the first 15min, and then 125V for 85min.

	Resolving Gel		Stacking gel
	10% Gel	12% Gel	4% Gel
40% Acrylamid	1.375ml	1.65ml	0.3ml
3x Tris/SDS pH 8,45	1.831ml	1.831ml	0.740ml
50% Glycerol	1.1ml	1.1ml	-
dd H ₂ O	1.16ml	0.890ml	1.935ml
10% APS	50µl	50µl	30µl
TEMED	2.5µl	2.5µl	2.5µl

5X Anode buffer

Tris	1M
in ddH ₂ O	
HCl	Adjust pH to 8.9

1x Cathode buffer

Tris	100mM
SDS	0.1%
Tricine	100mM
in ddH ₂ O	

3x Tris/SDS

Tris	3M
HCl	Adjust pH to 8.45
SDS	Filter and add 0.3%
in H ₂ O	

3.4.4 Western blot

Proteins were blotted on a polyvinylidene fluoride (PVDF) membrane using a wet-blot system. Before blotting, the membrane was activated with methanol. See figure 11



for order of preparation. Blots were running overnight at 25V and 4°C in 1x blotting buffer.

Figure 11: Design of a western blot.

10x Blotting buffer

Glycine	2M
Tris	50mM
SDS	0.2%
in ddH ₂ O	

1x Blotting buffer

10x blotting buffer	10%
Methanol	20%
ddH ₂ O	70%

3.4.5 Ponceau S staining

Ponceau S is a sodium salt that stains proteins on a PVDF membrane in a light red color. After the blotting, membranes were incubated in Ponceau S solution for 5 – 10min until protein bands were visible. Next, membranes were scanned, trimmed and finally destained by washing them in ddH₂O or washing buffer.

3.4.6 Detection of proteins

The membranes were blocked in 5% BSA for 30min and then incubated with a primary antibody solution over night at 4°C. On the next day, blots were washed 3 times over 30min in TBS containing Tween (TBST) and then incubated with the secondary antibody solution (either anti-rabbit or anti-mouse) for 1h at room temperature under constant shaking. After 3 – 5 washing steps for 30 – 60min, the membranes were covered with detection solution for 3 – 5min and then exposed to x-ray films. The quantification was performed using Image Quant 5.0. For a list of used antibodies and their distributors, see table 7.

Primary antibody solution

BSA	3%
Antibody	1:10000
TBST	Fill up to 10ml

Secondary antibody solution

BSA	3%
HRP conjugated antibody	1:10000
TBST	Fill up to 10ml

Washing buffer

0,1% Tween in 1xTBS

Antibody	monoclonal	polyclonal	Secondary AB	Distributor	MW
β-Actin	x		mouse	Sigma	42kDa
Akt	x		rabbit	Cell signaling	60kDa
pAkt (Ser 473)	x		rabbit	Cell signaling	60kDa
ERK 1/2		x	rabbit	Cell signaling	42/44kDa
pERK 1/2		x	rabbit	Cell signaling	42/44kDa
pFRS-2 (Y436)		x	rabbit	Cell signaling	80-85kDa
PLCy1		x	rabbit	Cell signaling	155kDa
pPLCy1 (Y783)		x	rabbit	Cell signaling	155kDa
S6	x		rabbit	Cell signaling	32kDa
pS6	x		rabbit	Cell signaling	32kDa
Stat3	x		rabbit	Cell signaling	79,86kDa
pSTAT3		x	rabbit	Cell signaling	79,86kDa

Table 7: Antibodies used in this project.

3.5 In vivo experiments

3.5.1 Xenograft tumors in SCID mice

1*10⁶ cells were infected with adenoviruses expressing sol4, dn4 or a control virus and injected subcutaneously into the right flank of SCID mice. Tumor size was measured periodically and the experiments were stopped when tumor size reached a threshold of

5.000mm³. Tumor and lungs of the animals were removed and fixed for 24h in 4% formaldehyde solution at room temperature in darkness. In the last step, tissue samples were washed in 1x PBS and stored in 70% EtOH at 4°C. Paraffin embedding was carried out as soon as possible.

3.5.2 Embedding and sectioning

Tumor samples were cut into 2 – 3 mm thick pieces and lobes of the lungs were separated. For the last fixation and paraffinization step, tissue samples were transferred into caps. Finally, paraffinization was performed at a Kos Histostation.

Conditions

Ethanol absolute	25min	65°C
Isopropanol	55min	68°C
Melted paraffin	75min	82°C

Fixed tissue was casted into paraffin blocks, sectioned in 4µm thick slices and mounted onto a microscope slide.

3.5.3 Tissue staining

3.5.3.1 Deparaffinization

Microscope slides with mounted tissue were incubated for 10min at 65°C. Afterwards, following protocol was carried out:

Xylol	2x 1min
Ethanol 100%	2x 1min
Ethanol 70%	2x 1min
ddH ₂ O	2x 1min

3.5.3.2 Hematoxylin and Eosin staining

Nuclei were stained with hematoxylin for 7min. After washing with water, slides were incubated with Sott's solution for 45sec. Next, slides were washed for 5min with warm water, followed by another washing step using floating water. Counter staining with eosin for 6sec and a last washing step finished the Hematoxylin-Eosin (HE) staining. Finally, water was removed using the following protocol:

Ethanol 70%	Dipping 3 times
Ethanol 96%	2x 1min
Ethanol 100%	2x 1min
Xylol	1x 1min
Xylol	2x 1min

Slides were sealed with Entellan.

3.5.3.3 Immunohistological staining

Endogenous Peroxidases were inactivated by incubating tissue slides in 0.3% H₂O₂ for 10min at room temperature. After washing 2 times in 1x PBS for 3min, slides were incubated in 10mM citrate buffer and heated up in a steamer for 30min. Next, we washed the slides 2 times for 3min using 1x PBS + 0.1% Tween and encircled the tissue on the slide using a fat pen. For detection an Ultravision LP Detection System HRP Polymer kit was used. Tissue was incubated with the Ultra V block solution for 5min and then with the primary antibody solution for 30 – 120min. For a complete list of used antibodies and their incubation time see table 8. After washing the slides 2 times with 1x PBS + 0.1% Tween, they were incubated for 10min with Primary Antibody Enhancer followed by 2 additional washing steps with 1x PBS + 0.1% Tween. Afterwards, slides were incubated for 15min with HRP polymere and washed 2 times using 1x PBS + 0.1% Tween. In the next step, the slides were incubated for 10min with DAB substrate, washed with ddH₂O and counter stained with hematoxylin for 10sec (6 dippings).

After a last washing step with H₂O, the remaining water was removed using the following protocol:

Ethanol 70%	Dipping 3 times
Ethanol 96%	2x 1min
Ethanol 100%	2x 1min
Xylol	1x 1min
Xylol	2x 1min

Slides were sealed with Entellan.

Antibody	Distributor	Dilution (in TBS-T)	Incubation time
Ki-67	Dako	1:100	30min
MT1-MMP	Millipore	1:100	60min
FGFR4	Santa Cruz	1:100	120min

Table 8: *Immuno-histological staining antibodies.*

0,3% H₂O₂

In 1x PBS

**Primary antibody
solution**

Antibody 1%

Goat serum 1%

in 1xPBS + 0,1% Tween

10mM Citrate buffer

Trisodium citrate 10mM

HCl Adjust pH to 6

Tween 20 0.05%

DAB substrate

DAB chromogen 2%

in DAB buffer

Material	Distributor
1000bp DNA ladder	Fermentas
100bp DNA ladder	Fermentas
10cm and 6cm petri dishes	Sarstedt
10x FastDigest Green Buffer	Thermo Scientific
10x Tango buffer	Fermentas
2x PCR-Mastermix (standard PCR)	Fermentas
50bp DNA ladder	Fermentas
5x Hot Fire Pol Probe q-PCR Mix Plus	Solis Biodyne
6well and 96well plates	Sarstedt
6x Loading dye	Fermentas
ABI 7500 Fast Real Time PCR System	Lifetechnologies
Acetic acid	Merck
Amphotericin B	Sigma
Ampicillin	Sigma
APC anti-human FGFR3	R&D Systems
APS	Sigma
Aspirator	KNF Laboratories
Bio Rad Gene Pulser	Bio Rad
Bovine serum albumin (BSA)	Sigma
CellTiter-Glo Luminescent Cell viability assay	Promega
Ciprofloxacin	Teva
Complete	Roche
Coomassie	Bio Rad
DAB kit	Thermo Scientific
Dimethyl sulfoxide (DMSO)	Sigma
DNA Serva Clear	Serva
dNTP Mix	Thermo Scientific
EcoRI FastDigest	Thermo Scientific
Ethylenediaminetetraacetic acid (EDTA)	Merck
EZ4U	Biomedika
FACS vials	BD Falcon, 5mL
Fetal calf serum (FCS)	GE Healthcare
FGFR4 blocking antibodies (in 1xPBS)	U3 Pharma
FGFR4 TK – TaqMan probe	Applied Biosystems
FGFR4 total – TaqMan probe	Applied Biosystems
GAPDH – TaqMan probe	Applied Biosystems
Geneticin (G418)	GE Healthcare
Glucose	Sigma
Glycerol	Sigma
Hexamer primer master mix	Thermo Scientific
Incubator	Haeraerus Function Line
KCl	Merck
MgSO ₄	Sigma
Minimum essential media (MEM)	Sigma
MMP14 – TaqMan probe	Applied Biosystems
MspI	Fermentas

NaCl	Sigma
Nano Drop	Peqlab
PBS/EDTA: 10mM EDTA in PBS	Merck
PD173074 (in DMSO)	Sigma
PE anti human CD334 (FGFR4)	Bio Legend
PE Rat anti-mouse IgG	BD Biosciences
Penicillin/Streptomycin (Penstrep)	Sigma
Phosphate Buffered Saline (PBS)	Sigma
Plasmid Mega Kits	Qiagen
Polyacrylamid (40%)	Bio Rad
Ponceau S	Sigma
Proline Biocontrol	Biohit
Puromycin	Sigma
PVDF membrane	VWR
Revert Aid M-MuLV reverse transcriptase	Fermentas
RNAse Inhibitor (Ribo Lock RNAse Inhibitor)	Thermo Scientific
RPMI-1640 media	Sigma
T100 Thermal cycler (PCR)	Bio Rad
TaqMan Mastermix (5x Hot Fire Pol Eva Green q-PCR Mix Plus)	Solis Biodyne
Tecan Infinity 200 PRO	Tecan
TEMED	Sigma
Trifast peq Gold	Peqlab
Tris	Sigma
Trypsin/EDTA	GE Healthcare
Tryptone	Fluka/Biochemika
Typhoon TR O	GE Healthcare
Ultravision LP Detection System HRP Polymer kit	Thermo Scientific
Vistra Green Nucleic Acid Stain	GE Healthcare
Yeast extract	Sigma

Table 9: *Materials used in this project and their distributors.*

4 Results

4.1 Establishing FGFR overexpressing Ba/F3 cell lines

Ba/F3 cells are murine pro B cells which lack any kind of RTKs on their cell surface. Therefore they are dependent on IL-3 which needs to be added to the standard cell culture media. The fact that there are no other interfering RTKs expressed in the background as well as the dependency on IL-3 makes these cells an attractive tool to study FGFR-signaling. For this reason Ba/F3 cells were transfected with FGFRs. Cell lines overexpressing FGFR4-Gly (Gly), FGFR4-Arg (Arg) - Glycin or Arginine at position 388 of the transmembrane (TM) domain - and the empty pcDNA3-vector (control) were already established in the lab according to the protocol described in the chapter *Material and Methods*. In parallel, new Ba/F3 cells were established while performing experiments with the already existing ones. New transfectants are referred to as Gly^{new}, Arg^{new}, control^{new}, FGFR3IIIc (R3c) and FGFR4-K504M (KD).

4.1.1 Evaluation of purified plasmids

To produce sufficient amounts of the required FGFR plasmids we transformed bacterial cells and prepared/isolated plasmid DNA as described in *Material and Methods*. For quality checking plasmids were digested with a single cutting restriction enzyme and the linearized as well as undigested plasmid was identified via electrophoresis.

For undigested plasmids different bands representing multimers, nicked/relaxed and supercoiled formation were expected. Naturally fused plasmids or multimers travel slowest. Nicked/relaxed DNA is faster but because of its partially open conformation still slower compared to linearized DNA, which is travelling according to its size. The majority of plasmids are supercoiled and run faster than predicted on an agarose gel. After restriction enzyme digestion, plasmids were linearized and we expected bands corresponding to their size (figure 12).

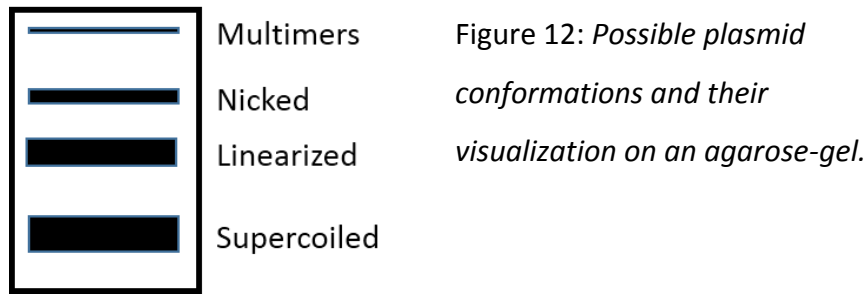


Figure 13 shows EcoRI digested and undigested FGFR4-pcDNA3 and -pMSCV-puro plasmids after running on a 1% agarose gel electrophoresis. As predicted, undigested DNA was heterogeneous and we saw 3 different bands according to their size and conformation: multimer (slowest), nicked/relaxed and supercoiled. The high amount of supercoiled plasmid, shown by the most prominent band at about 5000bp proves the good quality of our plasmids. Digested plasmids were successfully linearized and had the predicted size of 8261bp and 9144bp. We observed 2 bands for the digested pMSCV-puro vector without FGFR4-insert. One at the expected size of 6283bp and the other at about 8500bp as a result of partially digested plasmid DNA. For size comparisons we loaded a 1000bp ladder onto the gel.

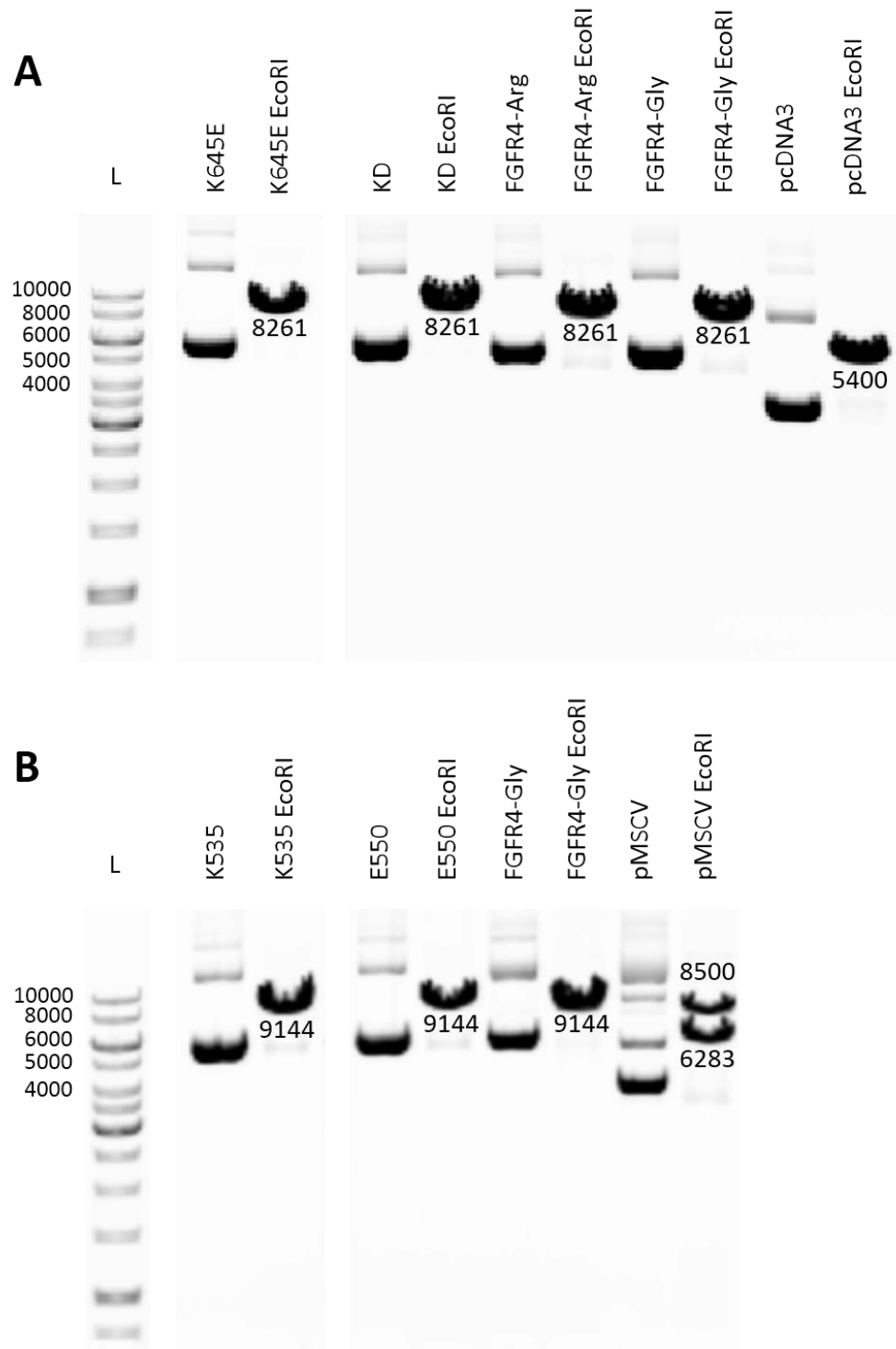


Figure 13: Quality control of prepared plasmids. A: pcDNA3 vectors. B: pMSCV-puro plasmids. Majority of undigested plasmids was supercoiled, characterized by a band around 5000bp for plasmids with insert. Linearized plasmid DNA had the predicted size of 8261bp (pcDNA3 plus insert) and 9144bp (pMSCVpuro plus insert), respectively. Plasmids without insert were respectively smaller. Digestion of empty pMSCVpuro vector resulted in 2 bands.

4.1.2 Transfection of Ba/F3 cells and sorting

Ba/F3 cells were transfected with pcDNA3 vectors expressing Gly^{new}, Arg^{new}, KD, R3c or empty pcDNA3 control vector (control^{new}). 7 to 10 days after transfection, the protein expression of FGFRs on the cell surface was measured by FACS using either a directly labelled PE-FGFR4- or APCy-FGFR3 surface-antibody. As a negative control a PE-labeled Rat surface binding antibody was used. FGFR-transfected Ba/F3 cultures were found to contain 8-12 % FGFR-expression, while cells transfected with the control vector remained FGFR-negative (figure 14).

Figure 15 shows the surface FGFR expression by FACS analysis of the final enriched cultures for FGFR-overexpressing Ba/F3 cells. By sorting the FGFR-positive cultures 2-3 times consecutively, we generated populations that were 60 – 80% positive for their respective receptor (figure 15 A, B, C, D) as compared to control transfectants (figure 15 E).

Already established Gly and Arg cell lines were 80-85% positive when treated with directly labeled PE-FGFR4 surface antibody while the control cells were negative (FACS analysis for already established cells not shown).

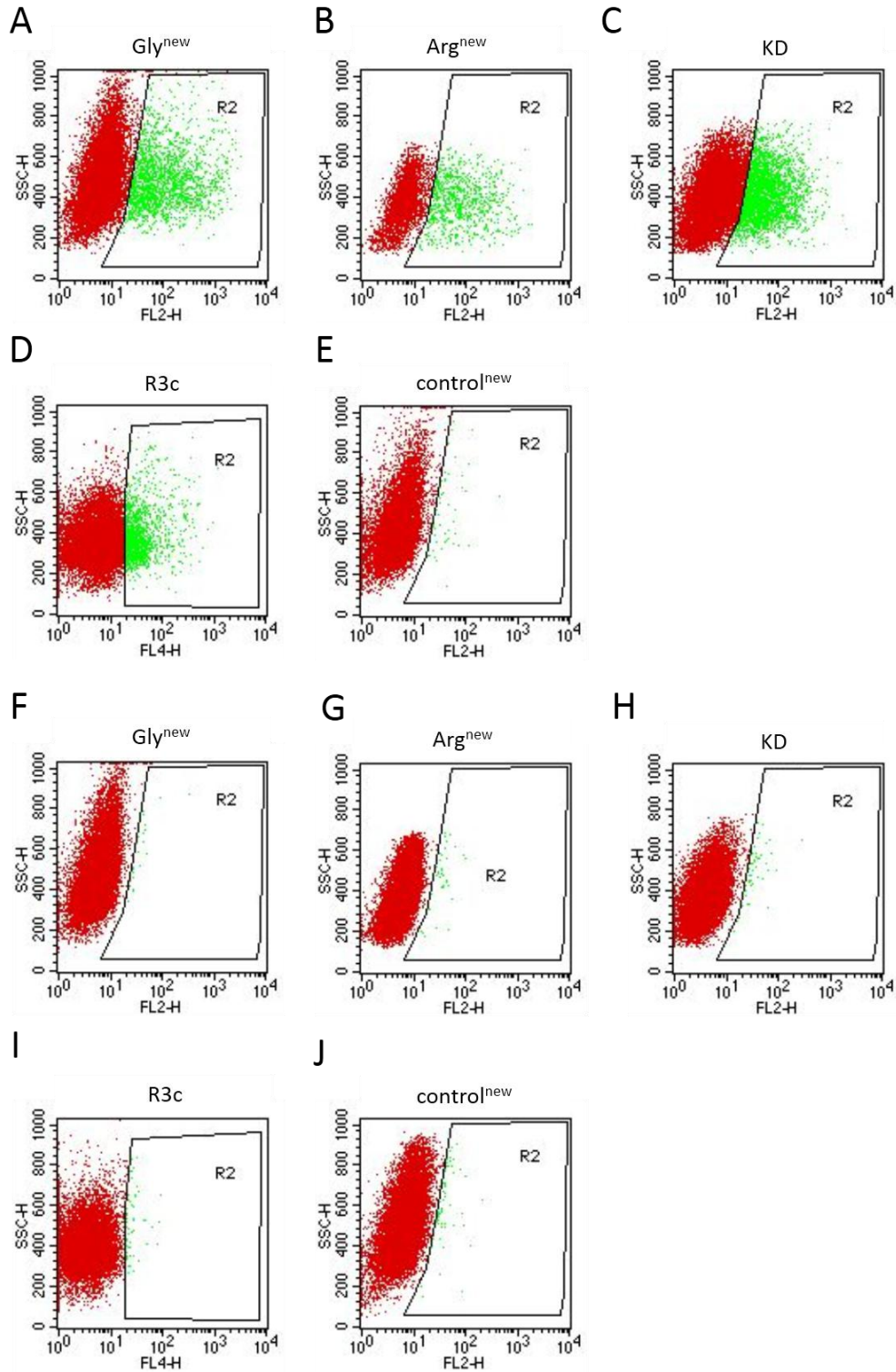


Figure 14: FACS Ba/F3 cells after transfection using an anti-FGFR4 PE-labeled or an anti-FGFR3 APCy surface antibody. A-E show FGFR surface expression of Ba/F3 transfectants. Gly^{new}, Arg^{new}, KD, and R3c (A, B, C, and D) were found to contain 8-12% FGFR expression, while control^{new} (E) remained FGFR negative. F-J show Ba/F3 transfectants treated with an unspecific control antibody to visualize unspecific antibody binding.

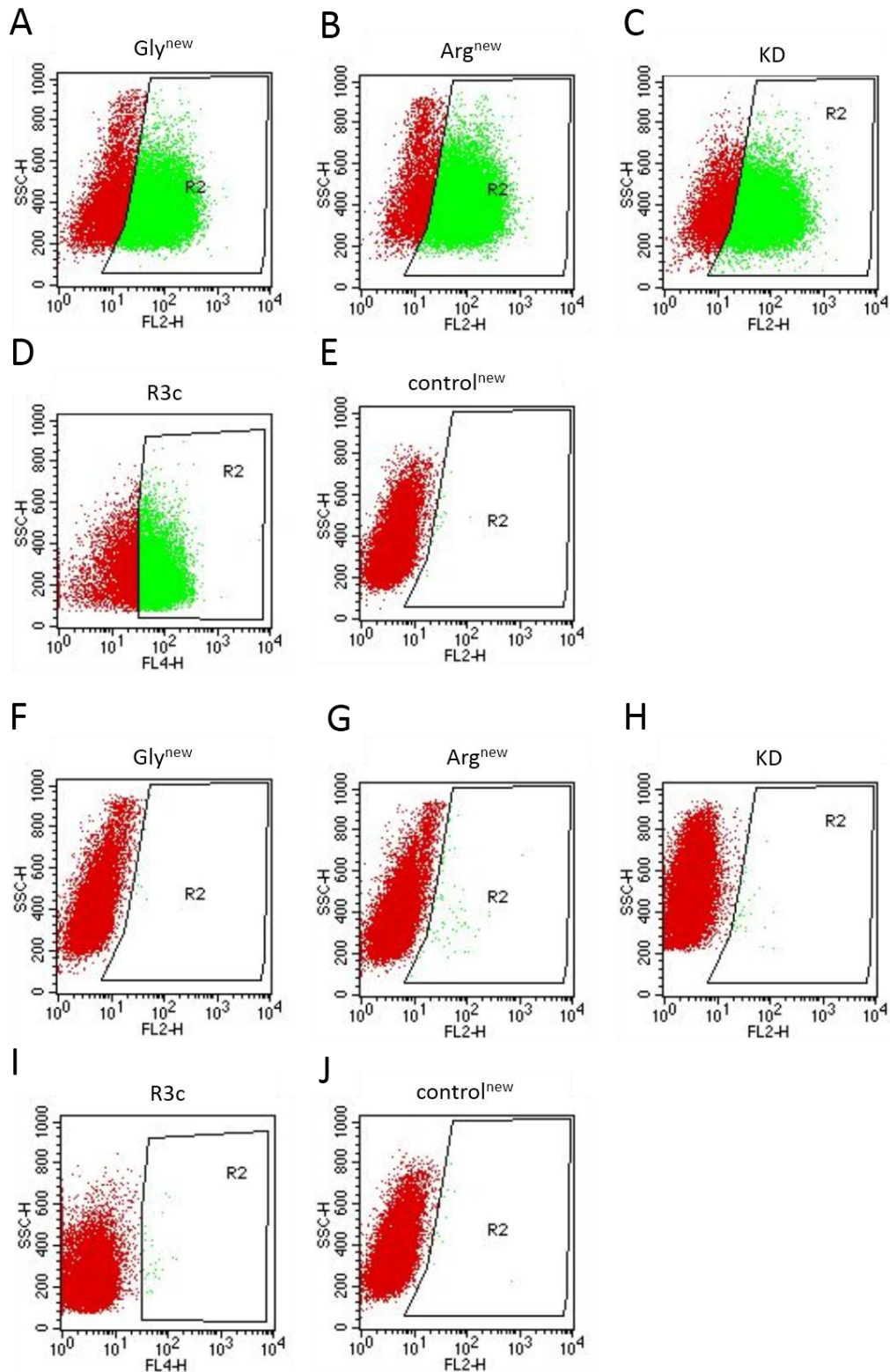


Figure 15: FACS plots of newly transfected Ba/F3 cells after 2-3 sorting cycles. A- E: Ba/F3 transfectants and their corresponding FGFR surface expression, measured by using PE- or APCy labeled specific antibodies. A-D were 60-80% positive for their respective receptor, while control^{new} cells did not express FGFRs. F-J: Ba/F3 cell lines treated with an unspecific control antibody.

4.1.3 Verification of FGFR overexpressing cells

Because we transfected the cells with different variants of FGFRs, it was important to validate, that the correct FGFR was expressed in each cell line. For FGFR3IIIb and IIIc overexpressing cells, we performed RNA isolation with subsequent cDNA synthesis and standard PCR with specific primers. Gly and Arg variants were determined by standard PCR and subsequent RFLP analysis.

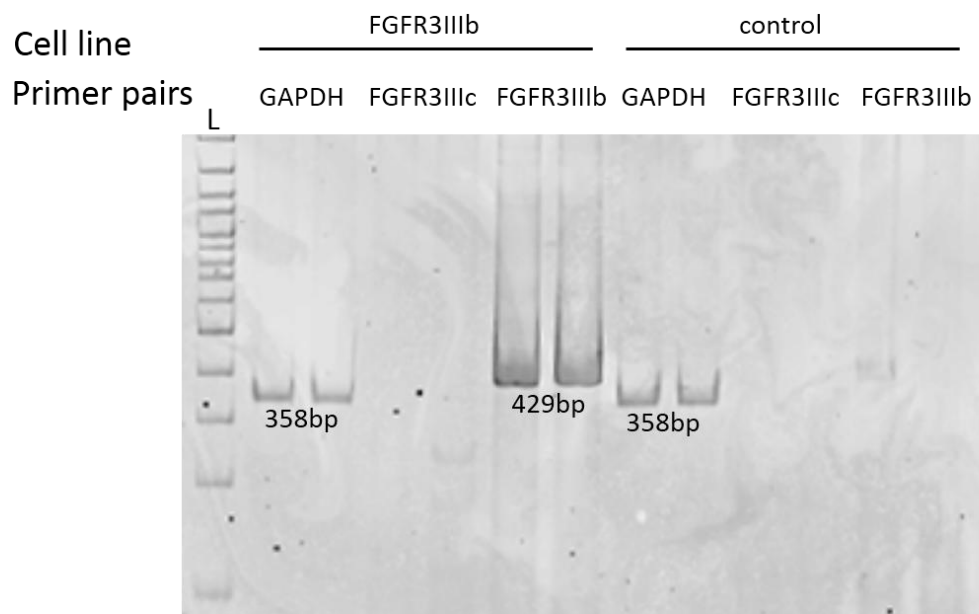
4.1.3.1 Standard RT-PCR for FGFR3IIIb and IIIc variants

We isolated RNA from the corresponding Ba/F3 cell lines and amplified FGFR3IIIb and IIIc from the cDNA using specific primers followed by PAGE analysis. As an internal control for the PCR GAPDH expression was additionally determined.

In Figure 16 A, we successfully detected GAPDH (358bp) for FGFR3IIIb overexpressing Ba/F3 cells. They showed no expression for R3c while the FGFR3IIIb (R3b) variant could be determined at 429bp. Cells transfected with the empty vector expressed GAPDH but neither FGFR3IIIb nor IIIc.

In B, R3c transfected Ba/F3 cells are shown. They express GAPDH (358bp) and FGFR3IIIc (435bp), but no FGFR3IIIb variant. For size comparison, we used a 100bp DNA ladder.

A



B

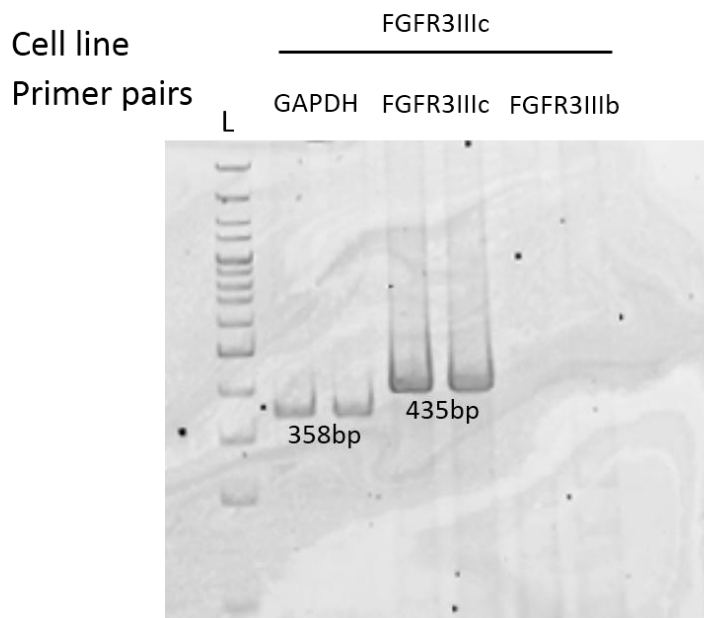


Figure 16: Verification of *FGFR3IIIb* and *IIIc* expression in *BaF3* transfectants using Standard PCR. A: *GAPDH*, *FGFR3 IIIb* and *FGFR3 IIIc* expression of *Ba/F3 FGFR3IIIb* transfectants and control. B: *GAPDH*, *FGFR3 IIIb* and *FGFR IIIc* expression of *Ba/F3 FGFR3IIIc* transfectants. *L*=100bp DNA ladder

4.1.3.2 FGFR4 G388R single nucleotide polymorphism

To evaluate the FGFR4 polymorphism in the Ba/F3 transfectants Gly^{new}, Arg^{new}, KD and control^{new}, a RFLP was performed. The restriction enzyme cuts the Gly variant into 3 pieces (85, 50 and 30bp) whereas one cutting site is hidden by the Arg variant resulting in only 2 bands (115 and 50bp). As positive controls, we used pure plasmid DNA with the sequence for either Gly or Arg.

In figure 17 A, there are no bands for the negative control. The positive Gly control (Gly pos co) was identified resulting in 3 fragments at 85, 50 and 30bp. The cleaved amplicon of positive Arg control (Arg pos co) showed 2 fragments with a length of 115 and 50bp. Gly^{new} and Arg^{new} cells had the same pattern as their corresponding positive control. At position 388 of the TM domain of the KD cell line is a glycine. Control^{new} cells do not express any FGFR4.

RLFP data of already established FGFR4 expressing Ba/F3 cells were carried out in another study and were similar to the result shown here.

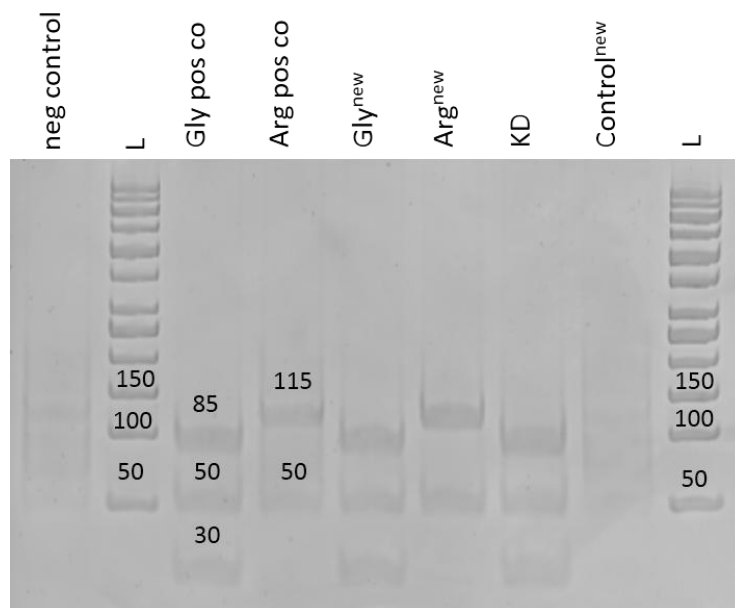


Figure 17: G388R RFLP of FGFR4-Ba/F3 transfectants. Numbers indicate length on fragments in bp. The cleaved amplicon of Gly^{new} resulted in 3 fragments, similar to the Gly positive control. Arg at position 388 of the TM domain altered the restriction pattern. There were only 2 fragments for the amplicon of Arg^{new} and the corresponding positive control. Cells expressing the KD receptor showed a glycine-specific restriction pattern. Control^{new} cells did not express any FGFR4. L=50bp+ ladder

4.2 Inhibition of FGFR4 and its effect on viability

4.2.1 IL-3 (in) dependency of Ba/F3 cells

We started to characterize growth behavior and factor-requirements of already established Ba/F3 cells as compared to empty vector.

As a first experiment, we wanted to investigate the viability of Ba/F3 cells overexpressing FGFR4 based on the IL-3 levels. As a positive control we use standard Ba/F3 culture media which contains IL-3 (1:10 dilution of WEHI-3 supernatant) and 10%FCS. Experimental groups contained less or no IL-3 supplementation as depicted in figure 18. No FGF was added to the media. In these factor-reduced media Gly overexpressing cells showed significantly higher viability compared to Arg or cells expressing an empty vector. Gly transfectant cells were also growing in absence of IL-3 which shows a required independency on IL-3 due to the FGFR4 wt.

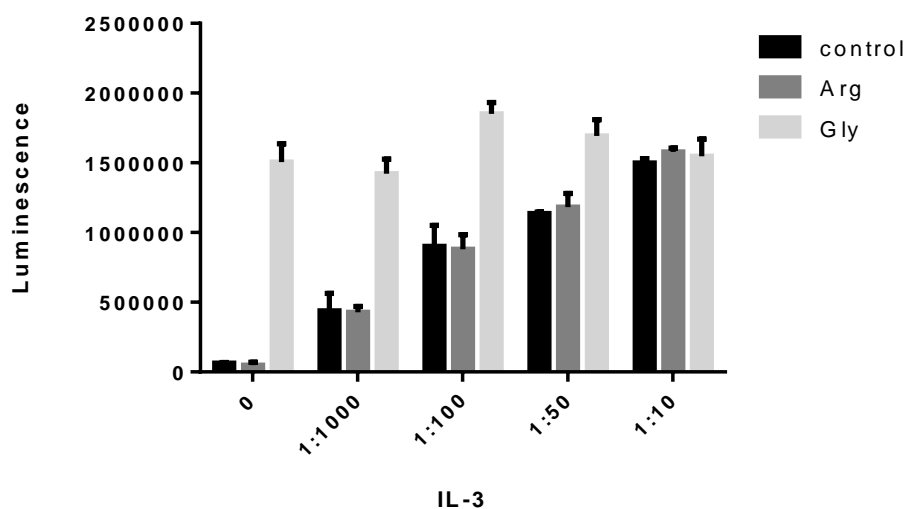


Figure 18: Viability of Ba/F3 cells using different amounts of IL-3. Concentration of 1:10 is equivalent to the amount of IL-3 usually used in standard cell culture.

4.2.2 Inhibition of FGFR4

To test if the IL-3 independency of Ba/F3 cells overexpressing Gly could be reversed by blocking the receptor we used dominant negative genetic constructs or the small molecule inhibitor PD173074 as detailed below and analyzed cell viability.

4.2.2.1 Blocking of FGFR4 via PD173074

The TKI PD173074 is a synthetic compound. There are various reports that treating tumor cells overexpressing or expressing mutant FGFR4 with higher doses of PD173074 (μM range) results in decreased cell proliferation (St Bernard, Zheng et al. 2005, Ho, Pok et al. 2009, Crose, Etheridge et al. 2012).

Ba/F3 control and Gly cells were seeded in medium plus or minus IL-3 and treated with different PD173074 concentrations. After 4 days, MTT assay was performed. In Figure 19, results of 3 independent experiments are pooled together. Treating control cells plus IL-3 with 0.1 μM or 5 μM of the TKI had no effect on viability (figure 19 A). Similar results were seen for Gly transfectants plus IL-3 (figure 19 B). By contrast, decreased (two tailed t-test, $p=0.019$) viability was seen in Gly cells without IL-3 when treated with 5 μM PD173074 (figure 19 C). However, treating any of those cells with a concentration of 10 μM or more of the inhibitor resulted in a dramatic reduction of viability independent of FGFR4-expression (figure 19 A-C). Control cells without IL-3 showed very low levels of viability (not shown).

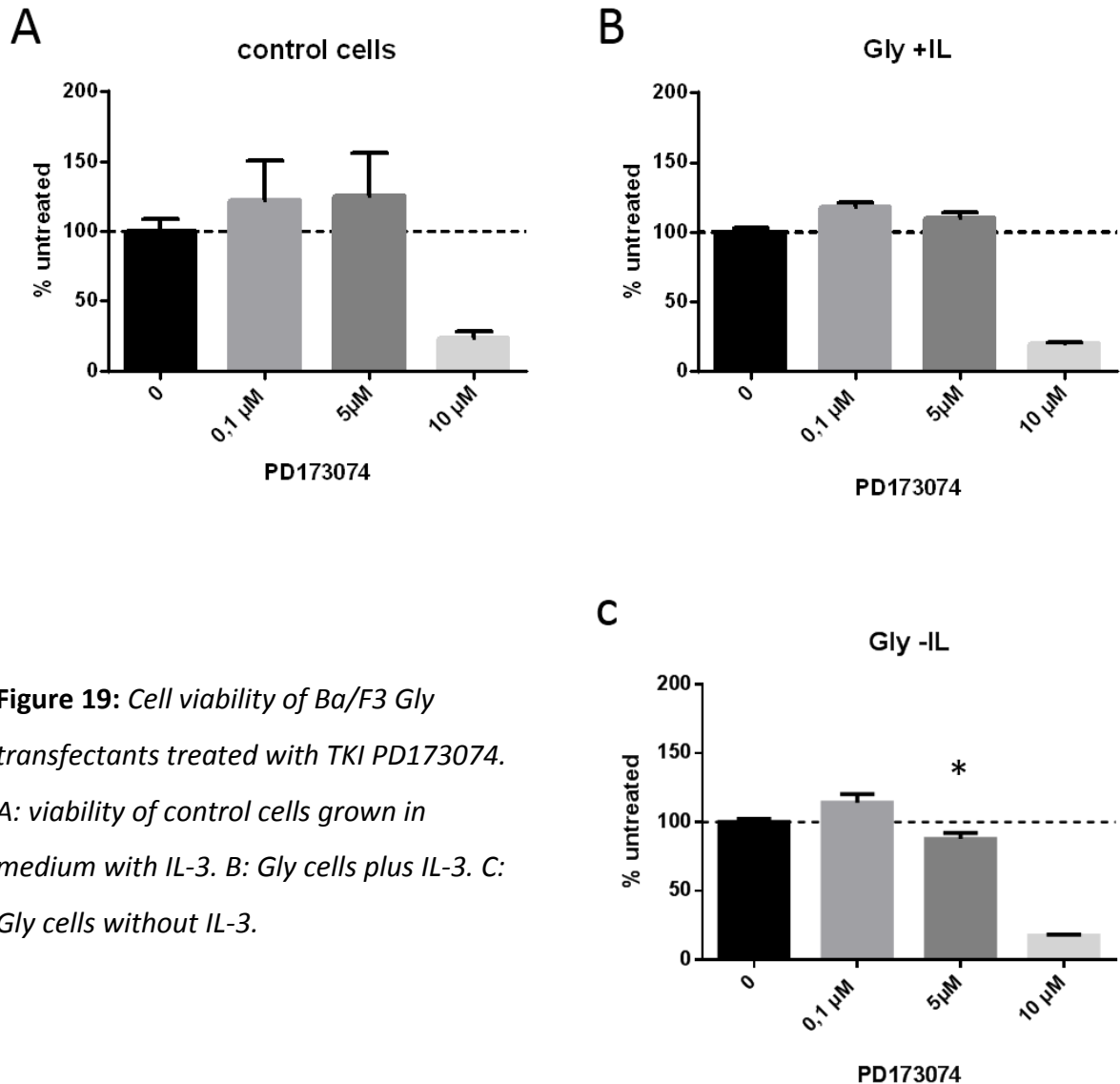


Figure 19: Cell viability of Ba/F3 Gly transfectants treated with TKI PD173074. A: viability of control cells grown in medium with IL-3. B: Gly cells plus IL-3. C: Gly cells without IL-3.

4.2.2.2 Inhibition of FGFR4 via adenovirus constructs

We used 2 different adenoviral constructs in this project. The dn4 construct lacks a tyrosine kinase domain, resulting in a dn4 FGFR4 dimer without autophosphorylation events, which inhibits signaling (Alberts 2008, Gaughfer, Paur et al. 2014).

The second construct expresses a sol4 mutant, as described in 3.1.6 Viral Transduction of cells, figure 10 B. This construct is able to engage the heparin binding site on FGFR4, thereby lowering FGF affinity and inhibiting signaling (Kalinina, Dutta et al. 2012).

For the assay, we infected Ba/F3 Gly and control cell line with 5 different adenoviral constructs at a multiplicity of infection (MOI) of 10. After four days cell viability was measured by MTT assay. In addition to dn4 and sol4 a control virus (co-v) which did not express a functional

construct and two FGFR adenoviruses expressing kinase dead mutants of the FGFRs 1 (KD1) and 3 (KD3) were used.

Figure 20 shows the results of 3 pooled MTT viability assays. No effect due to the infection of all 5 viruses on cell viability was observed for control (figure 20 A) and Gly (figure 20 B) cells in the presence of IL-3. We also monitored viability of control cells without IL-3, but due to their IL-3 dependency the viability was drastically reduced (data not shown). Viability of Gly cells without IL-3 (figure 20 C) and infected with dn4 was significantly reduced as compared to cells treated with co-v (two-tailed t-test, $p=0.0225$). We did not observe an effect for cells infected with the sol4 construct as well as KD3 and KD1.

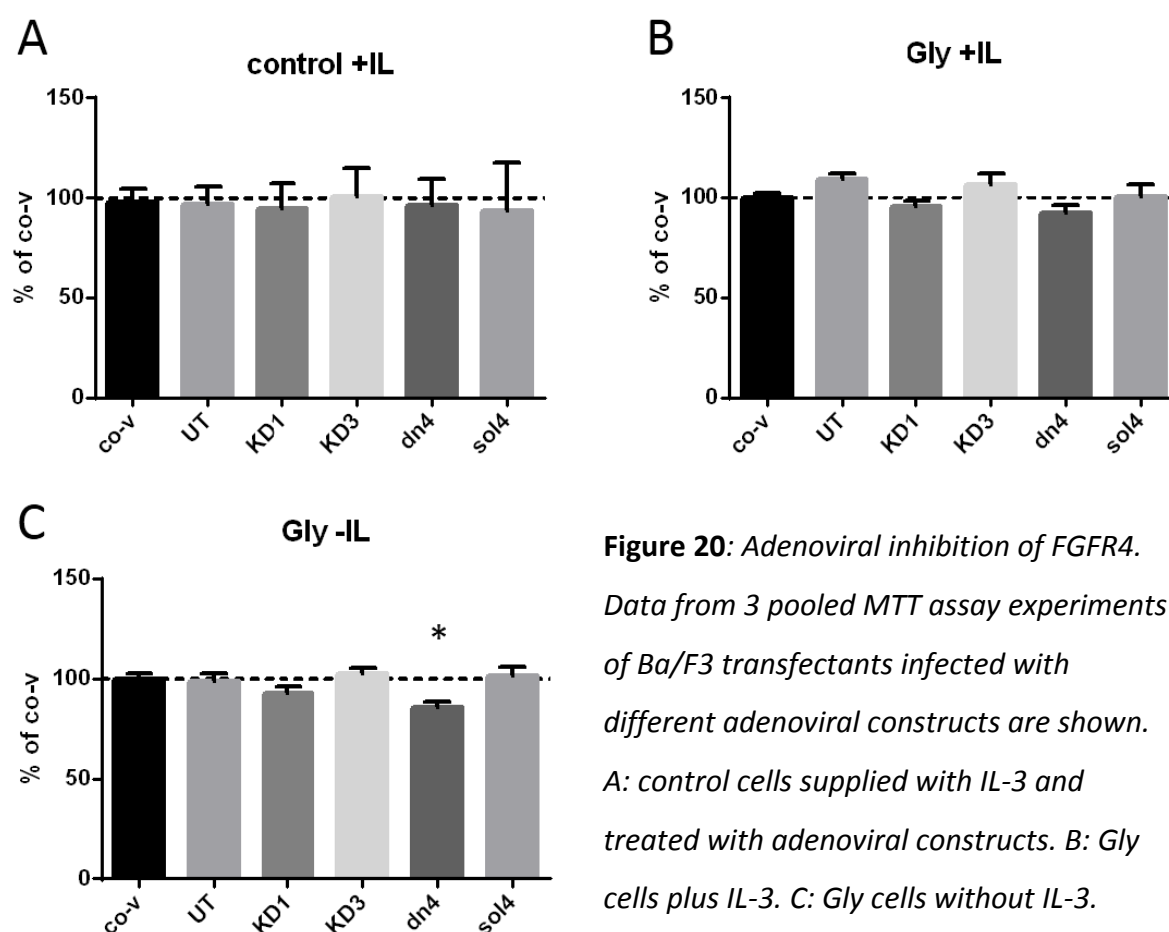


Figure 20: Adenoviral inhibition of FGFR4.
Data from 3 pooled MTT assay experiments of Ba/F3 transfectants infected with different adenoviral constructs are shown. A: control cells supplied with IL-3 and treated with adenoviral constructs. B: Gly cells plus IL-3. C: Gly cells without IL-3.

4.3 Viability of FGFR4 overexpressing Ba/F3 cells stimulated with FGF

Because viral inhibition of FGFR4 with the dn4 construct showed reduced viability of the Ba/F3 cells overexpressing Gly, we wanted to know if stimulation of those cells with FGF1 or FGF2, which both are strong activating ligands for FGFR4, would result in increased cell proliferation and viability. The cells were treated with 2 μ g/ml heparin and different FGF concentrations and viability assays were performed in presence or absence of IL-3.

The results of 2 independent experiments are pooled together in figure 21. We were not able to detect any effects on the viability of control cells when stimulated with FGF1 (figure 21 A, B). Gly cells plus IL-3 (figure 21 C) showed increased viability when stimulated with 5ng/ml FGF1 (two tailed t-test, $p=0.0231$). Without IL-3, we observed an increase of viability for Gly cells treated with 5ng/ml ($p=0.024$) and 10ng/ml ($p=0.0042$) FGF1 (figure 21 D).

When FGF2 was used in the same experimental setup, no increased viability was observed for control cells (figure 21 E, F). We were only able to detect an increased viability for Ba/F3 cells expressing Gly treated with 5ng/ml (two tailed t-test, $p=0.0001$) when they were supplemented with IL-3 (figure 21 G). There were no significant changes in the group without IL-3 (figure 21 H).

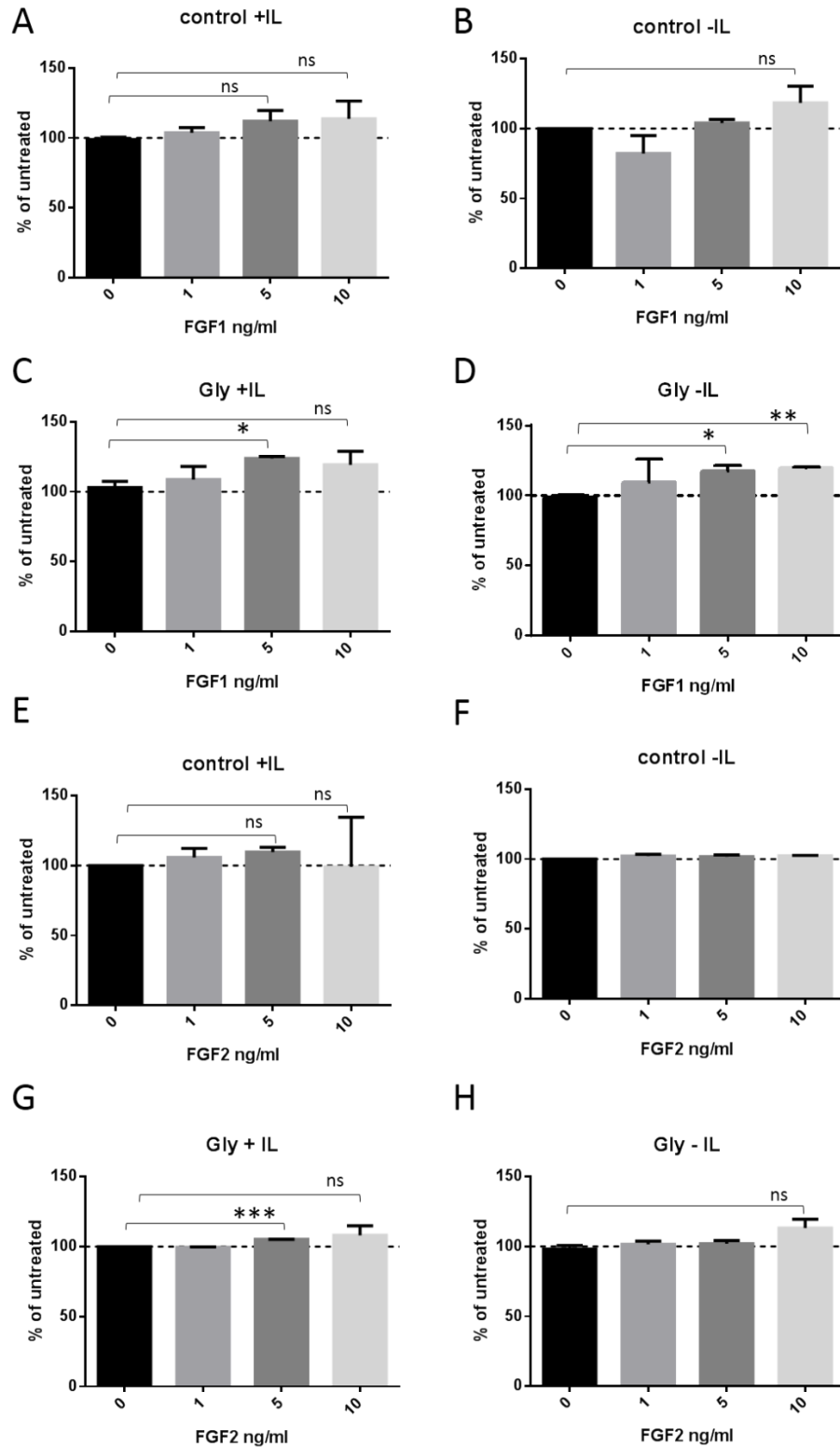


Figure 21: Viability assays of Ba/F3 transfectant cells stimulated with FGF1 and FGF2. A: control cells plus IL-3 treated with FGF1. B: control cells without IL-3 treated with FGF1. C: Gly cells plus IL-3 treated with FGF1. D: Gly cells without IL-3 treated with FGF1. E: control cells plus IL-3 treated with FGF2 F: control cells without IL-3 treated with FGF2. G: Gly cells plus IL-3 treated with FGF2 H: Gly cells without IL-3 treated with FGF2.

4.4 Impact of Genetic FGFR4 Blockade on the Signaling of Ba/F3 Cells Overexpressing FGFR4

After observing reduced viability of virally inhibited FGFR4 overexpressing cells but only weak stimulation effects when treated with FGF, we wanted to investigate the signaling of cells infected with adenoviruses expressing sol4 or dn4 constructs.

Ba/F3 Gly or control cells were starved with serum-free media without IL-3 containing 1% BSA and 10µg/ml heparin for 24h. Then they were infected with adenoviruses expressing the dn4, sol4 or control construct for another 24h. After 10min of stimulation with FGF1, protein lysates were obtained and western blots with antibodies against PLCγ, S6, ERK1/2 and STAT3 were performed using phospho-specific antibodies to assess the activation status of each protein.

Control (figure 22A) or Gly (figure 22 B) cells without FGF1 showed no or very weak phosphorylation of PLCγ1. pPLCγ1 signals could only be detected in FGFR4-overexpressing cells stimulated with FGF1 and they were sensitive to FGFR4 blocking constructs (figure 22). Figure 22 D and E show signaling blots for S6 and its phosphorylated forms that did not differ between the experimental groups

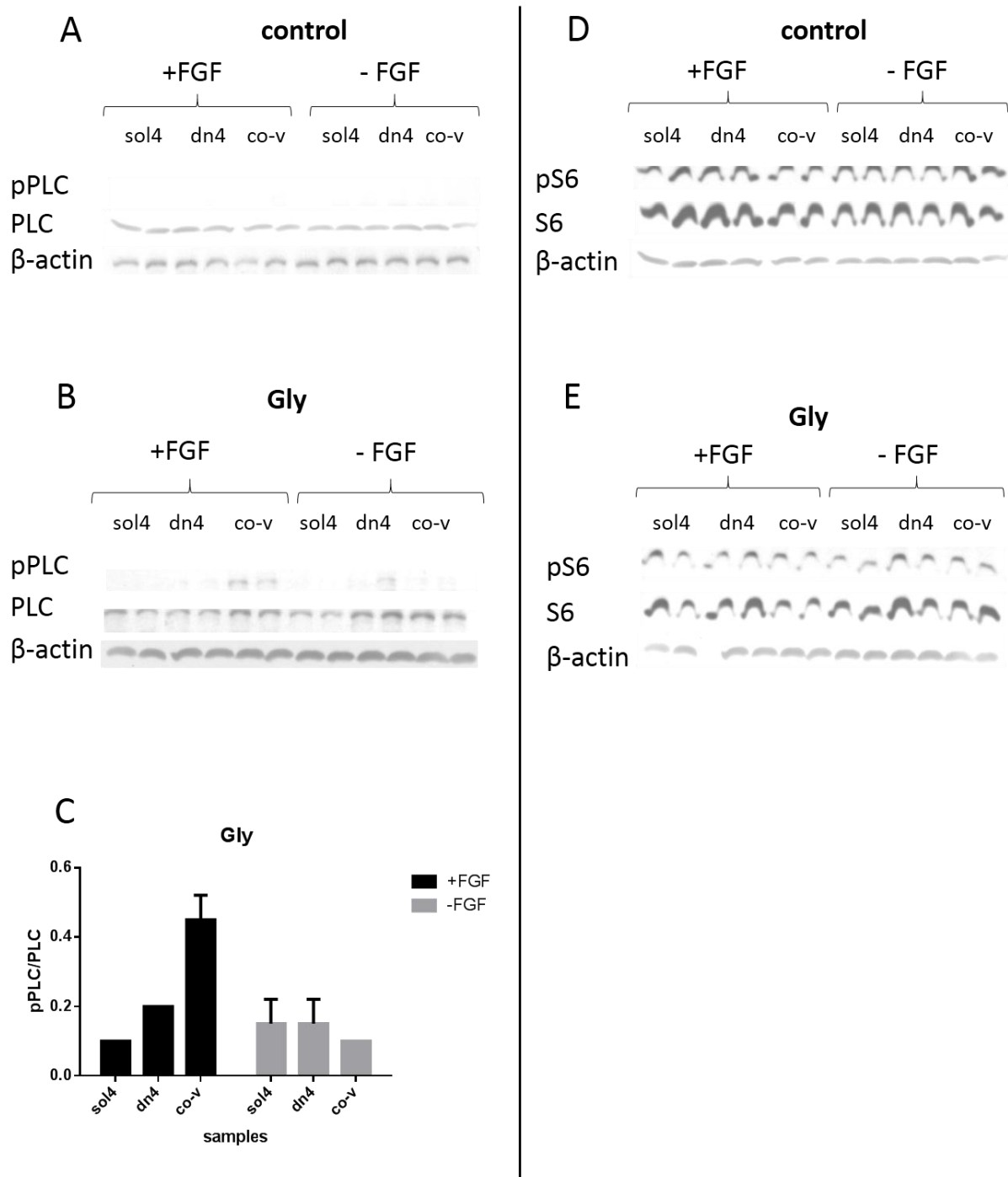


Figure 22: Effects of *sol4* and *dn4* constructs on PLC γ 1 and S6 signaling. A: PLC γ 1 signaling of infected control cells with or without FGF1 stimulation. B: PLC γ 1 signaling of infected Gly cells with or without FGF1 stimulation. C: quantification of pPLC/PLC signaling of Gly cells. D: S6 signaling of infected control cells with or without FGF1 stimulation. E: S6 signaling of infected Gly transfectant cells with or without FGF1 stimulation. +/- = with or without FGF

In figure 23 (top panel), we analyzed STAT3 signaling. There were no differences in the control group (figure 23 A, B), but a trend of decreased STAT3 signaling for Ba/F3 cells expressing Gly and sol4 or dn4 was observed, but not significant (figure 23 C, D).

With regard to ERK-activation Ba/F3 cells expressing the empty vector had increased pERK1/2 signals when stimulated with FGF compared to untreated control. In dn4 and sol4 infected cultures the signal was even higher (figure 23 E, F). Gly cells had higher baseline levels of pERK as compared to control cultures, but these were not affected by either FGF-addition to the culture or infection with a blocking virus (figure 23 G, H).

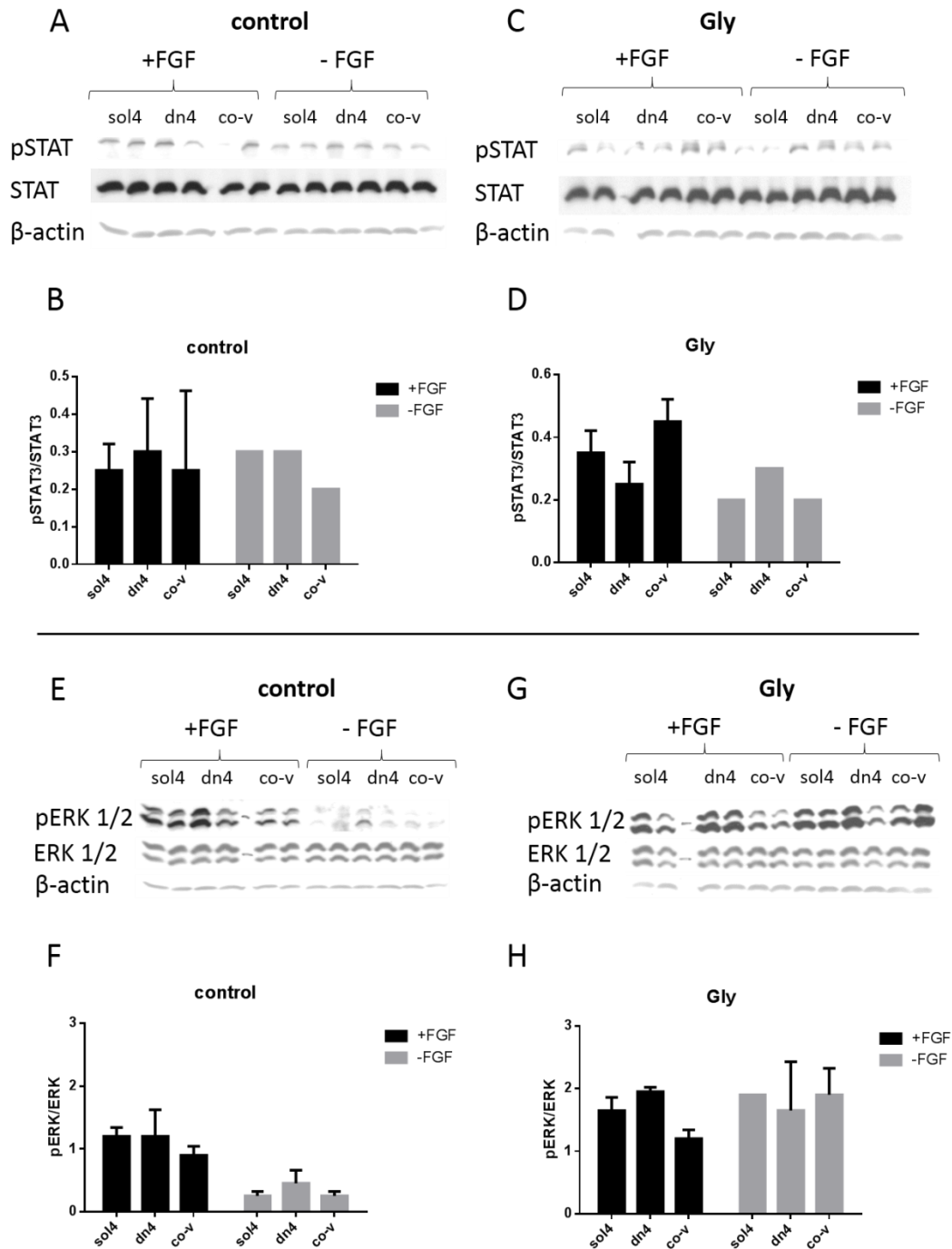


Figure 23: STAT3 and ERK1/2 signaling of virally inhibited Ba/F3 transfectants with or without FGF1. A: STAT3 signaling blots of control cells B: Quantification of STAT3 control cell signaling. C: Gly cells infected with adenoviruses expressing sol4 and dn4 constructs and the effects of FGF stimulation. D: Evaluation of pSTAT3/STAT3 signaling of Gly cells. E: ERK1/2 signaling blots of control cells with or without FGF1 and infected with adenoviruses dn4 and sol4. F: ERK signaling quantification of control cells. G: pSTAT3, STAT3 and β-actin blots of Gly expressing cells infected with adenoviruses and effects of FGF stimulation. H: Quantified pERK/ERK signaling of Gly cells. +/- = with or without FGF

4.5 Establishing new FGFR overexpressing Ba/F3 cell lines

In parallel to the inhibition and stimulation experiments, new Ba/F3 cell lines were established by transfecting them with Gly, Arg, empty pcDNA3, KD and R3c as described in *Material and Methods*. Similar to the experiments in chapter 4.2.1 *IL-3 (in)dependency of Ba/F3 cells*, we treated the cells with different concentrations of IL-3 produced by WEHI-3 cells and performed viability assays.

The results for these assays are shown in figure 24. “Old” in figure 24 A refers to Ba/F3 transfected cells we used for our inhibition and stimulation experiments. In B, the viability of newly transfected Ba/F3 cells is shown as comparison. We established a Gly^{new} cell line that expressed the receptor but was not IL-3 independent. Moreover, we also obtained cells overexpressing the empty vector (control^{new}) or Arg^{new} that were more viable at lower IL-3 concentrations compared to Gly^{new} cells. However, they were not IL-3 independent.

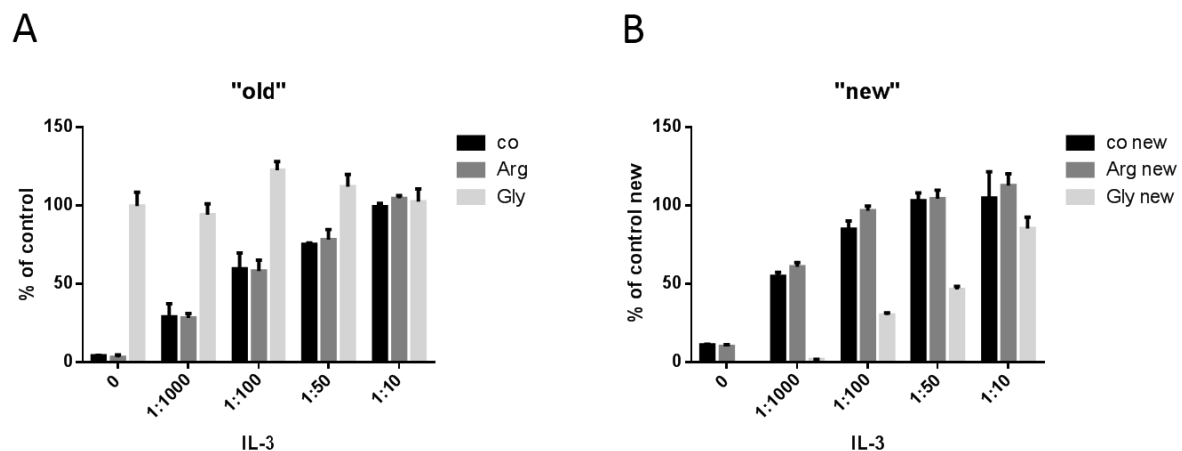


Figure 24: Comparing viability of Ba/F3 cell lines with different IL-3 concentrations.

Next, the viability of all 5 new cell lines was tested either with or without IL-3 (figure 25). Without IL-3, control^{new} and Arg^{new} cells had a more than 2-fold increased viability compared to the other cell lines.

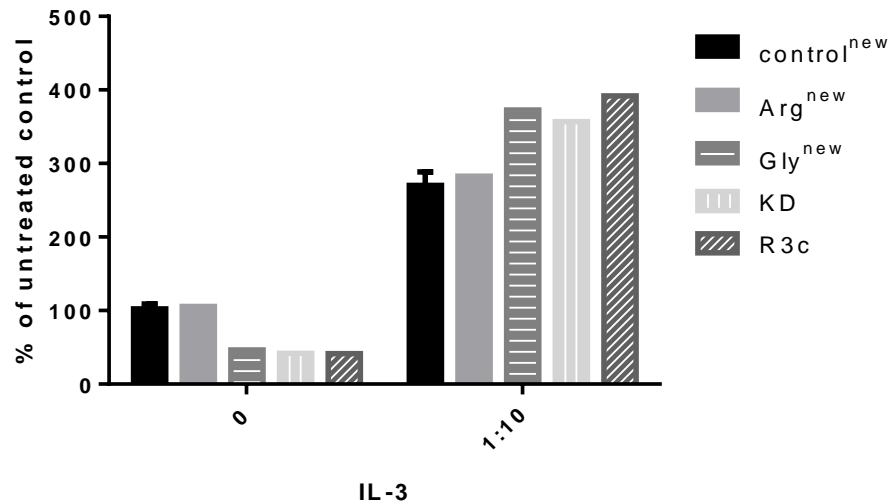


Figure 25: MTT assay of new transfected Ba/F3 cell lines. Plotted data is relative to untreated control (control^{new} without IL-3).

To test the stimulatory effect of FGF on those new cell lines, and to reveal possible differences in the signaling pathways of cells that are more viable without IL-3, western blots were performed.

4.6 Signaling of FGFR overexpressing cells induced with FGF

Signaling blots for the “old” IL-3 independent Gly and IL-3 dependent Arg and control cell line were already performed as part of an earlier project and showed higher baseline levels of pSTAT3, pS6, pAkt and pERK in IL-3 independent Gly cells compared to the Arg and control cell line. Now, we wanted to investigate the signaling of newly established Ba/F3 cell lines (Gly^{new}, Arg^{new}, control^{new}, R3c). For that purpose, equal amounts of cells were seeded into petri dishes and starved for 24h in serum free medium containing 1%BSA and 10μg/ml heparin. Cultures were stimulated with 10ng/ml FGF1 for 30min. Then cell lysates were harvested and western blots were performed using phosphospecific antibodies for STAT3, ERK, S6 and PLCγ1 as before. Results from 2 independent experiments are shown.

Detection of the very upstream PLCγ1 signaling was hampered by high background which resulted in large error bars (figure 26). Total PLCγ1 protein expression was slightly elevated for Gly cells stimulated with FGF1, but pPLCγ1 levels did not change (figure 26 A). There was a weak stimulation of pPLCγ1 for R3c (figure 26 B).

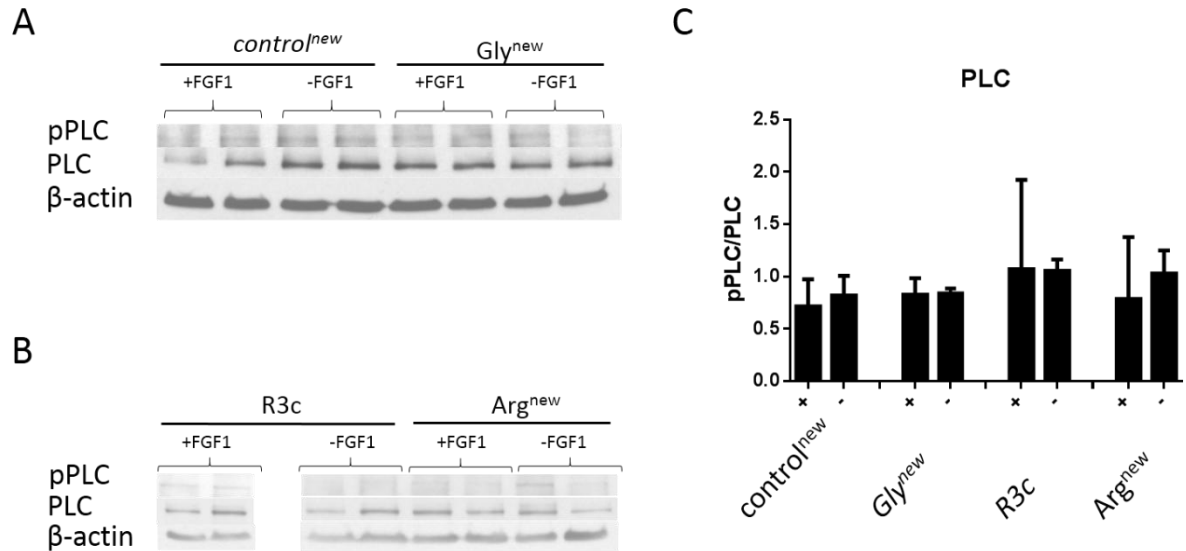


Figure 26: PLC γ 1 signaling of Ba/F3 transfectants stimulated with FGF1. A: pPLC γ 1, PLC γ 1 and β -actin of control^{new} and Gly^{new} cells. B: Effects of FGF1 stimulation on Arg^{new} and R3c overexpressing cells. C: Quantification of pPLC/PLC. Standardization relative to corresponding untreated sample. +/- = with or without FGF1

Arg^{new} and control^{new} cell lines showed a strong increase in S6 phosphorylation compared to the other 2 cell lines (figure 27 A and B). We were able to detect a weak stimulatory effect of FGF1 on S6 signaling for R3c cells (figure 27 C).

There was no FGF1 dependent stimulatory effect on ERK phosphorylation, as shown in figure 27 F, but increased baseline levels of pERK for Arg^{new} compared to the other three cell lines (figure 27 D, E).

We were not able to detect any STAT3 phosphorylation for FGF1 stimulated Ba/F3 transfectants (data not shown).

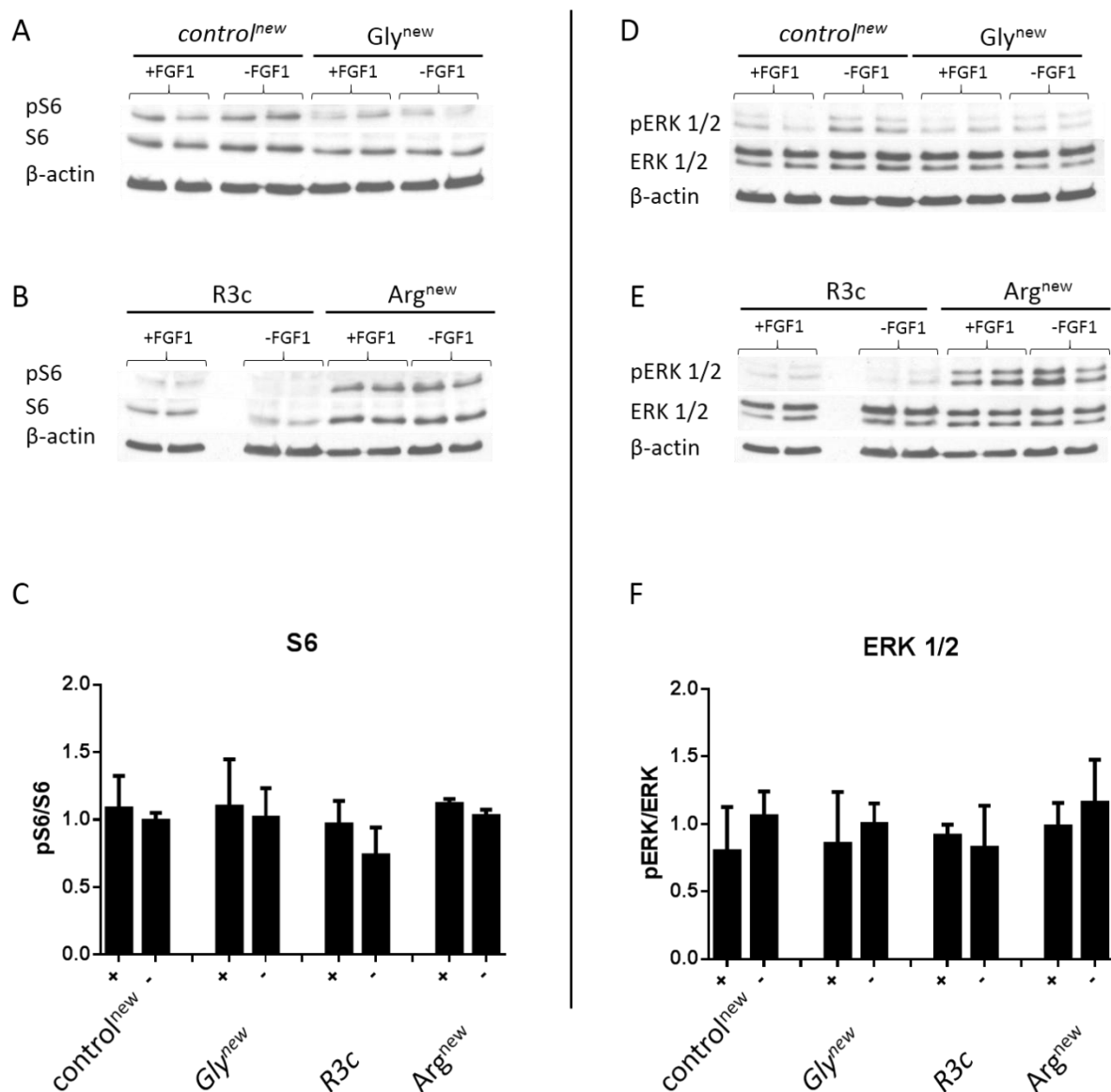


Figure 27: S6 and ERK signaling of FGF1 stimulated Ba/F3 transfectants. A: S6 signaling blots of *control^{new}* and *Gly^{new}* cells. B: *Arg^{new}* and *R3c* overexpressing cells and their S6 signaling. C: Quantification of S6 signaling. D: pERK, ERK and β-actin levels of *control^{new}* and *Gly^{new}* cells. E: ERK signaling blots of *R3c* and *Arg^{new}* cell lines. F: Effects of FGF1 stimulation on ERK signaling. Standardization relative to corresponding untreated sample. +/- = with or without FGF1

4.7 In vivo – SW480, HCT116 and HT29 xenografts

In an earlier project expression of FGFR4 in colon cancer cell lines has been determined. In the same project the focus has been laid on the Gly388Arg Polymorphism of FGFR4 and therefore also the allelotype of the colon cancer cell lines has been established. For further experiments 3 cell lines with different FGFR4 expression levels as well as allelotype have been chosen:

SW480, HCT116 and HT29. SW480 showed a low Gly expression level and were homozygous for this receptor. HCT116 were also Gly-homozygous but in contrast to SW480 had a higher FGFR4 expression level (figure 28). HT29 can be characterized as a heterozygous FGFR4-Gly/Arg colon cancer cell line that showed high expression level for preferentially Arg allele (Heinzle, Gsur et al. 2012).

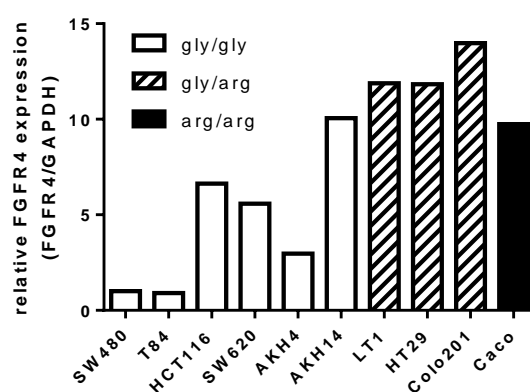


Figure 28: relative FGFR4 expression of different colon cancer cell lines.(Heinzle, Gsur et al. 2012)

The 3 CRC lines were infected with dn4 and sol4 expressing adenoviruses. HCT116 and HT29 cells were infected with a MOI=10, SW480 cells with a MOI=1. After 6h virus was removed from the cells by medium change. 24h after infection, cells were counted and 1×10^6 cells were subcutaneously injected into the right flank of SCID mice. Tumor growth was monitored, measured and before it reached the endpoint, mice were sacrificed. Tumors and lungs were obtained, fixed and immunohistochemistry was performed. For each experimental group 4 mice were used.

In figure 29 A, the kinetic of tumor growth is depicted for HCT116 cells infected with dn4-, sol4, and control virus. There was a trend towards reduced tumor growth in the dn4 virus group, but it was not significant (2-way ANOVA; $p=0.5150$). HCT116 cells that were infected with the sol4 virus failed to develop any tumor at all after 24 days (figure 29 A).

Figure 29 B shows the results for HT29 cells infected with the 3 different adenoviruses. Cells infected with the control virus developed tumors with a volume of about 2000mm^3 after 18 days. HT29 cells treated with the dn4 virus showed reduced growth rate compared to control (2-way ANOVA, $p=0.0021$). Moreover, cells infected with the sol4 virus had a significantly reduced growth rate in comparison to the control (2-way ANOVA, $p=0.0285$).

We performed 2 experiments using SW480 cells and the results are pooled in figure 29 C. Again, mice injected with the control cells developed tumors from about day 20. Infection with dn4 adenoviruses led to a reduction in tumor growth rate compared to the control (2-way ANOVA, $p=0.0191$). Sol4 reduced in vivo tumor growth of SW480 highly significantly (2-way ANOVA, $p<0.0001$).

Our experiments showed a reduction or even an inhibition of tumor growth in vivo for 3 different colon cancer cell lines with various FGFR4 expression and genotype when infected with dn4 or sol4.

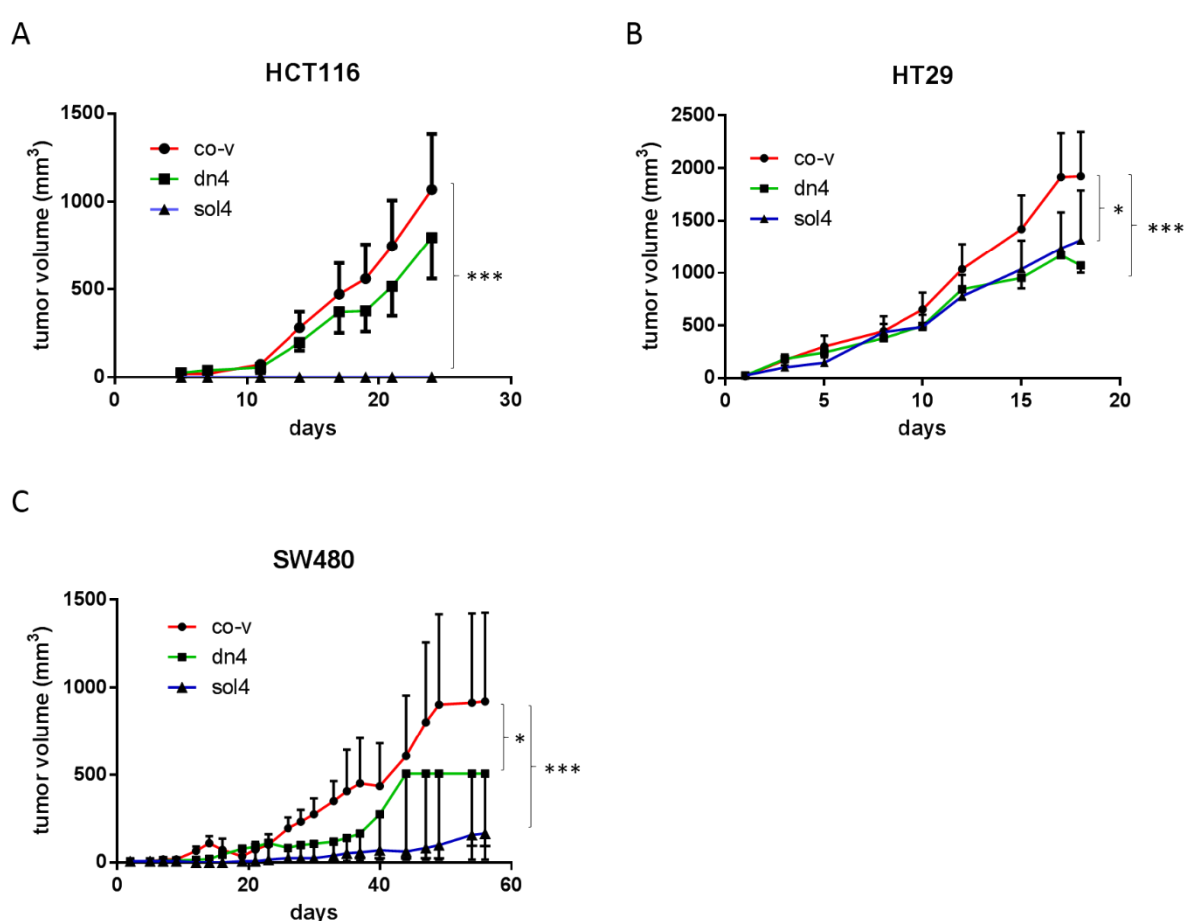


Figure 29: *In vivo* tumor growth of A: HCT116, B: HT29 and C: SW480 infected with co-v, dn4, and sol4.

Tumor samples of all in vivo experiments were stained with HE and Ki67. HE staining is used to get an overview of the tumor structure and to determine eventual necrotic areas. Ki-67 is a nuclear marker for proliferating cells and shows the growing and apoptotic potential of the tumor. Figure 30 shows pictures of HE and Ki67 staining of all tumors obtained by SW480

infected with dn4, sol4, and control virus. We were not able to detect any differences between the groups. For HCT116 cells, only pictures of dn4 and co-v infected cells were possible due to the lack of tumors in the sol4 treated group (figure 31). Because the stained tumor tissues of all 3 tested cell lines looked similar, only tumors originated from SW480 and HCT116 cells are shown.

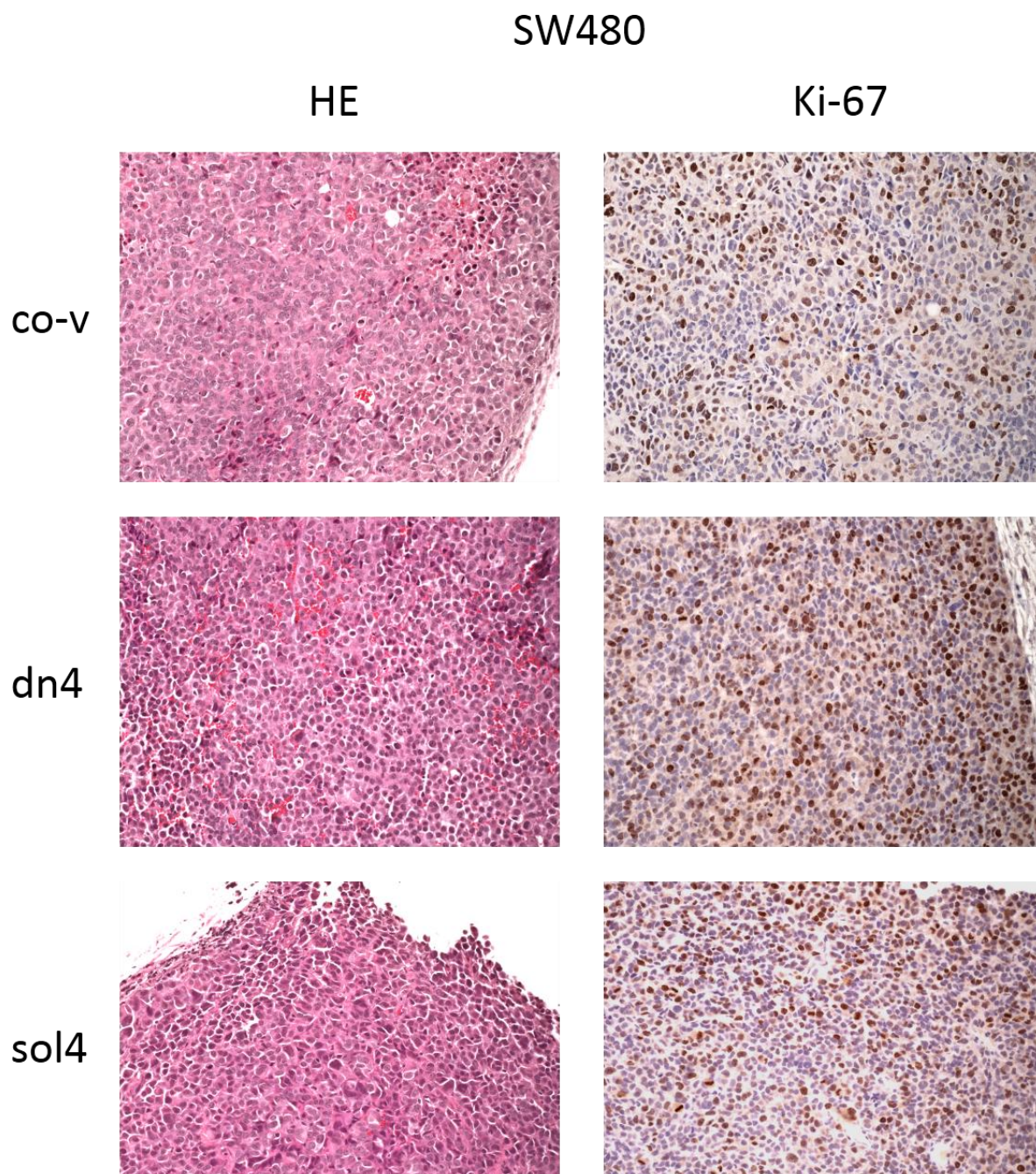


Figure 30: HE and Ki-67 staining of SW480 tumor tissue. HE stained tissue is shown on the left, Ki-67 immuno-histochemical staining on the right.

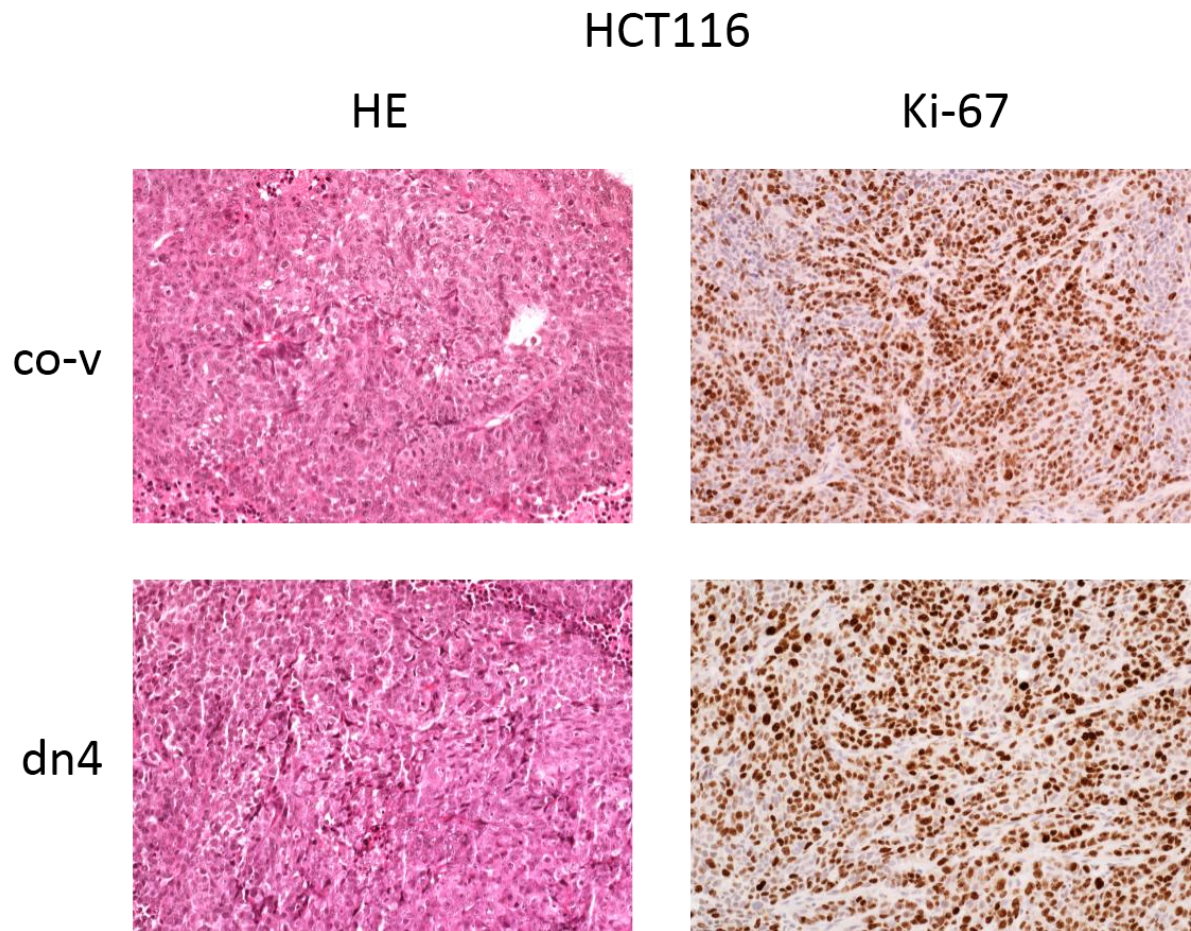


Figure 31: *HE and Ki-67 staining of HCT116 tumor tissue.. HE stained tumors are shown on the left, Ki-67 staining on the right.*

Because cells migrate from under the skin into the lung, lung tissue of all animals was obtained and Ki-67 staining was performed to detect metastasis. Lung tissue in adult animals is non-proliferative. Consequently all positive stained nuclei belong to the tumor tissue and represent metastasis. For mice injected with HCT116 cells, 1 micro metastasis in the control and 1 in the dn4 group were found (figure 32 left column). All other animals of the HCT116 experiment were negative for metastasis. As an example for metastasis free lungs, see figure 32 (figure 32 right column). Mice injected with HT29 or SW480 cells did not develop any metastasis in the lungs (data not shown).

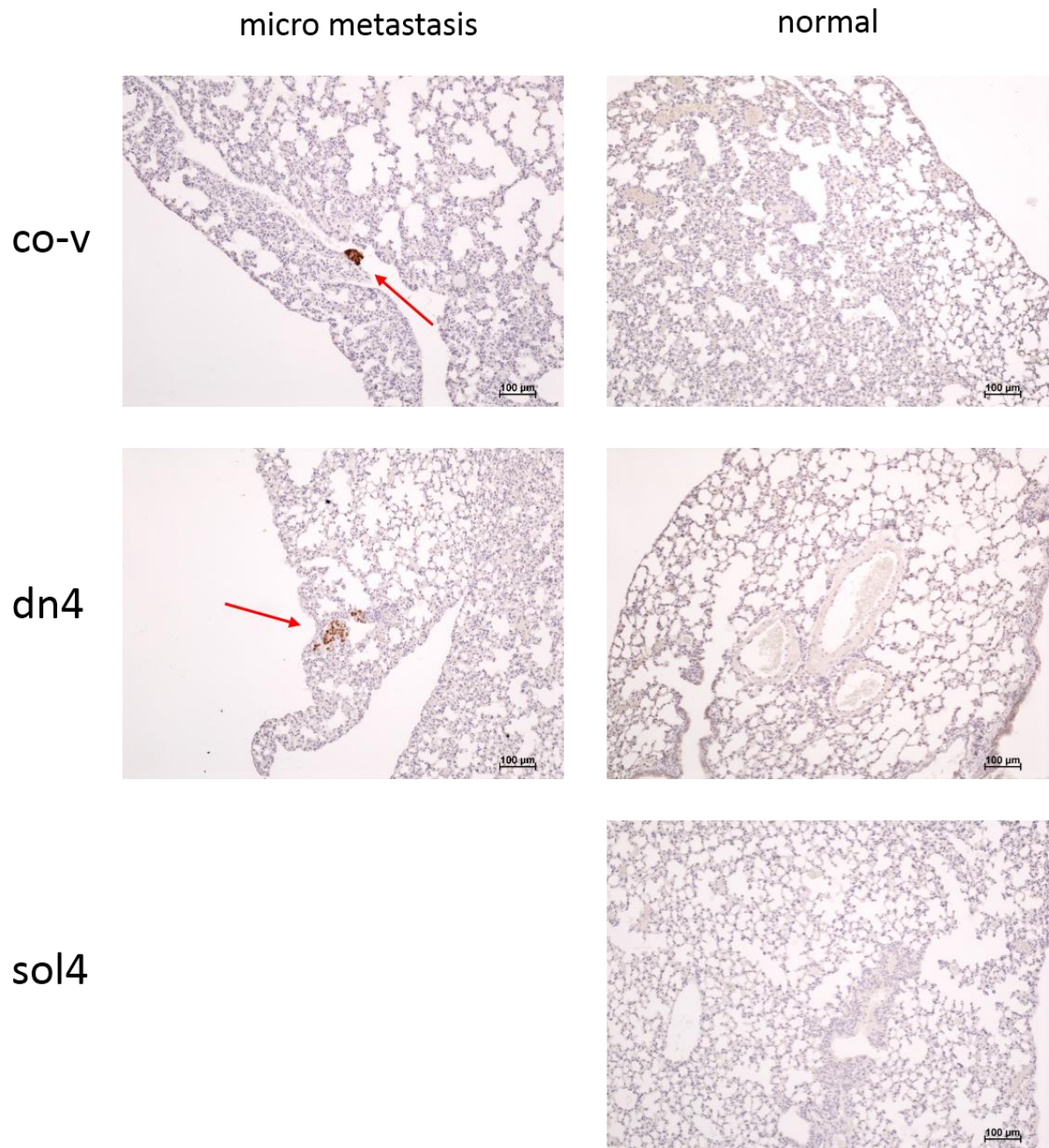


Figure 32: Ki-67 stained lungs of the experiment using HCT116 cell line. On the left, micro metastasis are indicated by a red arrow. Examples for normal lungs are shown in the right panel.

5 Discussion

During this master thesis we established Ba/F3 cells overexpressing FGFRs and tested their signaling, the inhibitory potential of TKI PD173074 and FGFR4 inhibiting adenoviral constructs. For the latter, significantly decreased viability as well as altered signaling of inhibited FGFR4 expressing cells was observed. In addition, the inhibitory adenoviral constructs attenuated tumor growth of colon cancer xenografts in SCID mice.

5.1 IL-3 (in)dependency of Ba/F3 cells

Upregulation of FGFR4 or its stimulating FGFs seems to play an important role in various tumor types and was observed for RMS (Taylor, Cheuk et al. 2009), liver (French, Lin et al. 2012), breast (Jaakkola, Salmikangas et al. 1993), prostate (Gowardhan, Douglas et al. 2005), and colon cancer (Desnoyers, Pai et al. 2008, Heinzle, Gsur et al. 2012) to name just a few. A very prominent SNP of FGFR4 results in either a glycine or an arginine at position 388 of the TM domain (Bange, Prechtel et al. 2002). Reports about the role of the SNP G388R are contradictory. At least some studies showed increased aggressiveness and tumor progression for patients expressing the Arg allele, whereas others failed to detect significant differences; for a summary see (Heinzle, Erdem et al. 2014). Findings of Wang et al. indicate that increased motility of cells expressing the Arg allele is a result of prolonged receptor stability and phosphorylation (Wang, Yu et al. 2008). In 2012, Heinzle et al. observed stimulation of both tumor growth and motility by either polymorphic allele of FGFR4 (Heinzle, Gsur et al. 2012). Identifying signaling events that correlate with Gly- or Arg-activation has been difficult however.

Ba/F3 cells are IL-3 dependent, murine bone marrow derived B-cells that lack endogenous RTKs (Palacios and Steinmetz 1985). Transfection with a specific receptor can create an IL-independent Ba/F3 population whose growth now relies on the transfected signaling pathway, as shown for FGF and its receptors (Ornitz, Yayon et al. 1992, Zhang, Ibrahimi et al. 2006). This constitutes a powerful tool to test inhibitory strategies using TKIs (Warmuth, Kim et al. 2007) as well as transforming potential of transfected RTKs (Daley and Baltimore 1988, Smedley, Demiroglu et al. 1999, Jiang, Paez et al. 2004, Jiang, Greulich et al. 2005, Ceccon, Mologni et al. 2013).

Daley et al. failed to induce spontaneous IL-3 independency in Ba/F3 cells, but detected IL-3 independency in cells expressing the bcr/abl fusion protein (Daley and Baltimore 1988). In our experiments, we observed IL-3 independency for one of the cell lines expressing the Gly variant of FGFR4. Although we observed a weak stimulatory effect of FGF1 towards increased viability of Gly cells, their mitogenic potential was strongly elevated compared to control even without IL-3 or FGF1. However, for a new batch of transfectants (Gly^{new}) this could not be reproduced.

Furthermore, we established cell lines Arg^{new} and control^{new} that showed increased viability at all tested IL-3 levels compared to other Ba/F3 cell lines, but were not completely IL-independent. This indicates that at least in some cases spontaneous decrease of IL-dependency can be observed. From this the question arose, whether transformation was dependent on signaling activity.

Alternatively, IL3-independency may have been acquired spontaneously during long-term cultivation of Ba/F3 cells as indicated by a report from Kazi et al. In their study, long term cultivation studies of Ba/F3 cells expressing Flt3-ITD and c-Kit-D816V in the absence of IL-3 showed an increase of proliferation compared to cells supplemented with IL-3 (Kazi, Sun et al. 2013). The authors suggested that cells cultured without IL-3 could be selected for stronger activation of receptors leading to enhanced oncogenic downstream signaling. Alternatively, chronic absence of IL-3 could alter gene expression patterns and response of cells towards cytokines like IL-3. Here, all media used for Ba/F3 cell culture were supplemented with IL-3 and we experienced enhanced viability as well as altered signaling also for cells without a transfected receptor. Further experiments will be useful to understand differential response of Ba/F3 cells.

5.2 FGF mediated signaling of transfected Ba/F3 cells

We investigated the signaling of Ba/F3 cell lines for further characterization. Western blots for a first set of Gly, Arg and control cell lines were already performed as part of an earlier project. Higher baseline levels of pERK, pS6 and pSTAT3 were observed for untreated as well as FGF stimulated IL-3-independent Gly cells compared to Arg and control. In contrast, equal phosphorylation levels of cells in the presence of IL-3 were observed (Christine Heinzle, unpublished data). Here, we investigated ERK, S6, STAT3 and PLCγ1 protein expression, as well

as their corresponding phosphorylated forms, for Gly^{new}, Arg^{new}, R3c and control^{new} and found distinct phosphorylation patterns.

PLCy1 binds to phosphorylated FGFRs via its SH2 domain and activates downstream signaling pathways (Turner and Grose 2010). Thus, PLCy1 plays an important role in cellular processes, for example, proliferation, survival, migration and death (Yang, Choi et al. 2012) and deregulation of PLCy1 can promote tumorigenesis (Park, Lee et al. 2012). For R3c treated with FGF1, we found stimulation of pPLCy1. Furthermore, Gly^{new} cells supplied with FGF1 showed elevated total PLCy1 levels, but no differences in phosphorylation. We did not observe any stimulatory effects after treatment of Arg^{new} and control^{new} cells with FGF1.

S6 is a downstream target of various RTKs, which activates multiple cellular processes upon phosphorylation, thereby regulating protein synthesis, proliferation, splicing and survival (Fenton and Gout 2011). For R3c, we detected a weak, FGF1 induced stimulatory effect on S6 phosphorylation. In addition to the already discussed increased viability, we observed strongly increased pS6 baseline levels of control^{new} and Arg^{new} compared to Gly^{new} and R3c. S6 is a downstream target of the PI3K pathway (Hemmings and Restuccia 2012), suggesting prolonged growth in IL-3 diminished media of control^{new} and Arg^{new} cells which resulted in an increased S6 phosphorylation. Similarly, Kazi et al. found in their long-term cultivation study with transfected Ba/F3 cells increased PI3K-and ERK1/2 signaling for cells without IL-3 (Kazi, Sun et al. 2013).

ERK1/2 is part of the MAPK pathway downstream of FGFR mediated signaling (Knights and Cook 2010). Activation of ERK1/2 leads to phosphorylation and in turn to degradation of pro-apoptotic protein BimEL (Ley, Balmano et al. 2003) as well as increased expression of pro-survival pathways (Balmano and Cook 2009). Although we did not observe an FGF1 dependent stimulatory effect on ERK1/2 signaling, we detected increased baseline pERK1/2 levels of Arg^{new} cells, similar to the viability experiments and S6 signaling, again indicating altered signaling response of this cell line. In contrast to the S6 signaling, we did not find an increased ERK1/2 phosphorylation of the control^{new} cells. However, increased ERK1/2 phosphorylation of Arg^{new} cells could also indicate a stress response. Ba/F3 cells treated with hydrogen peroxide, arsenite or incubated at higher temperatures showed dramatically increased pERK1/2 levels (Ng and Bogoyevitch 2000). In our experiments, all cells were incubated at 37°C and all manipulations were carried out as fast as possible and in a similar

manner for all cell lines. Nonetheless, the possibility of differing stress stimuli between different culture dishes and its impact on ERK phosphorylation cannot be excluded.

The transcription factor STAT3 plays an important role in various physiological processes, including metabolism, development, immunity as well as differentiation and its altered expression is linked to cancer (Siveen, Sikka et al. 2014). Moreover, tumor cells overexpressing FGFR1, 3 and 4 showed elevated STAT signaling (Heinzle, Sutterluty et al. 2011). Here, we were not able to detect any phosphorylated STAT3 for Gly^{new}, Arg^{new}, R3c or control^{new}.

5.3 FGFR4 inhibition - PD173074

Jiang et al. observed differential sensitivity of IL-3 independent Ba/F3 cells expressing EGFR-variants when treated with the TKI Gefitinib. Recently, Ba/F3 cells expressing mutated NPM-ALK proteins have been used to simulate crizotinib-resistant ALCL and to screen for possible inhibitors (Ceccon, Mologni et al. 2013). Here, we treated Gly and control Ba/F3 cells with the TKI PD173074. This small molecule inhibits FGFR1 (Nguyen, Tsunematsu et al. 2013), FGFR2, FGFR3 (Beenken and Mohammadi 2009) as well as FGFR4, although the inhibition of the latter is weaker compared to FGFR1-3 (Vainikka, Partanen et al. 1992, Wang, Gao et al. 1994, Shaoul, Reich-Slotky et al. 1995).

We detected decreased viability (two tailed t-test, $p=0.019$) of IL-3 independent Gly cells when treated with 5 μ M PD173074 in absence of IL-3. Control or Gly cells supplied with IL-3 showed no effects for the same concentration. This suggests that the IL-3 independency of Gly cells was at least in part dependent on FGFR4-signaling activity.

In addition, we observed a strong decrease of viability for all cell lines with or without IL-3 when treated with 10 μ M PD173074, suggesting a general toxicity of this TKI at high concentrations. In fact, clinical trials with PD173074 have been stopped due to toxicity problems (Knights and Cook 2010).

5.4 Blockade of FGFR4 by adenoviral constructs

Kalinina et al. described the inhibitory effect towards FGFRs of an adenovirally expressed construct consisted of an Igl loop linked to an AB by blocking the heparin binding site of FGFRs (Kalinina, Dutta et al. 2012). In addition, sol4 may compete with FGFRs for ligand binding

(Ezzat, Zheng et al. 2001) (Chen, Jiang et al. 2011). In contrast to soluble FGFRs, dnFGFRs are similar to wtFGFR but lack the TK domain, which prevents auto-phosphorylation and therefore FGFR mediated signaling (Alberts 2008). HCC cells infected with adenoviruses expressing sol4 or dn4 showed altered signaling as well as decreased motility and anchorage-independent growth (Gauglhofer, Paur et al. 2014). Here, we infected the IL-3 independent Gly cells as well as control cells with sol4, dn4 and co-v.

As expected, viability of the control cells was not altered by these constructs. Gly cells supplied with IL-3 also showed no differences in viability. However, IL-3 withdrawal resulted in reduced viability of cells infected with the dn4 construct, suggesting reacquired IL-3 dependency upon receptor blockade and therefore successful inhibition of FGFR4. However, we did not observe any inhibitory effects of cells treated with sol4. Although sol4 should exert its inhibitory potential by acting as a ligand trap (Ezzat, Zheng et al. 2001, Chen, Jiang et al. 2011) as well as blocking heparin binding sites (Kalinina, Dutta et al. 2012), recent studies indicated that Igl loop and AB play an important role in cell-to-cell contacts. Pituitary tumor derived cells expressing FGFR4 isoforms that lack the N-terminal Igl and AB showed less cell adhesion in vitro and increased invasiveness in vivo (Ezzat, Zheng et al. 2004). This suggests that the inhibitory function of the sol4 construct is, at least to some extent, involved in cell-to cell contacts. Ba/F3 are suspension cells (Palacios and Steinmetz 1985) and lack cell adhesion, which could explain why there was no impact on the viability of sol4 treated Ba/F3 cells.

However, we observed drastically reduced pPLC γ 1 levels and a trend to decreased STAT3 signaling of Gly cells stimulated with FGF1 and infected with dn4 as well as sol4, indicating FGFR4 blockade. We did not detect decreased S6 or ERK1/2 signaling of FGF1 stimulated cells infected with dn4 or sol4. In contrast to PLC γ 1 and STAT, S6 and ERK1/2 do not directly interact with the FGFR (Turner and Grose 2010) and could also be stimulated by another pathway. In addition, signaling mediated by FGFR4 is weak compared to other FGFRs (Vainikka, Partanen et al. 1992, Wang, Gao et al. 1994, Shaoul, Reich-Slotky et al. 1995). This suggests, that the activation of signaling pathways downstream of FGFR4 - S6 and ERK1/2 - was not sufficient to show inhibitory effects of dn4 and sol4.

5.5 Impact of FGFR4 Blockade on Tumor Growth

HCC cell lines infected with dn4 and sol4 showed decreased tumor growth rates when injected into SCID mice (Gauglhofer, Paur et al. 2014). Here, we tested FGFR4 blocking adenoviral constructs dn4, sol4 as well as co-v in vivo by injecting 3 different virally infected colon cancer cell lines subcutaneously into SCID mice, measured tumor growth rates and fixed/stained tumors when they reached the endpoint. The used cell lines SW480, HCT116 and HT29 varied in FGFR4 expression and allelotype (Heinzle, Gsur et al. 2012). Growth rates of tumors derived from dn4 infected cells were significantly decreased for HT29 and SW480. HCT116 derived tumors showed a trend to decreased tumor growth rates and failed to develop any tumors when infected with the sol4 construct. Attenuation of tumor growth rates was significant for all cell lines when infected with the sol4 construct. Our data suggest that the dn4 construct blocks FGFR4, therefore leading to decreased viability and tumor growth rates as well as variations in FGFR4 signaling. Furthermore, sol4 did not reduce viability in vitro in our Ba/F3 model, but altered signaling and drastically attenuated tumor growth rates in vivo, which indicates the already discussed role of FGFR4 and the Ig1-AB part in cell-to-cell contact. In addition to measuring tumor growth, we stained the tumors and lungs of the animals. Investigation of HE and Ki-67 stained tumor tissue slides revealed no differences between the experimental groups. Because we used non-propagating adenoviruses, the viral genome was transiently expressed and finally diluted out of the cell during cell division or degraded (Lanza 2013). This implies that tumor growth rates were successfully attenuated by viral treatment, but changes in tumor architecture, proliferation rates as well as expression of FGFR4 and invasive markers were already lost at the endpoints. Furthermore, for animals injected with HCT116 cells infected with dn4 and co-v, we detected 1 micro-metastasis in each of the lungs. There was no metastasis in the other groups, indicating, that this model is not suitable for studying invasion and metastasis.

5.6 Summary

In this master thesis, we investigated the impact of FGFR4 blockade towards viability, signaling and tumor growth. Using the Ba/F3 model system, we were able to show inhibitory effects of a small molecule inhibitor on viability of FGFR4 expressing cells. Furthermore, adenoviral constructs effectively altered signaling in vitro and reduced tumor growth rates of colon

cancer cells in vivo. Although we observed the effects of FGFR4 blockade in different model systems, the underlying pathways remain hidden. Further experiments to analyze FGFR4-dependent cellular reactions and their blockade will include gene set enrichment analysis of various FGFR4 overexpressing colon cancer cell lines. Comparing the expression data of different cell lines should allow us to identify FGFR4 mediated effects.

6 Abstract

Overexpression of FGFR4 and/or its stimulating ligands has been observed for various tumor types. Recently, the SNP G388R of FGFR4 has moved into the focus of interest as both allelic forms seem to play important roles in tumorigenesis. So far, inhibitory strategies for FGFR4 are limited, mainly because available drugs were initially designed to block other RTK and lack specificity for FGFR4. In this study, we were able to show the inhibitory potential of the TKI PD173074 towards Ba/F3 cells expressing only FGFR4. Using the same cell line, we evaluated blockade of FGFR4 via infection with adenoviral constructs. Treatment with the dn4 construct resulted in decreased viability, indicating successful inhibition. In addition, both dn4 and sol4 altered signaling pathways of FGFR4 expressing Ba/F3 cells. Moreover, we performed in vivo experiments using three CRC cell lines with varying FGFR4 expression and allelotype. Tumor growth rates for these xenografts were decreased compared to control, whereby efficiency of inhibition varied between the cell lines. This indicates, that blockade of FGFR4 could play an important role in cancer therapy of patients with altered FGFR4 background.

7 Kurzfassung

In verschiedenen Tumoren wurde erhöhte Expression von FGFR4 bzw. dessen stimulierenden Liganden detektiert. Weiters nimmt in immer mehr Studien der Einzelnukleotid-Polymorphismus G388R von FGFR4 eine besondere Rolle ein. Nach heutigem Wissensstand dürften beide Allele mit Tumorentstehung und –entwicklung in Verbindung stehen. Um FGFR4 zu blockieren, werden Inhibitoren verwendet die vorwiegend entwickelt wurden um andere RTK zu blockieren, weshalb es an Spezifität fehlt. In dieser Studie wurden Ba/F3 Zellenlinien verwendet die nur FGFR4 exprimieren, um auf diese Weise die inhibierende Wirkung von PD173074 auf FGFR4 nachzuweisen. Zusätzlich wurde dieselbe Zelllinie mit Adenoviren infiziert, um die blockierende Wirkung der genetischen Konstrukte dn4 und sol4 zu überprüfen. Eine verringerte Viabilität nach dn4 Expression bzw. Veränderungen von phosphorylierten Signalproteinen deutete auf erfolgreiche FGFR4 Blockade hin. Zusätzlich wurden in vivo Versuche mit drei verschiedenen Kolon-Krebs Zelllinien durchgeführt. Die verwendeten Zelllinien unterschieden sich sowohl im Ausmaß der FGFR4 Expression als auch im Allelotyp. Diese Zelllinien wurden mit dn4 und sol4 infiziert, in Mäuse injiziert und die daraus resultierenden Tumore in regelmäßigen Abständen gemessen. Die Wachstumsrate der dn4 und sol4 behandelten Tumore war verringert, wobei das Ausmaß der Reduzierung abhängig von der Zelllinie war. Eine gezielte FGFR4 Blockierung könnte also eine wichtige Rolle bei der Behandlung von Patienten mit mutierten oder FGFR4 überexprimierenden Tumoren spielen.

8 Bibliography

- Adams, J. M. and S. Cory (2007). "The Bcl-2 apoptotic switch in cancer development and therapy." Oncogene **26**(9): 1324-1337.
- Alberts, B. (2008). Molecular Biology of the Cell 5th edition, Garland Science.
- Armand, A. S., T. Launay, C. Pariset, B. Della Gaspera, F. Charbonnier and C. Chanoine (2003). "Injection of FGF6 accelerates regeneration of the soleus muscle in adult mice." Biochim Biophys Acta **1642**(1-2): 97-105.
- Armand, A. S., I. Laziz and C. Chanoine (2006). "FGF6 in myogenesis." Biochim Biophys Acta **1763**(8): 773-778.
- Armitage, P. and R. Doll (1954). "The age distribution of cancer and a multi-stage theory of carcinogenesis." Br J Cancer **8**(1): 1-12.
- Avet-Loiseau, H., T. Facon, A. Daviet, C. Godon, M. J. Rapp, J. L. Harousseau, B. Grosbois and R. Bataille (1999). "14q32 translocations and monosomy 13 observed in monoclonal gammopathy of undetermined significance delineate a multistep process for the oncogenesis of multiple myeloma. Intergroupe Francophone du Myelome." Cancer Res **59**(18): 4546-4550.
- Balmano, K. and S. J. Cook (2009). "Tumour cell survival signalling by the ERK1/2 pathway." Cell Death Differ **16**(3): 368-377.
- Bange, J., D. Prechtel, Y. Cheburkin, K. Specht, N. Harbeck, M. Schmitt, T. Knyazeva, S. Muller, S. Gartner, I. Sures, H. Wang, E. Imyanitov, H. U. Haring, P. Knayzev, S. Iacobelli, H. Hofler and A. Ullrich (2002). "Cancer progression and tumor cell motility are associated with the FGFR4 Arg(388) allele." Cancer Res **62**(3): 840-847.
- Beenken, A. and M. Mohammadi (2009). "The FGF family: biology, pathophysiology and therapy." Nat Rev Drug Discov **8**(3): 235-253.
- Berger, W., U. Setinek, T. Mohr, I. Kindas-Mugge, M. Vetterlein, G. Dekan, F. Eckersberger, C. Caldas and M. Micksche (1999). "Evidence for a role of FGF-2 and FGF receptors in the proliferation of non-small cell lung cancer cells." Int J Cancer **83**(3): 415-423.
- Berx, G. and F. van Roy (2009). "Involvement of members of the cadherin superfamily in cancer." Cold Spring Harb Perspect Biol **1**(6): a003129.
- Bhowmick, N. A., E. G. Neilson and H. L. Moses (2004). "Stromal fibroblasts in cancer initiation and progression." Nature **432**(7015): 332-337.
- Blasco, M. A. (2005). "Telomeres and human disease: ageing, cancer and beyond." Nat Rev Genet **6**(8): 611-622.
- Boland, C. R. and L. Ricciardiello (1999). "How many mutations does it take to make a tumor?" Proc Natl Acad Sci U S A **96**(26): 14675-14677.

- Carstens, R. P., J. V. Eaton, H. R. Krigman, P. J. Walther and M. A. Garcia-Blanco (1997). "Alternative splicing of fibroblast growth factor receptor 2 (FGF-R2) in human prostate cancer." Oncogene **15**(25): 3059-3065.
- Cavallaro, U. and G. Christofori (2004). "Cell adhesion and signalling by cadherins and Ig-CAMs in cancer." Nat Rev Cancer **4**(2): 118-132.
- Ceccon, M., L. Mologni, W. Bisson, L. Scapozza and C. Gambacorti-Passerini (2013). "Crizotinib-resistant NPM-ALK mutants confer differential sensitivity to unrelated Alk inhibitors." Mol Cancer Res **11**(2): 122-132.
- Chen, Q., Y. Jiang, Y. An, N. Zhao, Y. Zhao and C. Yu (2011). "Soluble FGFR4 extracellular domain inhibits FGF19-induced activation of FGFR4 signaling and prevents nonalcoholic fatty liver disease." Biochem Biophys Res Commun **409**(4): 651-656.
- Cheng, N., A. Chytil, Y. Shyr, A. Joly and H. L. Moses (2008). "Transforming growth factor-beta signaling-deficient fibroblasts enhance hepatocyte growth factor signaling in mammary carcinoma cells to promote scattering and invasion." Mol Cancer Res **6**(10): 1521-1533.
- Cho, J. Y., C. Guo, M. Torello, G. P. Lunstrum, T. Iwata, C. Deng and W. A. Horton (2004). "Defective lysosomal targeting of activated fibroblast growth factor receptor 3 in achondroplasia." Proc Natl Acad Sci U S A **101**(2): 609-614.
- Choi, M., A. Moschetta, A. L. Bookout, L. Peng, M. Umetani, S. R. Holmstrom, K. Suino-Powell, H. E. Xu, J. A. Richardson, R. D. Gerard, D. J. Mangelsdorf and S. A. Kliewer (2006). "Identification of a hormonal basis for gallbladder filling." Nat Med **12**(11): 1253-1255.
- Croze, L. E., K. T. Etheridge, C. Chen, B. Belyea, L. J. Talbot, R. C. Bentley and C. M. Linardic (2012). "FGFR4 blockade exerts distinct antitumorigenic effects in human embryonal versus alveolar rhabdomyosarcoma." Clin Cancer Res **18**(14): 3780-3790.
- Daley, G. Q. and D. Baltimore (1988). "Transformation of an interleukin 3-dependent hematopoietic cell line by the chronic myelogenous leukemia-specific P210bcr/abl protein." Proc Natl Acad Sci U S A **85**(23): 9312-9316.
- Datta, S. R., H. Dudek, X. Tao, S. Masters, H. Fu, Y. Gotoh and M. E. Greenberg (1997). "Akt phosphorylation of BAD couples survival signals to the cell-intrinsic death machinery." Cell **91**(2): 231-241.
- Davies, M. A. and Y. Samuels (2010). "Analysis of the genome to personalize therapy for melanoma." Oncogene **29**(41): 5545-5555.
- Desnoyers, L. R., R. Pai, R. E. Ferrando, K. Hotzel, T. Le, J. Ross, R. Carano, A. D'Souza, J. Qing, I. Mohtashemi, A. Ashkenazi and D. M. French (2008). "Targeting FGF19 inhibits tumor growth in colon cancer xenograft and FGF19 transgenic hepatocellular carcinoma models." Oncogene **27**(1): 85-97.
- Ezzat, S., L. Zheng and S. L. Asa (2004). "Pituitary tumor-derived fibroblast growth factor receptor 4 isoform disrupts neural cell-adhesion molecule/N-cadherin signaling to diminish

cell adhesiveness: a mechanism underlying pituitary neoplasia." Mol Endocrinol **18**(10): 2543-2552.

Ezzat, S., L. Zheng, S. Yu and S. L. Asa (2001). "A soluble dominant negative fibroblast growth factor receptor 4 isoform in human MCF-7 breast cancer cells." Biochem Biophys Res Commun **287**(1): 60-65.

Feinberg, A. P. and B. Vogelstein (1983). "Hypomethylation distinguishes genes of some human cancers from their normal counterparts." Nature **301**(5895): 89-92.

Fenton, T. R. and I. T. Gout (2011). "Functions and regulation of the 70kDa ribosomal S6 kinases." Int J Biochem Cell Biol **43**(1): 47-59.

Fong, C. W., M. S. Chua, A. B. McKie, S. H. Ling, V. Mason, R. Li, P. Yusoff, T. L. Lo, H. Y. Leung, S. K. So and G. R. Guy (2006). "Sprouty 2, an inhibitor of mitogen-activated protein kinase signaling, is down-regulated in hepatocellular carcinoma." Cancer Res **66**(4): 2048-2058.

French, D. M., B. C. Lin, M. Wang, C. Adams, T. Shek, K. Hotzel, B. Bolon, R. Ferrando, C. Blackmore, K. Schroeder, L. A. Rodriguez, M. Hristopoulos, R. Venook, A. Ashkenazi and L. R. Desnoyers (2012). "Targeting FGFR4 inhibits hepatocellular carcinoma in preclinical mouse models." PLoS One **7**(5): e36713.

Gauglhofer, C., J. Paur, W. C. Schrottmaier, B. Wingelhofer, D. Huber, I. Naegelen, C. Pirker, T. Mohr, C. Heinzle, K. Holzmann, B. Marian, R. Schulte-Hermann, W. Berger, G. Krupitza, M. Grusch and B. Grasl-Kraupp (2014). "Fibroblast growth factor receptor 4: a putative key driver for the aggressive phenotype of hepatocellular carcinoma." Carcinogenesis **35**(10): 2331-2338.

Gowardhan, B., D. A. Douglas, M. E. Mathers, A. B. McKie, S. R. McCracken, C. N. Robson and H. Y. Leung (2005). "Evaluation of the fibroblast growth factor system as a potential target for therapy in human prostate cancer." Br J Cancer **92**(2): 320-327.

Grivennikov, S. I. and M. Karin (2010). "Inflammation and oncogenesis: a vicious connection." Curr Opin Genet Dev **20**(1): 65-71.

Hammoud, S. S., B. R. Cairns and D. A. Jones (2013). "Epigenetic regulation of colon cancer and intestinal stem cells." Curr Opin Cell Biol **25**(2): 177-183.

Hanada, K., D. M. Perry-Lalley, G. A. Ohnmacht, M. P. Bettinotti and J. C. Yang (2001). "Identification of fibroblast growth factor-5 as an overexpressed antigen in multiple human adenocarcinomas." Cancer Res **61**(14): 5511-5516.

Hanahan, D. and J. Folkman (1996). "Patterns and emerging mechanisms of the angiogenic switch during tumorigenesis." Cell **86**(3): 353-364.

Hanahan, D. and R. A. Weinberg (2011). "Hallmarks of cancer: the next generation." Cell **144**(5): 646-674.

Haugsten, E. M., A. Wiedlocha, S. Olsnes and J. Wesche (2010). "Roles of fibroblast growth factor receptors in carcinogenesis." Mol Cancer Res **8**(11): 1439-1452.

- Heinzle, C., Z. Erdem, J. Paur, B. Grasl-Kraupp, K. Holzmann, M. Grusch, W. Berger and B. Marian (2014). "Is fibroblast growth factor receptor 4 a suitable target of cancer therapy?" Curr Pharm Des **20**(17): 2881-2898.
- Heinzle, C., A. Gsur, M. Hunjadi, Z. Erdem, C. Gauglhofer, S. Stattner, J. Karner, M. Klimpfinger, F. Wrba, A. Reti, B. Hegedus, A. Baierl, B. Grasl-Kraupp, K. Holzmann, M. Grusch, W. Berger and B. Marian (2012). "Differential effects of polymorphic alleles of FGF receptor 4 on colon cancer growth and metastasis." Cancer Res **72**(22): 5767-5777.
- Heinzle, C., H. Sutterluty, M. Grusch, B. Grasl-Kraupp, W. Berger and B. Marian (2011). "Targeting fibroblast-growth-factor-receptor-dependent signaling for cancer therapy." Expert Opin Ther Targets **15**(7): 829-846.
- Hemmings, B. A. and D. F. Restuccia (2012). "PI3K-PKB/Akt pathway." Cold Spring Harb Perspect Biol **4**(9): a011189.
- Ho, H. K., S. Pok, S. Streit, J. E. Ruhe, S. Hart, K. S. Lim, H. L. Loo, M. O. Aung, S. G. Lim and A. Ullrich (2009). "Fibroblast growth factor receptor 4 regulates proliferation, anti-apoptosis and alpha-fetoprotein secretion during hepatocellular carcinoma progression and represents a potential target for therapeutic intervention." J Hepatol **50**(1): 118-127.
- Ibrahimi, O. A., F. Zhang, S. C. Hrstka, M. Mohammadi and R. J. Linhardt (2004). "Kinetic model for FGF, FGFR, and proteoglycan signal transduction complex assembly." Biochemistry **43**(16): 4724-4730.
- Jaakkola, S., P. Salmikangas, S. Nylund, J. Partanen, E. Armstrong, S. Pyrhonen, P. Lehtovirta and H. Nevanlinna (1993). "Amplification of fgfr4 gene in human breast and gynecological cancers." Int J Cancer **54**(3): 378-382.
- Jiang, B. H. and L. Z. Liu (2009). "PI3K/PTEN signaling in angiogenesis and tumorigenesis." Adv Cancer Res **102**: 19-65.
- Jiang, J., H. Greulich, P. A. Janne, W. R. Sellers, M. Meyerson and J. D. Griffin (2005). "Epidermal growth factor-independent transformation of Ba/F3 cells with cancer-derived epidermal growth factor receptor mutants induces gefitinib-sensitive cell cycle progression." Cancer Res **65**(19): 8968-8974.
- Jiang, J., J. G. Paez, J. C. Lee, R. Bo, R. M. Stone, D. J. DeAngelo, I. Galinsky, B. M. Wolpin, A. Jonasova, P. Herman, E. A. Fox, T. J. Boggon, M. J. Eck, E. Weisberg, J. D. Griffin, D. G. Gilliland, M. Meyerson and W. R. Sellers (2004). "Identifying and characterizing a novel activating mutation of the FLT3 tyrosine kinase in AML." Blood **104**(6): 1855-1858.
- Kalinina, J., K. Dutta, D. Ilghari, A. Beenken, R. Goetz, A. V. Eliseenkova, D. Cowburn and M. Mohammadi (2012). "The alternatively spliced acid box region plays a key role in FGF receptor autoinhibition." Structure **20**(1): 77-88.
- Kazi, J. U., J. Sun and L. Ronnstrand (2013). "The presence or absence of IL-3 during long-term culture of Flt3-ITD and c-Kit-D816V expressing Ba/F3 cells influences signaling outcome." Exp Hematol **41**(7): 585-587.

Kim, R., M. Emi and K. Tanabe (2007). "Cancer immunoediting from immune surveillance to immune escape." Immunology **121**(1): 1-14.

Klagsbrun, M. and P. A. D'Amore (1991). "Regulators of angiogenesis." Annu Rev Physiol **53**: 217-239.

Knights, V. and S. J. Cook (2010). "De-regulated FGF receptors as therapeutic targets in cancer." Pharmacol Ther **125**(1): 105-117.

Korhonen, J., J. Partanen and K. Alitalo (1992). "Expression of FGFR-4 mRNA in developing mouse tissues." Int J Dev Biol **36**(2): 323-329.

Kunii, K., L. Davis, J. Gorenstein, H. Hatch, M. Yashiro, A. Di Bacco, C. Elbi and B. Lutterbach (2008). "FGFR2-amplified gastric cancer cell lines require FGFR2 and Erbb3 signaling for growth and survival." Cancer Res **68**(7): 2340-2348.

Kwabi-Addo, B., J. Wang, H. Erdem, A. Vaid, P. Castro, G. Ayala and M. Ittmann (2004). "The expression of Sprouty1, an inhibitor of fibroblast growth factor signal transduction, is decreased in human prostate cancer." Cancer Res **64**(14): 4728-4735.

Lanza, R. (2013). Principles of Tissue Engineering, Academic Press.

Ley, R., K. Balmano, K. Hadfield, C. Weston and S. J. Cook (2003). "Activation of the ERK1/2 signaling pathway promotes phosphorylation and proteasome-dependent degradation of the BH3-only protein, Bim." J Biol Chem **278**(21): 18811-18816.

Lo, T. L., P. Yusoff, C. W. Fong, K. Guo, B. J. McCaw, W. A. Phillips, H. Yang, E. S. Wong, H. F. Leong, Q. Zeng, T. C. Putti and G. R. Guy (2004). "The ras/mitogen-activated protein kinase pathway inhibitor and likely tumor suppressor proteins, sprouty 1 and sprouty 2 are deregulated in breast cancer." Cancer Res **64**(17): 6127-6136.

National-Cancer-Institute. (2014, 07.03.2014). "What is cancer?", from <http://www.cancer.gov/cancertopics/cancerlibrary/what-is-cancer>.

Ng, D. C. and M. A. Bogoyevitch (2000). "The mechanism of heat shock activation of ERK mitogen-activated protein kinases in the interleukin 3-dependent ProB cell line BaF3." J Biol Chem **275**(52): 40856-40866.

Nguyen, P. T., T. Tsunematsu, S. Yanagisawa, Y. Kudo, M. Miyauchi, N. Kamata and T. Takata (2013). "The FGFR1 inhibitor PD173074 induces mesenchymal-epithelial transition through the transcription factor AP-1." Br J Cancer **109**(8): 2248-2258.

Olsen, S. K., O. A. Ibrahimi, A. Raucci, F. Zhang, A. V. Eliseenkova, A. Yayon, C. Basilico, R. J. Linhardt, J. Schlessinger and M. Mohammadi (2004). "Insights into the molecular basis for fibroblast growth factor receptor autoinhibition and ligand-binding promiscuity." Proc Natl Acad Sci U S A **101**(4): 935-940.

Ornitz, D. M., A. Yayon, J. G. Flanagan, C. M. Svahn, E. Levi and P. Leder (1992). "Heparin is required for cell-free binding of basic fibroblast growth factor to a soluble receptor and for mitogenesis in whole cells." Mol Cell Biol **12**(1): 240-247.

Palacios, R. and M. Steinmetz (1985). "IL3-dependent mouse clones that express B-220 surface antigen, contain ig genes in germ-line configuration, and generate B lymphocytes in vivo." Cell **41**(3): 727-734.

Park, J. B., C. S. Lee, J. H. Jang, J. Ghim, Y. J. Kim, S. You, D. Hwang, P. G. Suh and S. H. Ryu (2012). "Phospholipase signalling networks in cancer." Nat Rev Cancer **12**(11): 782-792.

Poh, W., W. Wong, H. Ong, M. O. Aung, S. G. Lim, B. T. Chua and H. K. Ho (2012). "Klotho-beta overexpression as a novel target for suppressing proliferation and fibroblast growth factor receptor-4 signaling in hepatocellular carcinoma." Mol Cancer **11**: 14.

Polyak, K. and R. A. Weinberg (2009). "Transitions between epithelial and mesenchymal states: acquisition of malignant and stem cell traits." Nat Rev Cancer **9**(4): 265-273.

Rappolee, D. A., Y. Patel and K. Jacobson (1998). "Expression of fibroblast growth factor receptors in peri-implantation mouse embryos." Mol Reprod Dev **51**(3): 254-264.

Ricol, D., D. Cappellen, A. El Marjou, S. Gil-Diez-de-Medina, J. M. Girault, T. Yoshida, G. Ferry, G. Tucker, M. F. Poupon, D. Chopin, J. P. Thiery and F. Radvanyi (1999). "Tumour suppressive properties of fibroblast growth factor receptor 2-IIIb in human bladder cancer." Oncogene **18**(51): 7234-7243.

Roidl, A., P. Foo, W. Wong, C. Mann, S. Bechtold, H. J. Berger, S. Streit, J. E. Ruhe, S. Hart, A. Ullrich and H. K. Ho (2010). "The FGFR4 Y367C mutant is a dominant oncogene in MDA-MB453 breast cancer cells." Oncogene **29**(10): 1543-1552.

Schlessinger, J., A. N. Plotnikov, O. A. Ibrahimi, A. V. Eliseenkova, B. K. Yeh, A. Yayon, R. J. Linhardt and M. Mohammadi (2000). "Crystal structure of a ternary FGF-FGFR-heparin complex reveals a dual role for heparin in FGFR binding and dimerization." Mol Cell **6**(3): 743-750.

Shaoul, E., R. Reich-Slotky, B. Berman and D. Ron (1995). "Fibroblast growth factor receptors display both common and distinct signaling pathways." Oncogene **10**(8): 1553-1561.

Shaw, R. J. and L. C. Cantley (2006). "Ras, PI(3)K and mTOR signalling controls tumour cell growth." Nature **441**(7092): 424-430.

Shukla, N., N. Ameer, I. Yilmaz, K. Nafa, C. Y. Lau, A. Marchetti, L. Borsu, F. G. Barr and M. Ladanyi (2012). "Oncogene mutation profiling of pediatric solid tumors reveals significant subsets of embryonal rhabdomyosarcoma and neuroblastoma with mutated genes in growth signaling pathways." Clin Cancer Res **18**(3): 748-757.

Siveen, K. S., S. Sikka, R. Surana, X. Dai, J. Zhang, A. P. Kumar, B. K. Tan, G. Sethi and A. Bishayee (2014). "Targeting the STAT3 signaling pathway in cancer: role of synthetic and natural inhibitors." Biochim Biophys Acta **1845**(2): 136-154.

Smedley, D., A. Demiroglu, M. Abdul-Rauf, C. Heath, C. Cooper, J. Shipley and N. C. Cross (1999). "ZNF198-FGFR1 transforms Ba/F3 cells to growth factor independence and results in high level tyrosine phosphorylation of STATs 1 and 5." Neoplasia **1**(4): 349-355.

Smith, K., S. B. Fox, R. Whitehouse, M. Taylor, M. Greenall, J. Clarke and A. L. Harris (1999). "Upregulation of basic fibroblast growth factor in breast carcinoma and its relationship to vascular density, oestrogen receptor, epidermal growth factor receptor and survival." Ann Oncol **10**(6): 707-713.

Sonvilla, G., S. Allerstorfer, C. Heinzle, S. Stattner, J. Karner, M. Klimpfinger, F. Wrba, H. Fischer, C. Gauglhofer, S. Spiegl-Kreinecker, B. Grasl-Kraupp, K. Holzmann, M. Grusch, W. Berger and B. Marian (2010). "Fibroblast growth factor receptor 3-IIIc mediates colorectal cancer growth and migration." Br J Cancer **102**(7): 1145-1156.

Spinola, M., V. P. Leoni, J. Tanuma, A. Pettinicchio, M. Frattini, S. Signoroni, R. Agresti, R. Giovanazzi, S. Pilotti, L. Bertario, F. Ravagnani and T. A. Dragani (2005). "FGFR4 Gly388Arg polymorphism and prognosis of breast and colorectal cancer." Oncol Rep **14**(2): 415-419.

St Bernard, R., L. Zheng, W. Liu, D. Winer, S. L. Asa and S. Ezzat (2005). "Fibroblast growth factor receptors as molecular targets in thyroid carcinoma." Endocrinology **146**(3): 1145-1153.

Stark, K. L., J. A. McMahon and A. P. McMahon (1991). "FGFR-4, a new member of the fibroblast growth factor receptor family, expressed in the definitive endoderm and skeletal muscle lineages of the mouse." Development **113**(2): 641-651.

Sugiyama, N., M. Varjosalo, P. Meller, J. Lohi, K. M. Chan, Z. Zhou, K. Alitalo, J. Taipale, J. Keski-Oja and K. Lehti (2010). "FGF receptor-4 (FGFR4) polymorphism acts as an activity switch of a membrane type 1 matrix metalloproteinase-FGFR4 complex." Proc Natl Acad Sci U S A **107**(36): 15786-15791.

Sutterluty, H., C. E. Mayer, U. Setinek, J. Attems, S. Ovtcharov, M. Mikula, W. Mikulits, M. Micksche and W. Berger (2007). "Down-regulation of Sprouty2 in non-small cell lung cancer contributes to tumor malignancy via extracellular signal-regulated kinase pathway-dependent and -independent mechanisms." Mol Cancer Res **5**(5): 509-520.

Taylor, J. G. t., A. T. Cheuk, P. S. Tsang, J. Y. Chung, Y. K. Song, K. Desai, Y. Yu, Q. R. Chen, K. Shah, V. Youngblood, J. Fang, S. Y. Kim, C. Yeung, L. J. Helman, A. Mendoza, V. Ngo, L. M. Staudt, J. S. Wei, C. Khanna, D. Catchpoole, S. J. Qualman, S. M. Hewitt, G. Merlino, S. J. Chanock and J. Khan (2009). "Identification of FGFR4-activating mutations in human rhabdomyosarcomas that promote metastasis in xenotransplanted models." J Clin Invest **119**(11): 3395-3407.

Teng, M. W., J. B. Swann, C. M. Koebel, R. D. Schreiber and M. J. Smyth (2008). "Immune-mediated dormancy: an equilibrium with cancer." J Leukoc Biol **84**(4): 988-993.

Turner, N. and R. Grose (2010). "Fibroblast growth factor signalling: from development to cancer." Nat Rev Cancer **10**(2): 116-129.

Vainikka, S., J. Partanen, P. Bellosta, F. Coulier, D. Birnbaum, C. Basilico, M. Jaye and K. Alitalo (1992). "Fibroblast growth factor receptor-4 shows novel features in genomic structure, ligand binding and signal transduction." EMBO J **11**(12): 4273-4280.

- Vogelstein, B., E. R. Fearon, S. E. Kern, S. R. Hamilton, A. C. Preisinger, Y. Nakamura and R. White (1989). "Allelotype of colorectal carcinomas." Science **244**(4901): 207-211.
- Vorlova, S., G. Rocco, C. V. Lefave, F. M. Jodelka, K. Hess, M. L. Hastings, E. Henke and L. Cartegni (2011). "Induction of antagonistic soluble decoy receptor tyrosine kinases by intronic polyA activation." Mol Cell **43**(6): 927-939.
- Wang, J., D. W. Stockton and M. Ittmann (2004). "The fibroblast growth factor receptor-4 Arg388 allele is associated with prostate cancer initiation and progression." Clin Cancer Res **10**(18 Pt 1): 6169-6178.
- Wang, J., W. Yu, Y. Cai, C. Ren and M. M. Ittmann (2008). "Altered fibroblast growth factor receptor 4 stability promotes prostate cancer progression." Neoplasia **10**(8): 847-856.
- Wang, J. K., G. Gao and M. Goldfarb (1994). "Fibroblast growth factor receptors have different signaling and mitogenic potentials." Mol Cell Biol **14**(1): 181-188.
- Warmuth, M., S. Kim, X. J. Gu, G. Xia and F. Adrian (2007). "Ba/F3 cells and their use in kinase drug discovery." Curr Opin Oncol **19**(1): 55-60.
- Weinberg, R. A. (2007). The biology of cancer. 210 Madison Avenue, New York, NY 10016, USA, and
2 Park square, Milton Park, Abingdon, OX14 4RN, UK, Garland Science.
- White, E. and R. S. DiPaola (2009). "The double-edged sword of autophagy modulation in cancer." Clin Cancer Res **15**(17): 5308-5316.
- Yan, G., Y. Fukabori, G. McBride, S. Nikolaropolous and W. L. McKeehan (1993). "Exon switching and activation of stromal and embryonic fibroblast growth factor (FGF)-FGF receptor genes in prostate epithelial cells accompany stromal independence and malignancy." Mol Cell Biol **13**(8): 4513-4522.
- Yang, Y. R., J. H. Choi, J. S. Chang, H. M. Kwon, H. J. Jang, S. H. Ryu and P. G. Suh (2012). "Diverse cellular and physiological roles of phospholipase C-gamma1." Adv Biol Regul **52**(1): 138-151.
- Yu, C., F. Wang, C. Jin, X. Wu, W. K. Chan and W. L. McKeehan (2002). "Increased carbon tetrachloride-induced liver injury and fibrosis in FGFR4-deficient mice." Am J Pathol **161**(6): 2003-2010.
- Yu, C., F. Wang, M. Kan, C. Jin, R. B. Jones, M. Weinstein, C. X. Deng and W. L. McKeehan (2000). "Elevated cholesterol metabolism and bile acid synthesis in mice lacking membrane tyrosine kinase receptor FGFR4." J Biol Chem **275**(20): 15482-15489.
- Zhang, X., O. A. Ibrahimi, S. K. Olsen, H. Umemori, M. Mohammadi and D. M. Ornitz (2006). "Receptor specificity of the fibroblast growth factor family. The complete mammalian FGF family." J Biol Chem **281**(23): 15694-15700.

9 Curriculum Vitae

Name: Daniel Florian Mario Drev
Gender: Male
Nationality: Austria
e-mail: daniel.drev@gmx.net

Education

1990 - 1993 Primary School Leopoldgasse, 1020 Vienna
1993 - 1994 Primary School Fürst-Lichtenstein-Straße, 1230 Vienna
1994 - 2002 BRG & ORG Antonkriegergasse, 1230 Vienna (Grammar School)
2008 - 2012 University of Vienna, Bachelor Molecular Biology
Since 2012 University of Vienna, Master Molecular Biology

Working experience

2012, August - September **Bachelor thesis** at the Institute of Cancer Research, Borschkegasse 8a A-1090, Vienna, Austria
group of Priv. Doz. Mag. Dr. Hedwig Sutterlüty
Topic: Influence of co-cultivation of NSCLC derived cells and tumor associated fibroblasts on miR-21 expression
2013, July - August **Internship** at the Institute of Cancer Research, Borschkegasse 8a A-1090, Vienna, Austria
group of A.o Univ. Prof. Dr. Brigitte Marian
Since 2013, October **Master thesis** at the Institute of Cancer Research, Borschkegasse 8a A-1090, Vienna, Austria
group of A.o Univ. Prof. Dr. Brigitte Marian
Topic: FGFR4 blocking strategies in colorectal cancer and Ba/F3 cells